

ALMA MATER STUDIORUM – UNIVERSITÀ DI BOLOGNA
CAMPUS DI CESENA
SCUOLA DI INGEGNERIA E ARCHITETTURA

CORSO DI LAUREA MAGISTRALE IN INGEGNERIA BIOMEDICA

TITOLO DELLA TESI

**OPTIMISATION OF CHEMICAL LYSIS PROTOCOL FOR
POINT-OF-CARE LEUKOCYTE DIFFERENTIATION**

Tesi in

Sensori e Nanotecnologie LM

Relatore

Prof. Ing. Marco Tartagni

Presentata da

Alessandra La Gioia

Correlatore

Prof. Ing. Hywel Morgan

Dr. Daniel Spencer

Sessione I

Anno Accademico 2013/2014

Abstract

The full blood cell (FBC) count is the most common indicator of diseases. At present hematology analyzers are used for the blood cell characterization, but, recently, there has been interest in using techniques that take advantage of microscale devices and intrinsic properties of cells for increased automation and decreased cost. Microfluidic technologies offer solutions to handling and processing small volumes of blood (2-50 μL taken by finger prick) for point-of-care (PoC) applications. Several PoC blood analyzers are in use and may have applications in the fields of telemedicine, out patient monitoring and medical care in resource limited settings. They have the advantage to be easy to move and much cheaper than traditional analyzers, which require bulky instruments and consume large amount of reagents. The development of miniaturized point-of-care diagnostic tests may be enabled by chip-based technologies for cell separation and sorting. Many current diagnostic tests depend on fractionated blood components: plasma, red blood cells (RBCs), white blood cells (WBCs), and platelets. Specifically, white blood cell differentiation and counting provide valuable information for diagnostic purposes. For example, a low number of WBCs, called leukopenia, may be an indicator of bone marrow deficiency or failure, collagen-vascular diseases, disease of the liver or spleen. The leukocytosis, a high number of WBCs, may be due to anemia, infectious diseases, leukemia or tissue damage. In the laboratory of hybrid biodevices, at the University of Southampton, it was developed a functioning micro impedance cytometer technology for WBC differentiation and counting. It is capable to classify cells and particles on the base of their dielectric properties, in addition to their size, without the need of labeling, in a flow format similar to that of a traditional flow cytometer. It was demonstrated that the micro impedance cytometer system can detect and differentiate monocytes, neutrophils and lymphocytes, which are the three major human leukocyte populations. The simplicity and portability of the microfluidic impedance chip offer a range of potential applications in cell analysis including

point-of-care diagnostic systems. The microfluidic device has been integrated into a sample preparation cartridge that semi-automatically performs erythrocyte lysis before leukocyte analysis. Generally erythrocytes are manually lysed according to a specific chemical lysis protocol, but this process has been automated in the cartridge. In this research work the chemical lysis protocol, defined in the patent US 5155044 A, was optimized in order to improve white blood cell differentiation and count performed by the integrated cartridge.

Contents

Introduction	10
1 Full blood count	12
1.1 Blood	12
1.2 Leukocyte classification	14
1.3 FBC and existing methods for leukocyte differentiation and counting	17
2 Systems for single cell analysis	22
2.1 Sample preparation for improving WBC detection in single cell analysis	23
2.2 Flow cytometry	26
2.2.1 Fluidics system	28
2.2.2 Optical system	29
2.2.3 Optical-to-electronic coupling system	31
2.3 Impedance cytometry	33
2.3.1 Dielectric cell characterisation	33
2.3.1.1 Polarization	33
2.3.1.2 Complex permittivity in dielectric-conductive material and dielectric spectroscopy	36
2.3.1.3 Maxwell's mixture theory	41
2.3.1.4 Electrical double layer	43
2.3.1.5 Single shell model	45
2.3.2 Microfluidic Impedance Chip	46
2.3.2.1 Geometry of the chip	48
2.3.2.2 MIC fabrication	48
2.3.2.3 Flow profile	49
2.3.2.4 Impedance signal acquisition	50
2.3.2.5 Lock-in scheme detection	52
2.3.2.6 Impedance spectrum of a single cell	53
3 Materials and methods	56
3.1 Chemical protocols used for RBC lysis and WBC differentiation	57
3.1.1 Standard lysis protocol for 3-part leukocyte differentiation	57

3.1.2	Lysis protocol for differential determination of four leukocyte populations	60
3.2	Sample preparation cartridge for automated RBC lysis	64
3.2.1	Integrated cartridge components	65
3.2.2	Comparison of data acquired by the integrated system and that acquired by MIC after manual sample preparation	67
3.3	Variations in the 3-part leukocyte differential protocol	69
3.3.1	Saponin concentration variations in the lysis solution	70
3.3.2	Glutaraldehyde addition in the quench solution	71
4	Results and discussion	73
4.1	Leukocyte subpopulation gating and count	73
4.2	Saponin variation effects	74
4.2.1	Evaluation of results in bulk lysis	75
4.2.2	Evaluation of results in stirring lysis	77
4.3	Glutaraldehyde addition effects	81
4.3.1	Evaluation of results obtained using 0.05% saponin solution	81
4.3.2	Evaluation of results obtained using 0.1% saponin solution	82
4.3.3	Evaluation of results obtained using 0.075% saponin solution	84
4.4	Variability in the data acquisition	84
5	Conclusion and future direction	88
5.1	Conclusion	88
5.2	Future direction	89
5.2.1	CD4 T-cell labeling	90
5.2.2	Choice of the mixer	93
	Bibliography	95

List of Figures

1.1	Blood centrifugation [20].	13
1.2	Blood cells, fragments and proteins [20].	15
1.3	Schematic diagram of the detecting area in a conventional flow cytometer (http://www.andor.com).	19
1.4	Schematic diagram of the working principle of impedance cytometry (http://www.southampton.ac.uk/cmm/research/Impedance).	20
2.1	Scheme of the lysis protocol used in the experimental work.	24
2.2	CAD drawing of the microfluidic platform for FBC [41].	25
2.3	Schematic diagram of the integrated microfluidic leukocyte analysis system [11].	26
2.4	Schematics of a flow cytometer (www.electronicproducts.com).	27
2.5	Schematic diagram of data acquisition in a flow cytometer (from 'Introduction to Flow Cytometry: A Learning Guide').	28
2.6	Hydrodynamic focusing of the sample within the flow chamber (from 'Introduction to Flow Cytometry: A Learning Guide').	29
2.7	Leukocytes clusters of lysed whole blood in the scatter plot SSC vs FSC.[25]	30
2.8	Schematic illustration of antibody staining and scatter plot of CD3 FITC/CD4 PE.[25]	30
2.9	Schematic diagram of the optical system (from 'Introduction to Flow Cytometry: A Learning Guide').	31
2.10	Conversion of a light signal into a voltage pulse (from 'Introduction to Flow Cytometry: A Learning Guide').	32
2.11	Dipolar orientation when an external electrical field is applied.	34
2.12	Equivalent circuit of an idealized parallel-plate capacitor filled with a dielectric material (wikipedia.org/wiki/Dielectric).	36
2.13	Equivalent circuit of an idealized parallel-plate capacitor filled with material of relative permittivity ϵ and conductivity σ	37
2.14	Single time constant relaxation. At the top relative permittivity vs frequency; at the bottom conductivity vs frequency (From 'Transduction - Ionics' of Nanotechnology course).	39
2.15	Cole-Cole diagram for a single relaxation time (From 'Transduction - Ionics' of Nanotechnology course).	40

2.16	A dielectric permittivity spectrum over a wide range of frequencies (wikipedia.org/Dielectric_spectroscopy). The real and imaginary parts of permittivity are shown, and various processes are depicted: ionic and dipolar relaxation, and atomic and electronic resonances at higher energies.	41
2.17	Schematic of N particles in a spherical region.	42
2.18	Electrical double layer when a negative electrode is in contact with a water solvent (From 'Transduction - Ionics' of Nanotechnology course).	44
2.19	Equivalent capacitances of the stern layer and the diffusive layer.	45
2.20	Single shell model of a cell [3].	46
2.21	Schematic diagram of a Coulter counter (http://www.beatop.com).	47
2.22	Schematic diagram of the micro impedance cytometry system [37].	47
2.23	Top view of the chip showing two pairs of overlapping electrodes above and below the microchannel (Right image from [13]).	48
2.24	Typical data captured by the microfluidic impedance cytometry when a cell passes through the channel. The dotted lines indicate the positions of the electrode edges [37].	50
2.25	Example of the three main leukocyte populations in the scatter plot of opacity ($ Z _{2\text{ MHz}}/ Z _{500\text{ kHz}}$) vs low frequency impedance magnitude ($ Z _{500\text{ kHz}}$).	51
2.26	Complex Impedance detection by lock in amplifiers (From 'Transduction - Ionics' of Nanotechnology course).	52
2.27	Simplified schematic of the impedance detection. C_{dl} represents the electrical double layer capacitance at the liquid electrode interface, C_m and R_m are the equivalent capacitance and resistance of the medium respectively. R_{cyto} is equivalent resistance of the cell cytoplasm, C_{mem} is the equivalent capacitance of the cell membrane [21].	53
2.28	Typical frequency-dependent impedance magnitude signal for leukocytes [21].	54
3.1	Scheme of the lysis protocol for 3-part leukocyte differentiation.	58
3.2	On the left three leukocyte subsets in the scatter plot SSC vs FSC. On the right the same populations in the scatter plot opacity vs electrical volume.	59
3.3	WBC differentiation obtained by MIC after implementing the 3 part leukocyte differential protocol in different quench times: 1 minute, 3 minutes and 5 minutes.	60
3.4	Scheme of the lysis protocol for 4-part leukocyte differentiation.	61
3.5	Leukocyte clusters obtained by flow cytometry after performing the standard lysis protocol.	62

3.6	Leukocyte analysis by flow cytometry from the four part differential protocol. The four experiments were performed by immersing the lysed and fixed blood solution into a 70° C water bath with swirling for different times: a) no heating b) 15 seconds c) 20 seconds d) 30 seconds.	63
3.7	Leukocyte analysis by impedance cytometry after performing the 4 part differential protocol.	64
3.8	Schematic diagram of the integrated sample preparation cartridge.	65
3.9	Top view of the integrated cartridge.	66
3.10	Three leukocyte populations in the scatter plot opacity vs Z_{500kHz} : on the left, clusters from the bulk lysis; on the right, clusters from the stirring lysis.	67
3.11	Time traces (0.2 seconds) of impedance signals from leukocytes obtained after performing bulk lysis (on left) and stirring lysis (on right).	68
3.12	Scatter plots obtained after 1 minute, 3 minutes and 5 minutes of quench by implementing the bulk lysis and the stirring lysis according to the 3 part leukocyte differential protocol.	69
3.13	Protein cross-linkage by glutaraldehyde.	71
4.1	Cluster gating by polygons for sub-population count.	74
4.2	HemoCue for WBC count and monitor with the corresponding leukocyte percentages from a blood sample (Left image from [26]).	74
4.3	WBCs acquired in different quench times (1 minute, 3 minutes and 5 minutes) from bulk lysis using the 0.1% w/v saponin lysis solution. Clusters are compared with those from the standard bulk lysis.	75
4.4	WBCs acquired in different quench times (1 minute, 3 minutes and 5 minutes) from bulk lysis using the 0.075% w/v saponin lysis solution. Clusters are compared with those from the standard bulk lysis.	76
4.5	WBCs acquired in different quench times (1 minute, 3 minutes and 5 minutes) from bulk lysis using the 0.065% w/v saponin lysis solution.	77
4.6	On left, WBCs from stirring lysis using 0.1% w/v saponin lysis solution after a quench time of 1 minute; on right, WBCs from the standard bulk lysis.	78
4.7	WBCs acquired in different quench times (1 minute, 3 minutes and 5 minutes) from stirring lysis using the 0.075% w/v saponin lysis solution. Clusters are compared with those from the standard bulk lysis.	79
4.8	WBCs acquired in different quench times (1 minute, 3 minutes and 5 minutes) from stirring lysis using the 0.065% w/v saponin lysis solution.	80

4.9	WBCs from stirring lysis using the 0.065% w/v saponin lysis solution acquired after 1 minute and 3 minutes of quench and compared with the standard bulk lysis.	81
4.10	WBCs from bulk lysis using the 1% v/v glutaraldehyde quench solution acquired after 1 minute and 5 minutes of quench and compared with the standard bulk lysis.	81
4.11	WBCs from stirring lysis using 1% v/v glutaraldehyde quench solution acquired after 1 minute and 5 minutes of quench and compared with the standard bulk lysis.	82
4.12	WBCs from bulk lysis using 0.1% w/v saponin lysis solution and 1% v/v glutaraldehyde quench solution acquired after 1 minute and 5 minutes of quench and compared with the standard bulk lysis.	83
4.13	WBCs from bulk lysis using 0.075% w/v saponin lysis solution and 1% v/v glutaraldehyde quench solution acquired after 1 minute and 5 minutes of quench and compared with the standard bulk lysis.	84
4.14	WBC clusters acquired after 3 minutes from the bulk lysis mixing the 0.065% saponin lysis solution with the whole blood for 10 seconds and 20 seconds. Clusters are compared with the standard lysis protocol.	85
4.15	WBC acquisitions from the the standard bulk lysis obtained using the same blood sample a) after 30 minutes and b) after 5 hours from the collection.	86
4.16	Clusters from the stirring lysis with 0.065% saponin solution obtained by pumping the lysed blood continuously at the flow rate of 40 μ L/min, and acquired a) after 1 minute, and b) after 5 minutes of quench.	87
5.1	Scheme of the interaction between a lymphocyte and antigen specific antibodies (http://www.cancer.ca/the-immune-system/). . .	91
5.2	Scheme of the interaction of CD4 coated beads with T helper cells [14].	91
5.3	Dependence of the mean APC fluorescence from lymphocytes on the volume of the APC-CD4 staining antibody solution added to 20 μ L blood sample.	92
5.4	Evolution of the APC fluorescence from lymphocytes in the time. 20 μ L blood sample was stained with 2 μ L APC-CD4 antibody solution.	93

List of Tables

4.1	WBC sub-population count corresponding to data shown in figure 4.4	77
4.2	WBC sub-population count corresponding to data shown in figure 4.5	77
4.3	WBC sub-population count corresponding to data shown in figure 4.7	79
4.4	WBC sub-population count corresponding to data shown in figure 4.8	80
4.5	WBC sub-population count corresponding to data shown in figure 4.12	83

Introduction

The leukocyte count is a clinical test that measures the number of leukocytes in blood, reporting the total count of leukocytes and the differential count of leukocyte subtypes. Clinical laboratories normally perform leukocyte count with a three part differential including neutrophils, lymphocytes, monocytes, or a complete five part differential, including also eosinophils and basophils, which are present in lower percentages. The test provides valuable information for diagnostic purposes. For instance, an increase in the number of neutrophils is associated with such diseases as inflammations, myocardial infarction and leukemia, and a decrease in their number is associated with viral diseases, hypoplastic anemia and agranulocytosis. A low number of lymphocytes is a feature of infection or disorders such as leukemia and lymphoma, and a decrease of T lymphocytes is associated with increased infections and human immunodeficiency virus (HIV). The leukocyte count is generally performed by hematology analyzers in central clinical laboratories after taking the venous blood from patients. The procedure is time consuming and patients wait 3-4 days for having the report. Hematology analyzers are computerized, highly specialized machines that count the number of different types of red and white blood cells, blood platelets, haemoglobin, and haematocrit levels in a blood sample (FBC). The traditional hemocytometers are bulky, expensive and consume a large number of reagents. They are not suitable for on-site diagnosis and their cost is prohibitive for resource limited settings.

In recent years, there is an emerging interest in the development of devices for point-of-care tests due to the advancement of the microfluidics technology. Point-of-care leukocyte count offers applications in the fields of telemedicine, out patient monitoring and medical care in developing countries. Recently several point-of-care testing devices for leukocyte count, that are based on different operating principles, have been developed. Leukocytes can be detected by light scattering, microscopic imaging, optics (using fluorescent dye assays or fluo-

rochrome conjugated antibodies) and impedance measurements.

In the experimental work the micro impedance cytometry system, totally developed at the University of Southampton (UoS), was used for three-part differential leukocyte count. It has the advantage to use small volumes of capillary blood taken by finger prick and to require a short sample preparation phase. The micro-impedance cytometer detects and differentiates neutrophils, lymphocytes and monocytes, without the need of labeling, after lysing the erythrocytes (RBCs).

The RBC lysis prevents cell interferences in the WBC acquisition since the erythrocytes have a size comparable with that of lymphocytes and they outnumber leukocytes by a factor of 1000. There are a lot of methods used for RBC lysis. In the laboratory of hybrid biodevices (UoS) RBC lysis is performed according to a chemical protocol, that involves the use of a lysis and a quench solution. The lysis solution is effective toward erythrocytes and the quench solution extinguishes the lytic effect preventing WBC damage. The protocol is generally performed manually but different fluidic platforms have been developing to automate the RBC lysis process. Specifically, in this work it was used a semiautomatic cartridge, having active components, that was integrated into the microimpedance cytometry system. The cartridge has been validated and it has been found that the RBC lysis performed by the sample preparation cartridge was less effective than that performed manually resulting in interferences between erythrocytes and lymphocytes. Thus the aim of the work was the leukocyte differentiation improvement by optimising the chemical lysis protocol. The effects of some chemicals on RBC lysis and WBC differentiation were analysed by changing their concentration in the lysis and quench solutions.

In the thesis, the experimental details and the results are reported in the third and fourth chapters. The first chapter provides a brief description of the blood components and a discussion about some of the methods used for WBC differentiation and count. In the second chapter the working principles of flow cytometry and impedance cytometry, techniques used in the experimental work, were described in detail. Lastly, the purpose and the results of the work were summarised in the fifth chapter.

Chapter 1

Full blood count

1.1 Blood

Blood is a connective tissue and the only liquid tissue in the body. It consists of formed elements, cells and cell fragments, in a liquid intercellular matrix, the plasma. Average adult blood volume is around 5 liters and represent the 8% of body weight. It's almost four times more viscous than water. Its temperature is about 1°C higher than measured body temperature (38 degrees). Blood transports oxygen and nutrients to cells, carbon dioxide and waste away from cells, hormones to target tissues. It contributes to maintain stable body temperature, pH, water and electrolyte levels. In fact, plasma absorbs and distributes heat throughout the body [20]. The blood vessels in the dermis dilate and dissipate the excess heat through the integument; to conserve heat, the dermal blood vessels constrict. Blood plasma pH is continuously regulated at a value of 7.4 (7.35-7.45) for normal cellular functioning. If pH falls to 7.0, in a condition of acidosis, the Central Nervous System is depressed; if pH rises to 7.8, in a condition of alkalosis, the nervous system is hyperexcited and convulsions occur. Blood plasma contains compounds and ions, such as salts and some proteins, that may be distributed to the interstitial fluid (among tissues) to help maintain normal tissue pH. Water content of cells, in which ions and proteins are dissolved, is regulated through blood osmotic pressure. If too much fluid is absorbed in the blood, high blood pressure results. If too much fluid escapes the bloodstream and enters the tissues, blood pressure drops to unhealthy low levels, and the tissues swell with excess fluid (edema). Furthermore, white blood cells protect body against diseases. Blood can be broken down into its liquid and cellular components by centrifugation [20].



Figure 1.1: Blood centrifugation [20].

After centrifugation blood plasma rises to the top of the tube, as shown in the figure 1.1, and represents about 55% of blood. *Plasma* is composed of water (92%), dissolved proteins, salts, and nutrients. Water facilitates the transport of materials in the plasma. Proteins make up about 7% of the plasma and they include: albumins, globulins, fibrinogen and regulatory proteins. *Albumins* are the smallest and most abundant of the plasma proteins. They act as transport proteins that carry ions, hormones, and some lipids in the blood and regulate water movement between the blood and interstitial fluid. *Globulins* represent the second largest group and bind, support, and protect certain water-insoluble or hydrophobic molecules, hormones, and ions. Some kinds of globulins are produced by defense cells to protect the body against pathogens that may cause disease. *Fibrinogen* is responsible for blood clot formation. *Regulatory Proteins* include enzymes to accelerate chemical reactions in the blood and hormones being transported throughout the body to target cells. Erythrocytes, leukocytes and platelets are called *formed elements* and represent about 45% of blood. The hematocrit is the percentage of the volume of formed elements in the blood. Values vary slightly and are dependent on age and sex. They increase when the body requires a larger oxygen carrying capacity of blood. The viscosity of the blood increases with the hematocrit and may lead to heart failure [20].

Erythrocytes, also called red blood cells (RBCs), represent 98% of formed elements. Their principal function is to transport oxygen and carbon dioxide to and from the tissues and the lungs. The erythrocytes contain hemoglobin (Hb), a red-pigmented protein, which transports almost all the oxygen and some molecules of carbon dioxide. It's responsible for the characteristic bright

red color of arterial blood. Hb molecule has four protein building blocks: 2 alpha and 2 beta chains. All globin chains contain a heme group with an iron ion (Fe^{++}) in its center. So each Hb molecule binds four molecules of oxygen. Oxygen binding is fairly weak to ensure rapid attachment in the lungs and detachment in the tissues. The hemoglobin carries over 99% of oxygen and 23% of carbon dioxide. Most of the carbon dioxide is carried in the bicarbonate ion.

Platelets, also called thrombocytes, are less than 1% and they are cell fragments involved in blood clotting. Their size is around 2-3 μm , make up 1% of formed elements and contribute to defending the body against pathogens [20].

1.2 Leukocyte classification

Leukocytes defend the body against infections by mounting an immune response if a pathogen or an antigen is found. Plasma transports antibodies, which are molecules that can immobilize antigens until a leukocyte can completely kill or remove the antigen. All leukocytes are produced and derived from a multipotent cell in the bone marrow known as a hematopoietic stem cell. Leukocytes are about 1.5 to 3 times larger than erythrocytes and make up approximately 1% of the total blood volume in a healthy adult. There are five major types of white blood cells: neutrophils, lymphocytes (B cells and T cells), monocytes, eosinophils and basophils, as shown in figure 1.2. Neutrophils, eosinophils and basophils are also called granulocytes because they have granules in their cells that contain digestive enzymes. Analyzing them by microscope using Wright's stain, that is a histologic stain that facilitates WBC differentiation, basophils have purple granules, eosinophils have orange-red granules and neutrophils have a faint blue-pink color. When a granulocyte is released into the blood, it stays there for an average of four to eight hours and then goes into the tissues of the body, where it lasts for four or five days. During a severe infection, these times are often shorter [20].

The *neutrophils* make up 60-70% of the total number of leukocytes. They are the one of the body's main defenses against bacteria. Neutrophils kill bacteria by a process called phagocytosis, in which they completely surround the bacteria and digest them with specific enzymes. They can phagocytize five to 20 bacteria in their lifetime. Neutrophils have a multi-lobed, segmented or polymorphic nucleus.

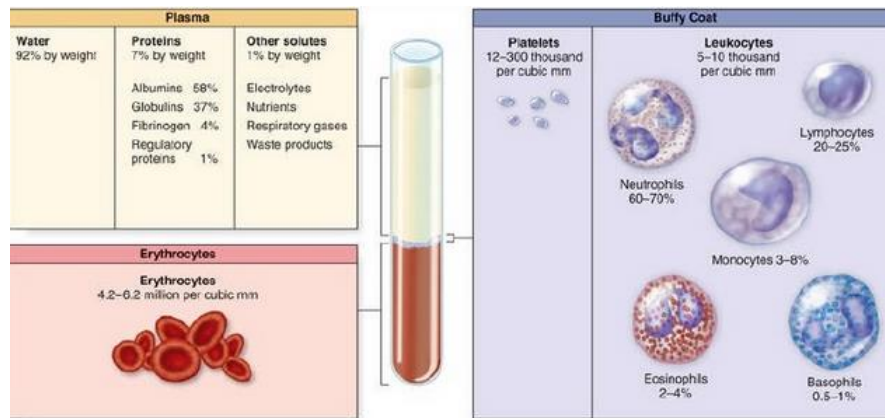


Figure 1.2: Blood cells, fragments and proteins [20].

The *eosinophils* make up about 2-4% of the total number of leukocytes. They kill parasites and have a role in allergic reactions. Their presence increases to phagocytize antigen-antibody complexes during parasitic infections. These proinflammatory white blood cells generally have nuclei with two lobes (bilobed) and cytoplasm filled with approximately 200 large granules containing enzymes and proteins with different functions. Eosinophils are formed exclusively in the bone marrow where they spend about 8 days in the process of maturation before moving into the blood vessels. They travel through the vessels for 8 to 12 hours before they finally arrive at destination tissues, where they remain for 1 to 2 weeks. Interleukin 5 (IL-5) appears to be the major growth factor for this type of cell.

The *basophils* are 1.5 times larger than erythrocytes and make up about 0.5-1% of the total number of leukocytes. They release histamine, which increases the diameter of blood vessels and heparin, which inhibits clotting in the infected area so that WBCs can reach the bacteria.

The *monocytes* make up 3-8% of all leukocytes. After an average of 10 to 20 hours in the circulation, monocytes move into tissues, where they become larger and turn into macrophages. There they can phagocytize bacteria throughout the body. These cells also destroy old, damaged and dead cells. Macrophages are found in the liver, spleen, lungs, lymphonodes, skin and intestine. Neutrophils and monocytes use several mechanisms to reach and kill invading organisms. They normally squeeze through openings in blood vessels by a process called diapedesis and move around using ameboid motion [20].

The *lymphocytes* are complex cells that direct the body's immune system. Lymphocytes are different from the other WBCs because they can recognize and have a memory of invading bacteria and viruses. Lymphocytes continually pass back and forth between lymph tissue, lymph fluid and blood. They can live for weeks, months or years. Lymphocytes are classified in 2 subsets: T lymphocytes and B lymphocytes. The first ones are involved in cell-mediated immunity and the second ones are primarily responsible for humoral immunity.

The T *lymphocytes* (T cells) start in the bone marrow from pluripotent hematopoietic stem cells, then travel to and mature in the thymus gland. The thymus is located in the chest between the heart and sternum. T cells make up about 75% of lymphocytes. There are many types of T cells that have specific functions, including:

- *Helper T cells*: have proteins on their cell membranes called CD4. Helper T cells direct the rest of the immune system by releasing cytokines. Cytokines stimulate B cells to form plasma cells, which form antibodies, stimulate the production of cytotoxic T cells and suppressor T cells and activate macrophages. Helper T cells are the cells the HIV infection attacks.
- *Cytotoxic T cells*: release chemicals that break and kill invading organisms.
- *NKT cells*: are a heterogeneous group of T cells that share properties of both T cells and natural killer (NK) cells. They seem to be essential for several aspects of immunity because their dysfunction or deficiency has been shown to lead to the development of autoimmune diseases, such as diabetes or atherosclerosis, and cancers.
- *Memory T cells*: help the immune system to respond more quickly if the same organism is encountered again.
- *Suppressor T cells*: suppress the immune response so that it does not get out of control and destroy normal cells once the immune response is no longer needed.

The *B lymphocytes* mature in the bone marrow and become plasma cells when exposed to an invading organism or when activated by helper T cells. B cells produce large numbers of antibodies, also called immunoglobulins. There are five types of immunoglobulins: IgG, IgM, IgE, IgA and IgD. These are Y-shaped molecules that have a variable segment that is a binding site for only one specific antigen. These bind to antigens, which cause them to clump and be neutralized. They also activate the complement system, which consists of a series of enzymes that help antibodies and other components of the immune system to destroy the invading antigen by attracting and activating neutrophils and macrophages, neutralizing viruses and causing invading organisms to break open. Memory B cells also remain for prolonged periods and, if the same antigen is encountered, it causes a more rapid response in producing antibodies [20].

1.3 FBC and existing methods for leukocyte differentiation and counting

The full blood count (FBC) consists in the measure of several parameters, such as hematocrit, haemoglobin, blood cell morphology and count, contributing to aid diagnosis and monitor disease progression.

A decrease in the red cell count is an indicator of anaemia. The rate of increase in haemoglobin could be used to monitor the treatment of anaemia and determine the amount of blood required for transfusion.

The platelet count and its size can also be used to determine the thrombopoietic activity of the bone marrow, and an increase or decrease in platelet numbers can be associated to disorders of haemostasis or liver disease [27].

Differentiation and counting of leukocytes in the blood provide valuable information for diagnostic purposes. For instance, an increase in the number of neutrophils is associated with such diseases as inflammations, myocardial infarction and leukemia, and a decrease in their number is associated with viral diseases, hypoplastic anemia and agranulocytosis. On the other hand an increase in the number of eosinophils is found in such diseases as parasitosis and allergosis. An increased number of monocytes occurs either during the convalescence period of patients suffering from infectious diseases. Furthermore, lymphocytosis is a feature of infection or disorders such as leukemia and lymphoma, and a decrease of T lymphocytes is associated with increased infections

and human immunodeficiency virus (HIV) [33].

Formerly, classification and counting of leukocytes have been made most commonly by the *visual counting method*. It consists in spreading a blood sample on a glass slide so that the blood corpuscles in the smear are fixed and stained for examination by microscopy. During the analysis by microscopy, the type of individual leukocytes is identified combining the degree of dye uptake to their morphological features, such as their size, the morphology of their nucleus and cytoplasm, and the presence or absence of granules. In this method, ordinarily, leukocyte classification is performed counting 100-200 leukocytes for each sample and the percentage of the total leukocyte count occupied by each type of cell is recorded as a measured value [33]. The differential counting method has several disadvantages, most of them are associated with procedures that precede the microscopic observation, such as smearing a blood sample on a glass slide, cell fixation and staining. The quality of the image depends mostly on the staining protocol and, then, on the type and the quantity of dyes involved in the experiment. Additionally, counting is time-consuming and is determined by technician's skill.

Several methods have been proposed for eliminating these disadvantages of the manual method by achieving automation. Automated techniques may be roughly divided into two types. The first method consists of recording the images of leukocytes with suitable imaging device and classifying them by custom image processing programs. This method is not an ideal alternative to the manual method because it requires sophisticated equipment which is large and costly [33]. The other approach toward automatic classification and counting of leukocytes is based on a flow system. In this method, after dilution, blood passes through a narrowed detecting area and leukocyte classification is made by analyzing the signal generated by the detector. There are two different techniques that make use of a flow system: flow cytometry and impedance cytometry, which will be discussed thoroughly in the next chapter.

The *flow cytometer* comprises a sheath fluid that permits the blood cells in a sample to flow one by one through a constricted channel, a light source, a photometric unit that detects light issuing from each blood cell, and an analyzer for processing the detected signals [35]. In the figure 1.3 the detecting area of the flow cytometer is schematized. In this method, leukocytes can be classified without the need of labelling. However, white blood cell differentiation may be improved combining the intensity of fluorescent signals, obtained from stained cells, with that of scattered light, collected from each cell. Two kinds of staining

may be used: intracellular staining and cell surface staining. There are a lot of different protocols regarding the *intracellular staining* and some of them comprise steps such as cell fixation and permeabilization. For example, the most common intracellular staining used to classify granulocytes involves the use of peroxidase for identifying eosinophils and neutrophils, esterase for distinguishing monocytes and alcian blue for basophils [19]. The cell *surface staining* involves the use of fluorescent labeled antibodies which bind to antigens present on cell surface. As leukocyte subsets have individual antigenic surface markers, it is possible to differentiate white blood cells using specific labeled antibodies [32].

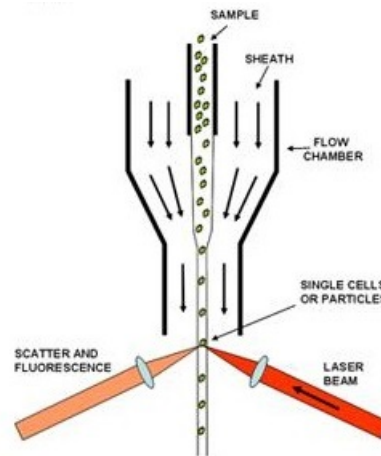


Figure 1.3: Schematic diagram of the detecting area in a conventional flow cytometer (<http://www.andor.com>).

The *impedance cytometry* enables cell differentiation on the base of the dielectric properties of individual cells in a flow format similar to that of a traditional flow cytometer. In this method all red cells have to be lysed so that only leukocytes are permitted to flow through a microchannel and perturb the electrical field generated by electrodes. When each corpuscle passes through the channel a change in electrical impedance occurs and the magnitude of the detected signal is used as a basis for classification of leukocytes [2]. The working principle of microfluidic impedance cytometer is schematized in figure 1.4.

Erythrocytes in the blood sample emit only fluorescence of very low intensity, so if all that is needed is to measure the intensity of fluorescence by flow cytometry, erythrocytes will not interfere with the counting of leukocytes even if coincidence of erythrocytes and leukocytes occurs (i.e., erythrocytes and leuko-

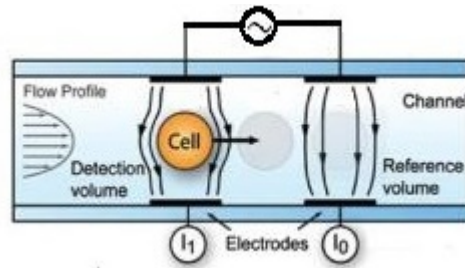


Figure 1.4: Schematic diagram of the working principle of impedance cytometry (<http://www.southampton.ac.uk/cmm/research/Impedance>).

cytes pass through the detecting portion simultaneously) [10].

If WBC differentiation is performed by flow cytometry or impedance cytometry without the use of fluorescent molecules, it is necessary to eliminate the interference due to erythrocytes as their size is comparable to that of leukocytes. Blood sample for leukocyte counting that are free from erythrocytes are commonly prepared by the following methods:

- Lysing of erythrocytes
 - a) Treatment with a surfactant
 - b) Treatment with an ammonium salt
 - c) Hypotonic treatment
 - Separation
 - d) Centrifugation
 - e) Sedimentation
- (a) *Treatment with a surfactant.* This method inhibits subsequent staining and in addition to lysing of erythrocytes, it causes morphological changes in leukocytes such as loss of cytoplasm and membrane swelling, making it difficult to achieve leukocyte differentiation [33].
- (b) *Treatment with an ammonium salt.* It inhibits subsequent staining. In addition, the ammonium salt does not have a great ability to lyse erythrocytes and it takes about 3-5 minutes to achieve complete lysis [33].

- (c) *Hypotonic treatment.* This one makes use of the fact that leukocytes are more resistant than erythrocytes in hypotonic solutions. However, at a physiological pH and under conditions that cause complete lysis of erythrocytes, part of leukocytes can be destroyed. Some methods involve the use of a hypertonic solution after the hypotonic treatment to prevent WBC damage [18].
- (d) *Centrifugation* and (e) *Sedimentation.* Both methods have such disadvantages as lengthy procedures, and high incidence of leukocyte loss and fluctuations in each leukocyte count and ratio [33]. Furthermore, techniques based on centrifugation are not convenient in microfluidics, where small amounts of blood, mostly taken by finger prick, are processed.

Chapter 2

Systems for single cell analysis

Introduction

Cell separation and sorting are essential steps in cell biology research and in many diagnostic and therapeutic methods. Tools such as flow cytometry have allowed scientists and clinicians to quantitatively investigate single-cell characteristics used in distinguishing cell subpopulations [7]. Flow cytometry is the one by one measurement of cells or particles as they flow through an analysis volume. The particle-by-particle analysis has made flow cytometry the primary method to count specific cell populations. Single cell analysis techniques are very suitable to miniaturization and integration in microfluidic devices [31]. Several devices using different operating principles have been developed in microfluidic field for cell differentiation and counting. The analysis and sorting of particles have several highly interrelated steps, which include sample preparation, delivery, analysis, and sorting [7]. After a brief introduction to the sample preparation step, flow cytometry and impedance spectroscopy techniques will be described in detail. Flow cytometry is a technology that simultaneously measures and then analyzes multiple physical characteristics of single particles, usually cells, as they flow in a fluid stream through a beam of light. The properties measured include particles' relative size, internal complexity, and relative fluorescence intensity. These characteristics are determined using an optical-to-electronic coupling system that records how the cell or particle scatters incident laser light and emits fluorescence[32]. Impedance spectroscopy (IS) represents a powerful label-free method for cell analysis. The technique allows quantitative

measurement of the inherent electrical and dielectric properties of cells, which directly reflect the cell's biological structure and metabolic state. These properties are detected studying the perturbation of the electrical field applied to a channel when the cell or the particle passes through it. Specifically, the microfluidic impedance cytometer, developed in the laboratory for hybrid biodevices, at the University of Southampton, consists of two pairs of micro-electrodes fabricated within a micro-channel connected to an electrical system. It was demonstrated that it can differentiate between the three main populations of leukocytes [21]. The simplicity and portability of the microfluidic impedance chip enable applications in point-of-care diagnostic systems, which have the potential to decrease analysis costs and enable fast treatment of patients. Precisely, it has been integrated into a cartridge, that performs semi automatically the blood sample preparation in order to enhance WBC differentiation. It will be showed in the next chapter.

2.1 Sample preparation for improving WBC detection in single cell analysis

The sample preparation step concerns the optimization of particle concentration and the sample washing [31]. The particle concentration optimization in flow cytometry is performed to avoid coincidences in the detecting area, or rather to ensure that particles are detected one by one. Specifically, for WBC analysis it is necessary to dilute the whole blood sample and lyse erythrocytes, that outnumber leukocytes by a factor of 1:1000 [41]. The most common approach to lyse RBCs and to prevent their interferences with WBCs concerns the use of specific solutions. The solutions, used for RBC lysis, dilute the blood sample, so that WBC concentration is reduced and coincidence of events in the analysis volume is limited. The WBC concentration may be further adjusted via dilution and RBC debris may be removed using wash steps. One of the most effective lysis methods consists of two solutions: lysis and quench solutions. The first one that has low pH and osmolality is selective toward erythrocytes, and the quench solution (alkaline salt solution) that has high pH and osmolality retards the lytic effect in order to prevent leukocyte damage. This lysis protocol has the advantage to preserve the chemical balance of the leukocytes, as chemical changes in the physiological environment of the leukocyte population can alter

the immunochemical response of the leukocyte surface markers [18]. In the figure 2.1 the RBC lysis protocol is schematized but it will be described accurately in the chapter of experimental details.

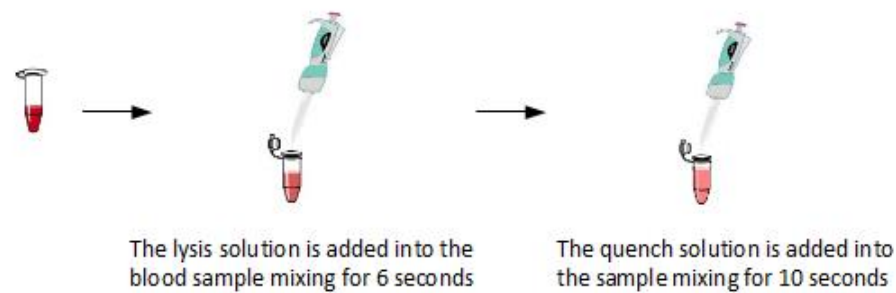


Figure 2.1: Scheme of the lysis protocol used in the experimental work.

The lysis solution is added into a small volume of blood in the quantity $12 \mu\text{L}$ per $1 \mu\text{L}$ of whole blood mixing the sample by pipettes at room temperature for 6 seconds. After that, the quench solution is added in the quantity $5.3 \mu\text{L}$ per $1 \mu\text{L}$ of blood mixing for 10 seconds [18]. In this way the blood is diluted about 20 times, and as $1 \mu\text{L}$ of whole blood contains about 6000 cells, after performing the protocol, in $1 \mu\text{L}$ of solution there are about 300 cells. That concentration avoids the coincidence of events during WBC acquisition by flow and impedance cytometry.

Conventionally, RBC lysis and blood dilution are performed by pipettes but recently these processes have been automated by microfluidic platform technologies. In the laboratory of hybrid biodevices (at the University of Southampton) different microfluidic systems that perform RBC lysis have been developed. They were integrated into the microfluidic impedance cytometer, that is capable to detect blood cells. Cees van Berkel et al. developed a microfluidic platform that performs the sample preparation for 3-part leukocyte count, together with erythrocytes and thrombocytes. The microfluidic sample preparation block is shown in figure 2.2 and performs sample loading, RBC lysis and dilution in two separate fluid channels followed by impedance analyses. The upper block is involved in the pre-processing related to WBC differentiation and hemoglobin concentration detection; the bottom block performs sample dilution to detect erythrocytes and platelet, that make up the 99% of the all formed elements [41]. The dilution of the sample permits that most particles pass through the detect-

ing area separately in order to avoid overlapping events. The WBC differentiation and count performed by the integrated microfluidic system is comparable to that obtained by impedance cytometry after manual RBC lysis, except that the RBC fragment content is higher [41].

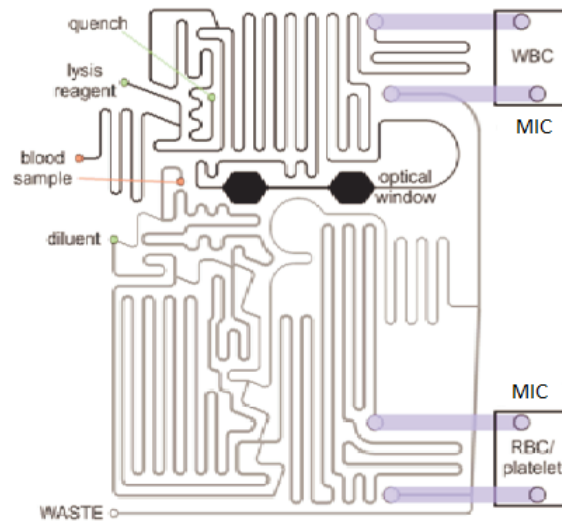


Figure 2.2: CAD drawing of the microfluidic platform for FBC [41].

The same type of design was used for the development of an integrated microfluidic system that performs only WBC analysis. The schematic 3-part system is shown in figure 2.3. The microfluidic platform consists of micro-channels having different size so that the two solutions are mixed by diffusion with the blood sample for different times. Because of the different channel length and the different mixing times the blood, the lysis solution and the quench solution are pushed by syringe pumps at different flow rates [11]. The lysate flows into the microfluidic impedance cytometer and the resulting current signals from leukocytes are processed by a custom electronic circuit. The RBC lysis from the microfluidic platform is comparable with that performed manually although the data shows a high RBC fragment content. This is due to the passive mixing (by diffusion) that limits the contact area between the blood and the two solutions. Furthermore the total leukocyte count is lower than that obtained by a traditional hematology analyzer because of the cell sedimentation in the syringe pump. The cell sedimentation occurs because of the low flow rate and the long fluidic channels [11]. The microfluidic platform involved in the lysis process

consists of long channels since the two solutions increase the blood volume by a factor of 20.

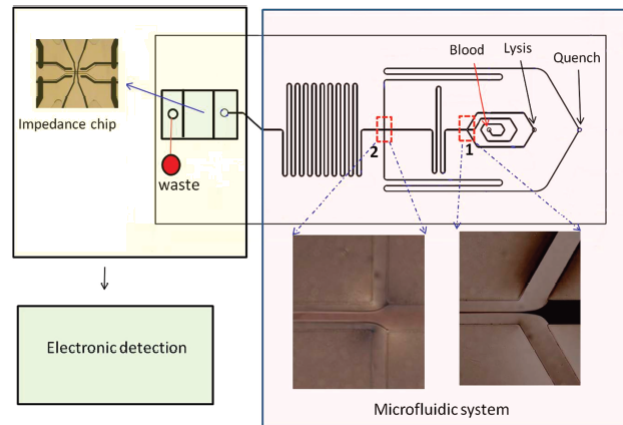


Figure 2.3: Schematic diagram of the integrated microfluidic leukocyte analysis system [11].

These results confirm that microfluidic systems are not entirely suitable for RBC lysis and led to the development of new platforms having larger fluidic channels and active mixers that make the lysis process faster. In the experimental work a new integrated cartridge with active components was used for WBC count. It overcomes some of the limits associated with the passive mixing except that in the leukocyte differentiation the RBC fragment content is higher. However, in this work, the WBC differentiation by the integrated system was improved by optimising the lysis protocol.

2.2 Flow cytometry

Flow cytometry is a technology that enables differentiation of cells (or particles), on the base of their size, complexity and fluorescence, through side and forward scatter light, produced and collected when a laser beam is directed onto the stream of the sample.[35] The forward scatter light increases linearly with the dimension of the cell and the side scatter light increases linearly with the complexity of the cell. The fluorescence is detected, after exciting the cell by wavelengths within its absorption spectrum, through the emitted wavelengths, which are longer than those absorbed because part of the energy is consumed

during absorption. A flow cytometer is made up of three main systems: fluidics, optics, and electronics. The fluidics system transports particles in a stream to the laser beam for interrogation. The optics system consists of lasers to illuminate the particles in the sample stream and optical filters to direct the resulting light signals to the appropriate detectors [25]. The electronics system converts the detected light signals into electronic signals that can be processed by the computer. The three principal components of the flow cytometer are illustrated in figure 2.4.

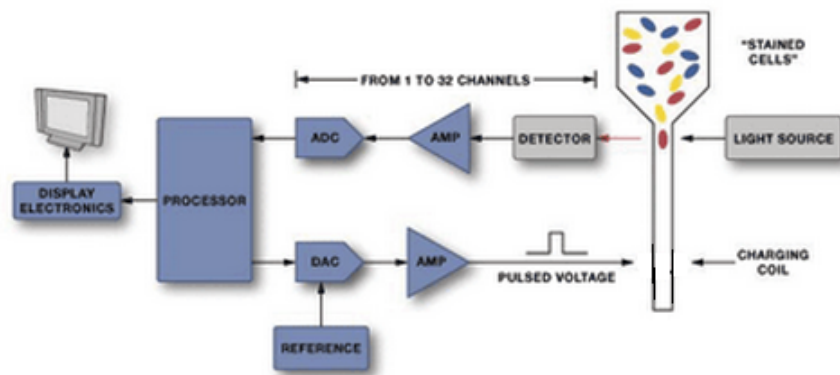


Figure 2.4: Schematics of a flow cytometer (www.electronicproducts.com).

In the flow cytometer, particles are carried to the laser intercept in a fluid stream. Any suspended particle or cell from 0.2–150 micrometers in size is suitable for analysis. The portion of the fluid stream where particles are located is called the sample core [35]. When particles pass through the laser intercept, they scatter laser light. Any fluorescent molecules present on the particle fluoresce. The scattered and fluorescent light is collected by appropriately positioned lenses. A combination of beam splitters and filters steers the scattered and fluorescent light to the appropriate detectors [32]. The detectors produce electronic signals proportional to the optical signals striking them. The characteristics or parameters of each event are based on its light scattering and fluorescent properties. The data is collected and stored in the computer. This data can be analyzed to provide information about subpopulations within the sample. A scheme of data acquisition is shown in figure 2.5.

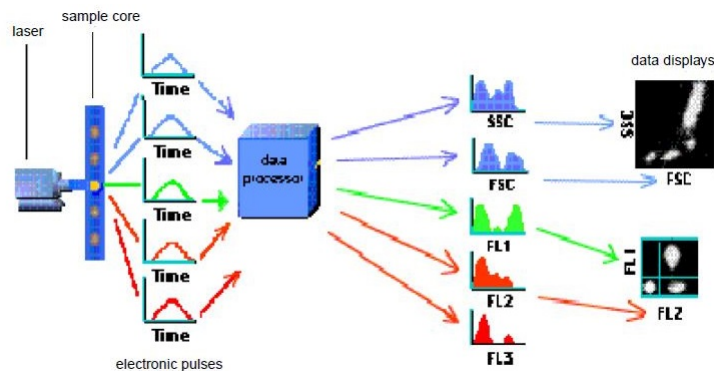


Figure 2.5: Schematic diagram of data acquisition in a flow cytometer (from 'Introduction to Flow Cytometry: A Learning Guide').

2.2.1 Fluidics system

The purpose of the *fluidics system* is to transport particles in a fluid stream to the laser beam for interrogation. For optimal illumination, the stream transporting the particles should be positioned in the center of the laser beam. In addition, only one cell or particle should move through the laser beam at a given moment. To accomplish this, the sample is injected into a stream of sheath fluid within the flow chamber. The flow of sheath fluid accelerates the particles and restricts them to the center of the sample core where the laser beam then interact with them [4]. This process is known as *hydrodynamic focusing* and is illustrated in figure 2.6.

The sample pressure and the sheath fluid pressure are different from each other. The sample pressure is always larger than the sheath fluid pressure. The sample pressure regulator controls the sample flow rate by changing the sample pressure relative to the sheath fluid. Increasing the sample pressure increases the flow rate by increasing the width of the sample core. Furthermore, this allows more cells to enter the stream within a given moment. With a wider sample core, some cells could pass through the laser beam off-center and intercept the laser beam at a less optimal angle [25].

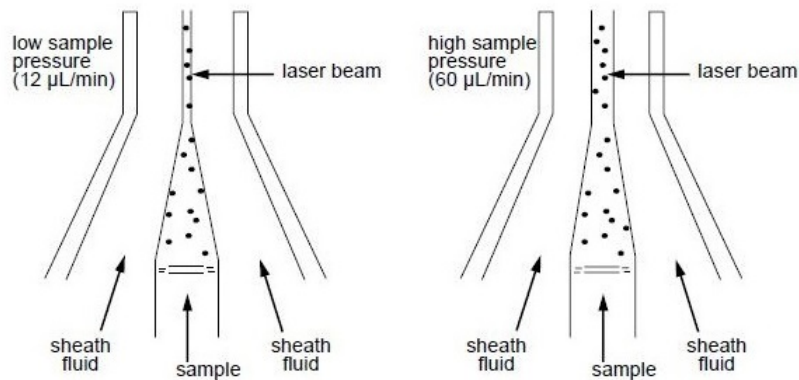


Figure 2.6: Hydrodynamic focusing of the sample within the flow chamber (from 'Introduction to Flow Cytometry: A Learning Guide').

2.2.2 Optical system

When a cell or particle passes through the laser light, deflects incident laser light and light scattering occurs. The extent to which this occurs depends on the physical properties of a particle, mainly its size and internal complexity. Factors that affect light scattering are cell shape, surface topography, cell membrane, nucleus and any granular material inside the cell [35]. *Forward-scattered light* (FSC), which is proportional to cell size, is a measurement of mostly diffracted light and is detected along the axis of the incident laser beam in the forward direction by a photodiode [35]. *Side-scattered light* (SSC), which is proportional to cell granularity or internal complexity, is a measurement of mostly refracted and reflected light that occurs at any interface within the cell where there is a change in refractive index [35]. SSC is collected at approximately 90 degrees to the laser beam by a collection lens and then redirected by a beam splitter to the appropriate detector [32]. Correlated measurements of FSC and SSC allow differentiation of cell types in heterogeneous cell population. As illustrated in figure 2.7, the three major leukocyte subpopulations can be differentiated using FSC and SSC.

Further subsets of leukocytes can be identified, on the base of their individual antigenic surface markers, by using fluorescent labeled antibodies. In a mixed population of cells, different fluorochromes can be used to distinguish separate subpopulations. The staining pattern of each subpopulation, combined with

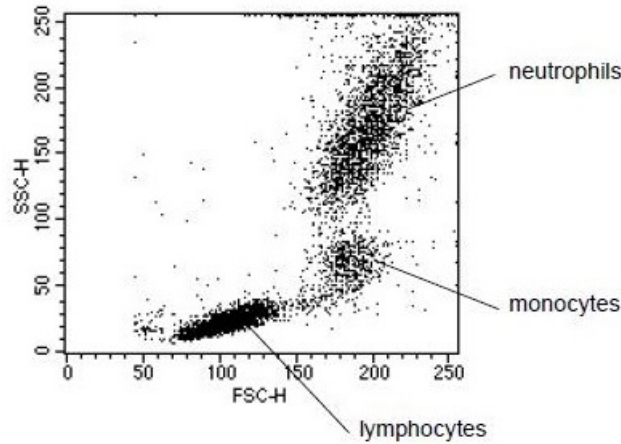


Figure 2.7: Leukocytes clusters of lysed whole blood in the scatter plot SSC vs FSC.[25]

FSC and SSC data, can be used to identify which cells are present in a sample and to count their relative percentages. An example is shown in figure 2.8.

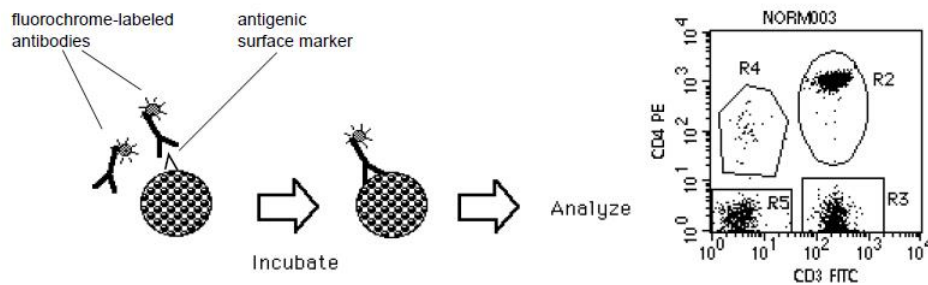


Figure 2.8: Schematic illustration of antibody staining and scatter plot of CD3 FITC/CD4 PE.[25]

The amount of fluorescent signal detected is proportional to the number of fluorochrome molecules on the cell and then to the number of antibodies bound to the cell. The range over which a fluorescent compound can be excited is termed its absorption spectrum. The range of emitted wavelength, which are longer than those absorbed, is termed its emission spectrum. Emission wavelengths, that are far enough from each other, are detected by separate detectors [25].

The *optical system* is composed of photomultiplier tubes (PMTs), photodiode, mirrors and optical filters. PMTs detect SSC and fluorescence signals, which are often weak [35]. The specificity of a detector for a particular fluorescent dye is optimized by placing a filter in front of the PMT, which allows only a narrow range of wavelengths to reach the detector. This spectral band of light is close to the emission peak of the fluorescent dye. Such filters are called band-pass filters. Beam splitters are devices that direct light of different wavelengths in different directions. Dichroic mirrors are a type of beam splitter and transmit specific wavelengths of light and reflect longer wavelengths [25]. Emitted FSC signals are stronger than SSC and fluorescence signals; therefore they are collected by a photodiode, which is less sensitive to light signals than the PMTs [35]. In the figure 2.9 the optical system is schematized.

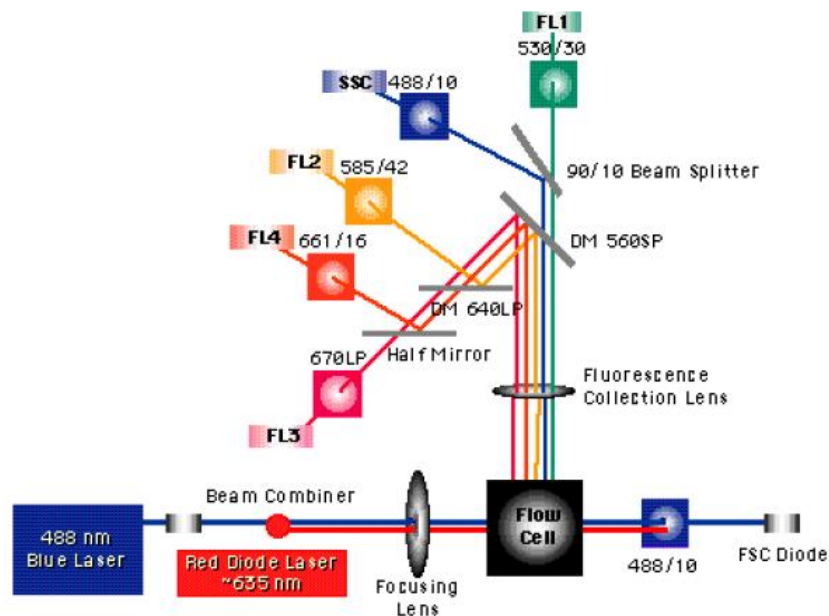


Figure 2.9: Schematic diagram of the optical system (from 'Introduction to Flow Cytometry: A Learning Guide').

2.2.3 Optical-to-electronic coupling system

The photodetectors, such as PMTs and the photodiode, convert light signals into *voltage signals*. A voltage pulse is created when a particle enters the laser

beam and starts to scatter light or fluorescence. Once the light signals, or photons, strike one side of the PMT or the photodiode, they are converted into a proportional number of electrons that are multiplied, creating a greater electrical current. The electrical current travels to the amplifier and is converted to a voltage pulse. The highest point of the pulse occurs when the particle is in the center of the beam and the maximum amount of scatter or fluorescence is achieved [32]. As the particle leaves the beam, the pulse comes back down to the baseline, as shown in figure 2.10.

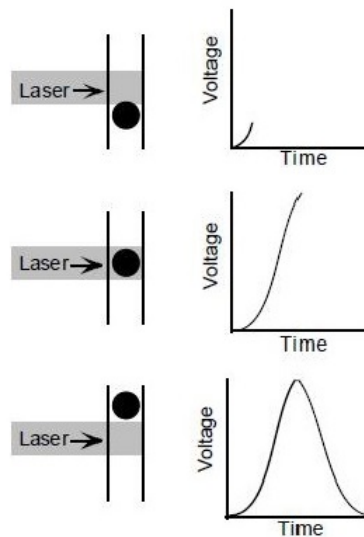


Figure 2.10: Conversion of a light signal into a voltage pulse (from 'Introduction to Flow Cytometry: A Learning Guide').

Signals can be amplified by applying a voltage to the PMTs, thus creating a greater electrical current, or by increasing the amplification gain [25]. The voltage pulse is assigned a digital value by the Analog-to-Digital Converter. The channel number is transferred to the computer and the light signal is then displayed in an appropriate position on the data plot. An electronic threshold can be used to limit the number of events that the flow cytometer acquires. When a threshold value is defined, only signals with an intensity greater than or equal to the threshold channel value will be processed and sent to the computer [35].

2.3 Impedance cytometry

After red blood cell lysis, white blood cell differentiation can be also performed by microfluidic single cell impedance systems which are portable and cheaper than optical devices. The impedance cytometry allows quantitative measurement of the inherent electrical and dielectric properties of cells; such as membrane capacitance and cytoplasmic conductivity and permittivity [5]. In the follow paragraphs the physical fundamentals, which represent the theoretical basis of impedance cytometry, are defined. In particular, then, it is described the microfluidic impedance chip used for WBC differentiation and counting in the experimental work.

2.3.1 Dielectric cell characterisation

The electrical properties of tissues and cell suspension are important in the measurement of physiological parameters using impedance techniques, studies of biological effects of electromagnetic fields, electrocardiography, muscle contraction, and nerve transmission [34]. In particular, biological dielectric studies are allowed to characterize different types of cells. The recent years have seen the development of computer-controlled instrumentation for precise and rapid measurements of dielectric properties of particles and cells. It has been possible to analyze effects of cellular structure on the dielectric properties of tissues using the coupling between externally applied electromagnetic fields and intracellular compartments, including membranes [30]. Thus specific theories have been developed to explain the dielectric features of cells. In this paragraph, after describing the polarization of materials, specific theories and models are discussed for characterizing the behavior of cells in suspension when an electrical field is applied. The structure of cells is simplified using the single shell model so that the Maxwell's theory for concentrated suspensions can be implemented.

2.3.1.1 Polarization

Electric polarization may be defined as the electric field induced disturbance of the charge distribution in a region. Dielectrics are materials which have no free charges; all electrons are bound and associated with the nearest atoms. An external electric field causes a small separation of the electron cloud and

the positive ion core so that each infinitesimal element of volume behaves as an electric dipole [29]. Dielectrics may be subdivided into two groups : non polar and polar. The polar dielectrics differ from the other ones because their molecules possess a permanent dipole moment which is ordinarily oriented but it changes orientation after the application of an external electrical field. The induced dipole field opposes the applied field [8]. In the figure 2.11 the volume element could represent an atom, a molecule, or a small region.

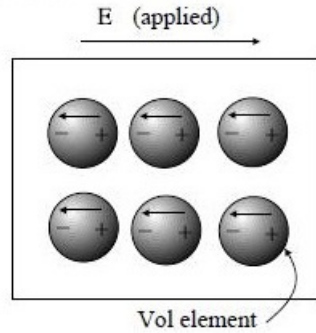


Figure 2.11: Dipolar orientation when an external electrical field is applied.

The type of polarization may be additionally subdivided into the following categories: *electronic* when there is a displacement of the electronic cloud around the nucleus, *ionic* when positive ions are separated from negative ones in the crystal, *orientational* when permanent dipoles (molecules) are aligned, *space-charge* when free electrons are present, but are prevented from moving by barriers such as grain boundaries [30]. In a dielectric material the presence of an electric field E causes the bound charges in the material (atomic nuclei and their electrons) to slightly separate, inducing a local electric dipole moment. The *electric polarization* P is the dipole moment per unit volume at a given point. It represents the average dipole moment p of N particles included in an infinitesimal volume dV [29]. The mathematical expression is:

$$P = \lim_{\Delta V \rightarrow 0} \frac{\Delta N}{\Delta V} \langle p \rangle = \lim_{\Delta V \rightarrow 0} \frac{\sum_{i=1}^{\Delta N} p_i}{\Delta V} \quad (2.1)$$

In dielectric materials the polarization is described by the *surface density of bound charges* σ_b and the *volume density of bound charges* ρ_b which can be written as a function of the electric polarization:

$$\sigma_b = P \cdot n \quad (2.2)$$

$$\rho_b = -\nabla \cdot P \quad (2.3)$$

P is a vector field whose divergence yields the density of bound charges ρ_b in the material. The electric field satisfies the first Maxwell equation:

$$\nabla \cdot E = \frac{1}{\epsilon_0}(\rho_f + \rho_b) = \frac{1}{\epsilon_0}(\rho_f - \nabla \cdot P) \quad (2.4)$$

where ρ_f is the *volume density of free charges* and hence:

$$\nabla \cdot (\epsilon_0 E + P) = \rho_f \quad (2.5)$$

The argument of the differential operator is the *displacement field* D that is defined as:

$$D = \epsilon_0 E + P \quad (2.6)$$

where ϵ_0 is the vacuum permittivity, also called permittivity of free space. The displacement field therefore satisfies Gauss's law in a dielectric:

$$\nabla \cdot D = \rho - \rho_b = \rho_f \quad (2.7)$$

In a linear, homogeneous, isotropic dielectric with instantaneous response to changes in the electric field, P depends linearly on the electric field:

$$P = \epsilon_0 \chi E \quad (2.8)$$

where the constant of proportionality χ is called the *electric susceptibility* of the material. Thus:

$$D = \epsilon_0(1 + \chi)E = \epsilon E \quad (2.9)$$

where $\epsilon = \epsilon_0 \epsilon_r$ is the permittivity, and $\epsilon_r = 1 + \chi$ the relative permittivity of the material. In linear, homogeneous, isotropic media, ϵ is a constant. In nonlinear materials it may depend on the electric field and have a time dependent response. Explicit time dependence can arise if the materials are physically moving or changing in time. A different form of time dependence can arise in a time-invariant medium, in that there can be a time delay between the imposition of the electric field and the resulting polarization of the material. In this case, P is a convolution of the impulse response susceptibility χ and the electric

field E [8]. The convolution takes on a simpler form in the frequency domain by Fourier transforming the relationship and applying the convolution theorem. The following relation is obtained for a linear time-invariant medium:

$$D(\omega) = \varepsilon(\omega)E(\omega) \quad (2.10)$$

where ω is frequency of the applied field.

2.3.1.2 Complex permittivity in dielectric-conductive material and dielectric spectroscopy

Assume to have a parallel plate capacitor, of plate area A and separation d , which contains a dielectric material, as illustrated in the figure 2.12.

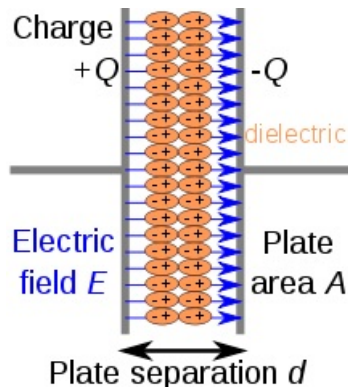


Figure 2.12: Equivalent circuit of an idealized parallel-plate capacitor filled with a dielectric material (wikipedia.org/wiki/Dielectric).

Initially, let the region between the plates be a vacuum. A constant voltage difference V between the plates will induce a charge density D given by:

$$D = \varepsilon_0 \frac{V}{d} \quad (2.11)$$

where ε_0 is the vacuum permittivity ($8.85 \cdot 10^{12}$ F/m). The capacitance C is the ratio of the total induced charge on the plates to the applied voltage:

$$C = \varepsilon_0 \frac{A}{d} \quad (2.12)$$

If a dielectric is introduced between the plates, an additional charge density P is induced on the plates from the polarization of charges within the material. The new charge density is defined in the equations 2.6 and 2.9. And the capacitance can be written:

$$C = \epsilon_0 \epsilon_r \frac{A}{d} \quad (2.13)$$

In this way it was demonstrated that when a dielectric material is introduced between the plates of a capacitor, the capacitance increases because the charge density enhances [34].

Assume that the material between the plates has a conductivity σ , besides a relative permittivity ϵ_r . In this case the material can be schematized as a conductance G in parallel with the capacitance. G is the inverse ratio of the resistance and is defined as:

$$G = \sigma \frac{A}{d} \quad (2.14)$$

The equivalent circuit is shown in the figure 2.13.

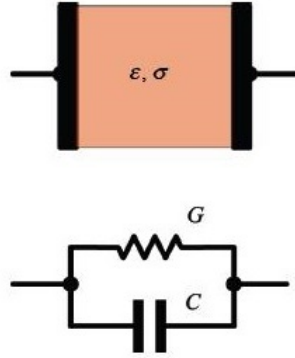


Figure 2.13: Equivalent circuit of an idealized parallel-plate capacitor filled with material of relative permittivity ϵ and conductivity σ .

If relaxation processes are present, the response of the material to a voltage step is a function of time [8]. For this circuit the time constant τ is:

$$\tau = \frac{C}{G} = \frac{\epsilon}{\sigma} \quad (2.15)$$

Then, the corresponding response to a sinusoidal field is characterized by dielectric properties that vary with frequency. For sinusoidal fields, at circular frequency ω the complex impedance Z^* can be written:

$$Z^* = R + \frac{1}{j\omega C} = \frac{d}{A} \frac{1}{\sigma + j\omega\epsilon} \quad (2.16)$$

From which is defined the complex conductivity σ^* of the material:

$$\sigma^* = \sigma + j\omega\epsilon \quad (2.17)$$

The complex conductivity and permittivity are related by:

$$\sigma^* = j\omega\epsilon^* \quad (2.18)$$

The complex relative permittivity ϵ^* is defined as:

$$\epsilon^* = \epsilon - j\frac{\sigma}{\omega} = \epsilon' - j\epsilon'' \quad (2.19)$$

where ϵ' is the real part of the permittivity, which is related to the stored energy within the medium;

ϵ'' is the imaginary part of the permittivity, which is related to the dissipation or loss of energy within the medium;

The series equivalent impedance Z^* can be rewritten:

$$Z^* = \frac{d}{A} \frac{1}{\sigma^*} = \frac{d}{A} \frac{1}{j\omega\epsilon^*} \quad (2.20)$$

The response of a material to a voltage step involves the physical displacement of charge, whose kinetics determine the frequency dependence of the bulk properties. Typically, relaxational effects are described by first order differential equations that lead to single time constant responses [34]. Moreover, in biological materials, several relaxation processes may occur in parallel, and the total response of the material might be characterized by several time constants [30].

Debye relaxation is the dielectric relaxation response of an ideal, non-interacting population of dipoles to an alternating external electric field. The dielectric response of a first order system in the frequency domain can be obtained by Laplace transformation:

$$\epsilon^* = \epsilon_\infty + \frac{\epsilon_s - \epsilon_\infty}{1 + j\omega\tau} \quad (2.21)$$

Where ϵ_{inf} refers to the permittivity at infinite frequencies due to electronic polarizability, ϵ_s is the static, low frequency permittivity, and is the characteristic relaxation time τ of the medium. The equation does not include the possible existence of currents at infinite time, the model can be expanded including a static conductivity σ_s :

$$\epsilon^* = \epsilon_\infty + \frac{\epsilon_s - \epsilon_\infty}{1 + j\omega\tau} - \frac{\sigma_s}{\omega\tau} \quad (2.22)$$

Separating the equation into real and imaginary parts yields:

$$\begin{aligned}\epsilon^* &= \epsilon' - j\epsilon'' \\ \epsilon' &= \epsilon_\infty + \frac{\epsilon_s - \epsilon_\infty}{1 + (\omega\tau)^2} \\ \epsilon'' &= \frac{\sigma_s}{\omega\epsilon_0} + \frac{(\epsilon_s - \epsilon_\infty)\omega\tau}{1 + (\omega\tau)^2} \\ \sigma &= \sigma_s + \frac{(\sigma_\infty - \sigma_s)(\omega\tau)^2}{1 + (\omega\tau)^2}\end{aligned}\quad (2.23)$$

In which the limit values are interrelated by:

$$\frac{(\epsilon_s - \epsilon_\infty)\epsilon_0}{\tau} = \sigma_\infty - \sigma_s \quad (2.24)$$

The figure 2.14 shows the variation in the real and imaginary parts of the complex permittivity with frequency for a single time constant relaxation.

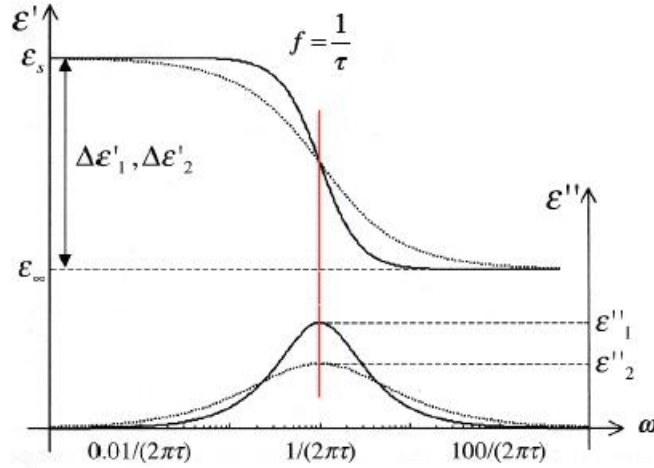


Figure 2.14: Single time constant relaxation. At the top relative permittivity vs frequency; at the bottom conductivity vs frequency (From 'Transduction - Ionics' of Nanotechnology course).

The maximum dissipation of energy in the medium is in correspondence of the frequency of relaxation, when the value of permittivity is intermediate between ϵ_s and ϵ_{inf} [30]. Dielectric relaxation behavior can be conveniently plotted on the complex plane, such as in the Cole–Cole diagram in figure 2.15.

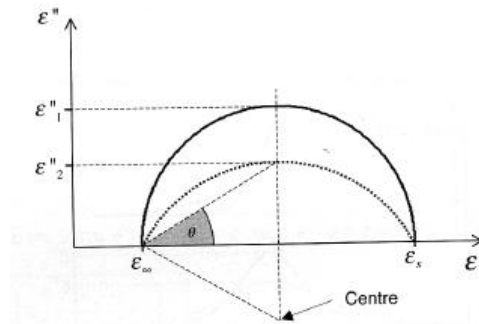


Figure 2.15: Cole-Cole diagram for a single relaxation time (From 'Transduction - Ionics' of Nanotechnology course).

A plot of ϵ'' vs ϵ' produces a semicircle for single time constant relaxation. The center of the semicircle is on the real axis at the point $(\epsilon_s + \epsilon_{in})/2$ and its apex occurs where $\omega = 2\pi f_c$. If a distribution of relaxation times is present, the corresponding plot in the complex permittivity may resemble semicircular arcs with centers below the real axis [34].

Hence *dielectric spectroscopy* or *impedance spectroscopy* measures the dielectric properties of a medium as a function of frequency. It is also an experimental method of characterizing electrochemical systems and cell suspension [22]. In the figure 2.16 a dielectric permittivity spectrum over a wide range of frequencies is illustrated.

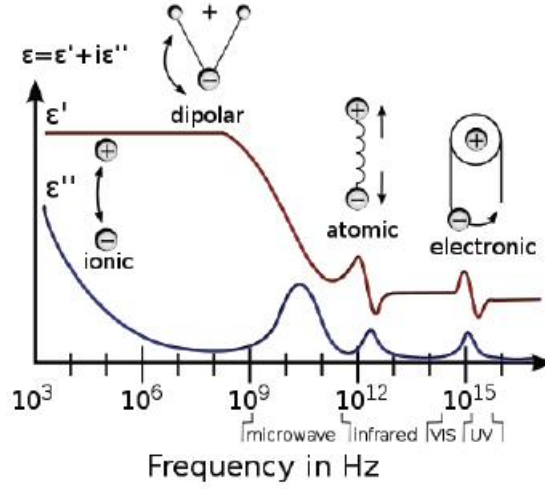


Figure 2.16: A dielectric permittivity spectrum over a wide range of frequencies (wikipedia.org/Dielectric_spectroscopy). The real and imaginary parts of permittivity are shown, and various processes are depicted: ionic and dipolar relaxation, and atomic and electronic resonances at higher energies.

The dipolar relaxation occurs at microwave frequencies, while atomic and electronic ones occur at higher frequencies.

2.3.1.3 Maxwell's mixture theory

Maxwell derived an analytical solution for the permittivity of a dilute suspension of non-interacting spherical particles. The equivalent complex permittivity of the mixture is dependent on the electrical properties of the mixture components and their geometry. It is calculated considering the induced dipole moment of the particles in a spherical region of the suspension [39]. The electrical polarization of the suspension is:

$$p_{susp}^* = N_{part} p_{part}^* \quad (2.25)$$

The induced dipole for a particle with complex permittivity ϵ_2^* in a suspending medium with complex permittivity ϵ_1^* and applied field E_0^* is defined as:

$$p_{part}^* = 4\pi\epsilon_1 \left(\frac{\epsilon_2^* - \epsilon_1^*}{\epsilon_2^* + 2\epsilon_1^*} \right) a^3 E_0^* \quad (2.26)$$

As the total dipole within the spherical region of suspension is the sum of the N part individual particle dipoles:

$$p_{susp}^* = N_{part} 4\pi\epsilon_1 \left(\frac{\epsilon_2^* - \epsilon_1^*}{\epsilon_2^* + 2\epsilon_1^*} \right) a^3 E_0^* \quad (2.27)$$

We can also write this dipole as if the region of suspension was a larger particle with effective suspension permittivity ϵ_{eff}^* :

$$p_{susp}^* = 4\pi\epsilon_1 \left(\frac{\epsilon_{eff}^* - \epsilon_1^*}{\epsilon_{eff}^* + 2\epsilon_1^*} \right) R^3 E_0^* \quad (2.28)$$

As schematized in figure 2.17, R_0 is the radius of the spherical region.

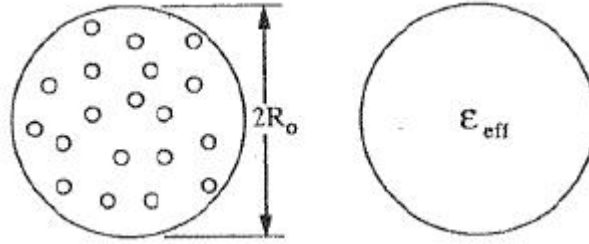


Figure 2.17: Schematic of N particles in a spherical region.

Set the previous two expressions equal to each other, and note that the volume fraction of the particles is $\varphi = N_{part}^* \frac{a^3}{R_0^3}$:

$$\frac{\epsilon_{eff}^* - \epsilon_1^*}{\epsilon_{eff}^* + 2\epsilon_1^*} = \varphi \frac{\epsilon_2^* - \epsilon_1^*}{\epsilon_2^* + 2\epsilon_1^*}$$

Solving for the *equivalent complex permittivity of the mixture* $\epsilon_{mix}^* = \epsilon_{eff}^*/\epsilon_1^*$ it is obtained the equation:

$$\tilde{\epsilon}_{mix} = \tilde{\epsilon}_m \frac{1 + 2\Phi f_{CM}}{1 - \Phi f_{CM}} \quad (2.29)$$

Where f_{CM} is the Clausius Mossotti factor:

$$f_{CM} = \frac{\tilde{\epsilon}_p - \tilde{\epsilon}_m}{\tilde{\epsilon}_p + 2\tilde{\epsilon}_m} \quad (2.30)$$

and ϵ_m and ϵ_p are the complex permittivity of the suspending medium and particle respectively. Φ is the volume fraction, the ratio of the volume of the particles to the detection volume [39].

2.3.1.4 Electrical double layer

When a metallic conductive electrode is brought in contact with a liquid electrolyte, a common interface among the two phases appears. The electrode-electrolyte interface is called double layer. The electrical properties of such a layer are important, since they significantly affect the electrochemical measurements [1]. In an electrical circuit used to measure the current that flows at a particular working electrode, the double layer can be viewed as a capacitor C_{DL} . The double-layer structure and its capacity depend on several parameters such as: electrode material, type of solvent, type of supporting electrolyte, extent of specific adsorption of ions and molecules, and temperature [28]. An imposition of a potential from an external source to a metallic electrode results in two layers of polarized ions. One layer of ions is in the surface lattice structure of the electrode. The other layer, with opposite polarity, originates from dissolved and solvated ions distributed in the electrolyte and has moved in direction of the polarized electrode. These two layers of polarized ions are separated by a monolayer of solvent molecules [16]. The molecular monolayer forms the *inner Helmholtz plane* (IHP), as shown in figure 2.18. It adheres by physical adsorption on the surface of the electrode and separates the oppositely polarized ions from each other, becoming a molecular dielectric. The forces that cause the adhesion are not chemical bonds but physical forces applied by polarized solvated ions. The *outer Helmholtz plane* (OHP) defines the area in which the dissolved and solvated ions have opposite polarity. The *stern layer* include the two Helmholtz planes. The diffusion layer is represented by free molecules in the solution [28].

The inner Helmholtz plane is 0.2 nm long. In correspondence of it the potential increases because of adsorbed ions and because solvated molecules cannot polarise. That means the dielectric constant is low [28].

The outer Helmholtz plane is 0.7 nm long and include dissolved and solvated molecules which have opposite polarity and then make the potential decrease linearly [28].

In the diffusion layer the potential decreases exponentially because of free molecules which increase with the distance from the electrode.

The *debye length* determinates the distance at which the solution is affected by the electrode. In an electrolyte or a colloidal suspension, the Debye length is usually denoted with symbol κ^{-1} (or λ_D) and is defined as:

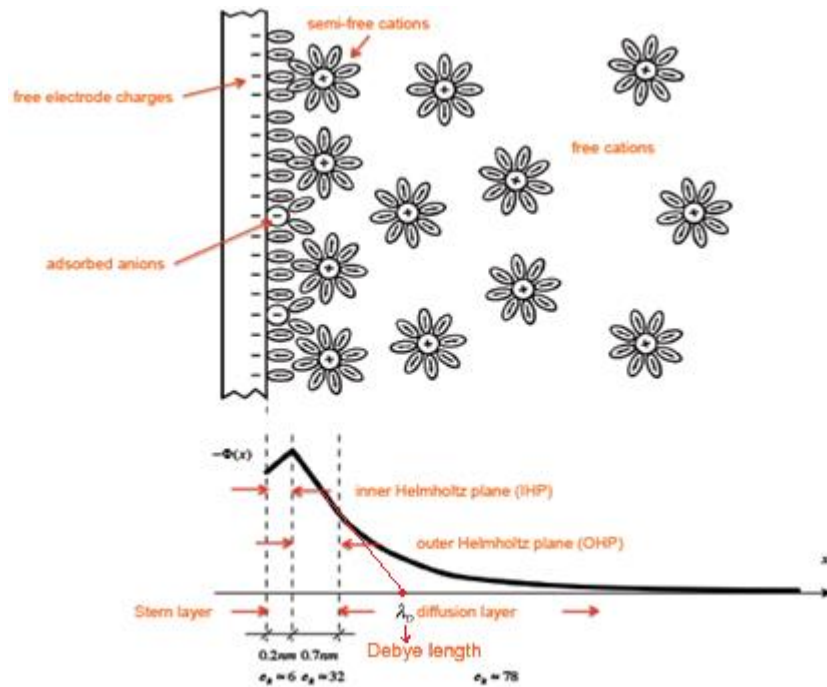


Figure 2.18: Electrical double layer when a negative electrode is in contact with a water solvent (From 'Transduction - Ionics' of Nanotechnology course).

$$\kappa^{-1} = \sqrt{\frac{\epsilon_0 \epsilon_r k_B T}{2 N_A e^2 I}} \quad (2.31)$$

where

I is the ionic strength of the electrolyte, and here the unit should be mole/ m^3 .

ϵ_0 is the permittivity of free space,

ϵ_r is the dielectric constant,

k_B is the Boltzmann constant,

T is the absolute temperature in kelvins,

e is the elementary charge,

N_A is the Avogadro number.

It is possible to schematise the electrical double layer with two capacitances, one relative to the stern layer, calculated as the series of the capacitances in the Helmholtz planes, and the other one relative to the diffusive layer [1]. The scheme is shown in figure 2.19.

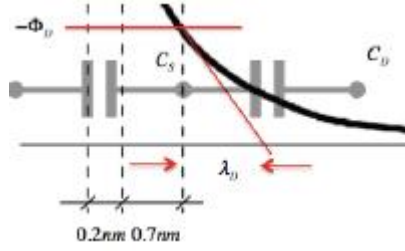


Figure 2.19: Equivalent capacitances of the stern layer and the diffusive layer.

From the debye length the capacitance of the diffusive layer can be calculated with the formula:

$$C_D = \epsilon \kappa \equiv \left[\frac{F}{m^2} \right] \quad (2.32)$$

The expression is intuitive, since the capacitance is inversely proportional to the debye length. The specific capacitance of the stern layer is defined as:

$$C_S = \frac{\epsilon}{d} \equiv \left[\frac{F}{m^2} \right] \quad (2.33)$$

where d is the length of the stern layer. Thus the *double layer capacitance* C_{DL} is given by:

$$\frac{1}{C_{DL}} = \frac{1}{C_D} + \frac{1}{C_{S1}} + \frac{1}{C_{S2}} \quad (2.34)$$

2.3.1.5 Single shell model

This Maxwell model is based on the assumption that the particles are solid homogeneous objects [39]. It can be extended to the case of a biological cell using the shell model, which treats the particle as a homogeneous object surrounded by a thin membrane [3]. The *single shell model* is schematized in figure 2.20.

Models for effective permittivity of cell suspensions provide insight into composition and morphology of cell suspensions: cell concentration, membrane capacitance, cytoplasm conductivity. For a cell suspension ϵ_p is given by:

$$\tilde{\epsilon}_p = \tilde{\epsilon}_{mem} \frac{\left(\frac{R}{R-d} \right)^3 + 2 \left(\frac{\tilde{\epsilon}_i - \tilde{\epsilon}_{mem}}{\tilde{\epsilon}_i + 2\tilde{\epsilon}_{mem}} \right)}{\left(\frac{R}{R-d} \right)^3 - \left(\frac{\tilde{\epsilon}_i - \tilde{\epsilon}_{mem}}{\tilde{\epsilon}_i + 2\tilde{\epsilon}_{mem}} \right)} \quad (2.35)$$

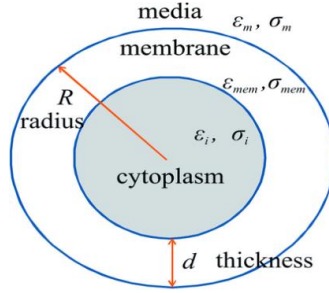


Figure 2.20: Single shell model of a cell [3].

where ϵ_{mem} and ϵ_i are the complex permittivity of the cell membrane and cell inside (cytoplasm), respectively. R is the radius of the cell and d ($d \ll R$) is the thickness of the membrane.

2.3.2 Microfluidic Impedance Chip

The first high-speed measurements of the electrical properties of single cells were performed by Coulter in 1950s. It was shown that individual blood cell can be counted and discriminated using a single low frequency (or DC) electrical signal. In a Coulter counter, a small aperture on the wall is immersed into a container that has particles suspended in low concentrated electrolyte solution. Two electrodes are placed: one in front and one behind the aperture, and a current path is provided by the electrolyte when an electric field is applied. The schematic diagram of a Coulter Counter is shown in figure 2.21. When a particle passes through the ‘sensing zone’, that is the aperture, it causes a short-term change in the impedance across the aperture [5]. This change can be measured as a voltage pulse or a current pulse. The pulse height is proportional to the volume of the sensed particle. If a constant particle density is assumed, the pulse height is also proportional to the particle mass.

The Coulter counter uses large electrodes which restrict high frequency measurements in consequence of high values of parasitic capacitances. Impedance microfluidic devices are more sophisticated because they allow high frequency measurements so that cell differentiation occurs on the base of electrical properties of the cell, in addition to its size [21]. It was demonstrated that the microfluidic impedance chip (MIC) developed in the laboratory of Hybrid Biodevices, at the University of Southampton, can differentiate the three major human

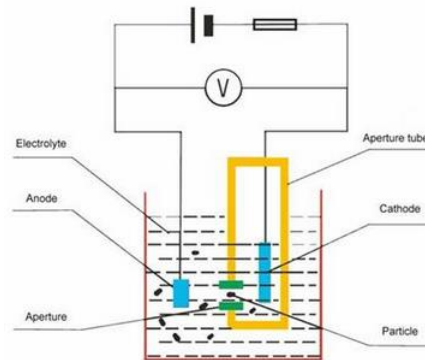


Figure 2.21: Schematic diagram of a Coulter counter (<http://www.beatop.com>).

leukocyte sub-populations (neutrophils, lymphocytes and monocytes) without the need for labeling [15]. The general principle of the single cell impedance cytometry system is shown in the figure 2.22.

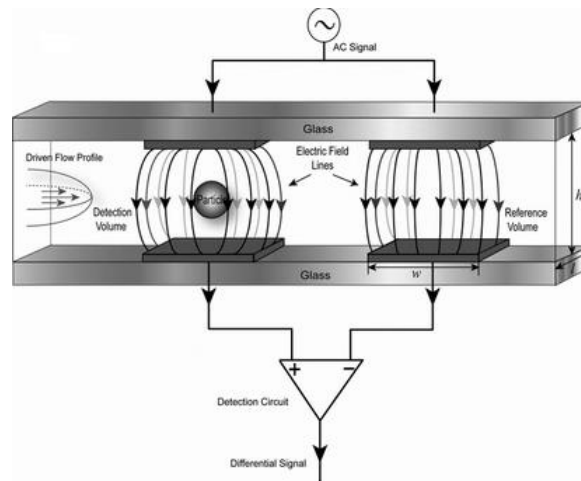


Figure 2.22: Schematic diagram of the micro impedance cytometry system [37].

A voltage signal is applied to the top two electrodes and as the cells pass through the channel they perturb the electric field in the detection volumes. The resulting differential current signal acquired from the two bottom electrodes is processed to provide the impedance signal using a custom detection circuit [37].

2.3.2.1 Geometry of the chip

The impedance of single cells is measured using micro-electrodes fabricated within a micro-channel. The length of the channel is 8 mm; in the correspondence of the inlet and the outlet the channel is 200 μm deep, the narrow part of the channel is 40 μm deep and represents the detecting area made of two pairs of microelectrodes. The micro-channel is a rectangular cross section, 30 μm x 40 μm , and the electrodes are 30 μm wide and 40 μm deep with a 50 μm gap, so that center-to-center distance between the two pairs of electrodes is 80 μm . The figure 2.23 shows the impedance chip that is 15 mm x 20 mm. The two electrodes are overlapped: the signal input is in the top pair; the bottom pair is connected to a differential virtual ground current sensing electronics [13].

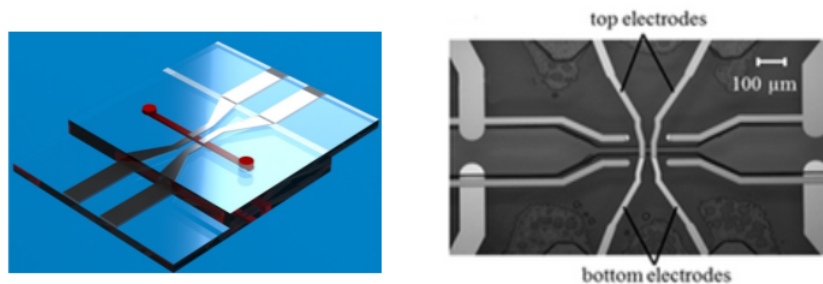


Figure 2.23: Top view of the chip showing two pairs of overlapping electrodes above and below the microchannel (Right image from [13]).

2.3.2.2 MIC fabrication

The chips were fabricated using photolithography and full wafer thermal bonding [37]. Photolithography is a process used in microfabrication to pattern parts of a thin film of a substrate on the surface of a wafer. A thin layer of titanium and then a layer of platinum was sputtered onto a glass wafer so that metal electrodes were lithographically patterned. The titanium layer is an adhesion layer because platinum does not stick directly to glass. Approximately 30 μm thick SU-8 photoresist was deposited onto the surface and fluidic channels were defined using standard photolithography [36]. Two wafers with patterned electrodes were bonded in a vacuum bonder; individual chips were diced from bonded wafers [21]. Inlet and outlet holes were drilled using a CO_2 laser. Electrical connectors were used to make contact with the chip electrodes

and miniature O-rings used to seal the fluidic connection between the block and the chip. The entire assembly was mounted on an x-y-z stage on an optical bench above a bespoke confocal microscope [37].

2.3.2.3 Flow profile

When a fluid flows through a channel, its movement depends on inertial and viscous forces. In microfluidics inertial forces can be ignored because of the small size of the devices and the low velocity of the fluids [5]. The motion of an incompressible Newtonian fluid is described by the Navier-Stokes equation:

$$\rho \frac{Dv}{Dt} = -\nabla p + \mu \nabla^2 v + \rho f \quad (2.36)$$

Where ρ and μ are the density and kinematic viscosity of the fluid, v is the velocity of the fluid, p is the pressure and f is an external applied force.

The ratio of the inertial term to the viscous term is known as the Reynolds number Re :

$$Re = \frac{\rho v D}{\mu} \quad (2.37)$$

Where v is the mean fluid velocity, D is the characteristic length that, in the case of a spherical tube, is the diameter, ρ and μ are the density and dynamic viscosity of the fluid. The Reynolds number is a dimensionless quantity that is used to help predict similar flow patterns in different fluid flow situations. If its value is close to 1 ($Re \simeq 1$) viscous forces dominate and the flow is laminar; if it is much larger ($Re \gg 1$) the flow is turbulent.

The corresponding Reynolds number relative to the water that passes through the narrow section of the channel is:

$$Re = \frac{\rho \frac{Q}{A} D}{\mu} = \frac{1000 \cdot \frac{40 \cdot 10^{-9} \cdot \frac{1}{60}}{40 \cdot 30 \cdot 10^{-12}} \cdot 30 \cdot 10^{-6}}{0.001} = 16.7 \quad (2.38)$$

The average linear velocity is the volumetric flow rate divided by the channel cross section. The flow rate normally used is 40 $\mu\text{L}/\text{min}$ and the channel cross section A is $30\mu\text{m} \times 40\mu\text{m}$. For water at 20°C ρ is $1000 \text{ kg}/\text{m}^3$ and μ is $0.001 \text{ Pa}\cdot\text{s}$.

2.3.2.4 Impedance signal acquisition

An AC voltage signal is applied to the top two electrodes and the resulting differential current signal acquired from the two bottom electrodes. The current signal is amplified and converted into a differential voltage signal by a feedback resistor [21]. The phase and the amplitude of the impedance signal are obtained using lock-in principles. Data is captured with custom software written in Lab-View and processed in Matlab. Cells in suspension are pumped through the chip using a syringe pump at a rate of approximately 200 cells per second. Dilution of the sample ensures that most particles arrive separately at random intervals (300 cells/ μl) and prevents coincidence of events. The figure 2.24 shows a typical data captured by the system, which consists of a pair of anti-symmetric Gaussian peaks [37]. The positive peak originates when the cell passes between the first pair of electrodes and the negative one in correspondence of the second pair. The time between the two peaks corresponds to transit time of the cell between electrodes and it can be used to measure the cell speed. The amplitude of the impedance signal depends on the particle size, the channel and electrode geometry, the applied voltage and any gain in the electronics.

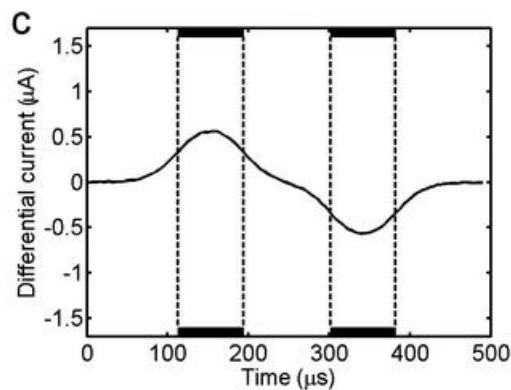


Figure 2.24: Typical data captured by the microfluidic impedance cytometry when a cell passes through the channel. The dotted lines indicate the positions of the electrode edges [37].

The frequency range of acquisition depends on electrical double layer, that affects signals at frequencies lower than 500 KHz, and parasitic capacitances, which limit the signal acquisition at high frequencies. In the frequency range 1MHz to 10 MHz the impedance of the cell decreases rapidly due to the in-

terfacial relaxation of the cell membrane. Through the microfluidic impedance cytometer the signal is acquired two times at different frequencies, 500 KHz and 2 MHz, to provide the electrical properties of the cell, in addition to its volume [21]. The low frequency in-phase impedance signal is used to trigger data acquisition and it is associated to the cell dimension. It enables only discrimination of lymphocyte population from the larger cells that make up the monocyte and neutrophil populations. Dual frequency measurement enables discrimination of the cell according to both membrane capacitance and cell size. The three main populations of leukocytes are differentiated in the opacity diagram ($|Z|_{2MHz} / |Z|_{500kHz}$ vs $|Z|_{500kHz}$), as shown in figure 2.25. Leukocytes are detected using a small amount of blood (20-50 μ L) taken by finger prick and after lysing RBCs according to the method described in the next chapter. The lysed blood is pumped at 40 μ L/min flow rate and about 15000 leukocytes are shown in the scatter plot. Each point corresponds to a cell and the debris are RBC fragments. Each cell subtype has been confirmed by labelling it with a specific fluorochrome and using a custom fluorescence detection system. Furthermore, the impedance system was validated comparing MIC leukocyte count with that obtained by a commercial hematology analyzer [21].

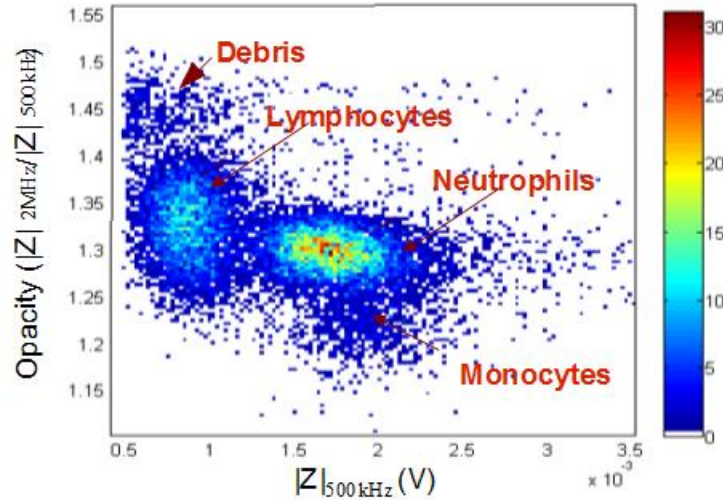


Figure 2.25: Example of the three main leukocyte populations in the scatter plot of opacity ($|Z|_{2MHz} / |Z|_{500kHz}$) vs low frequency impedance magnitude ($|Z|_{500kHz}$).

2.3.2.5 Lock-in scheme detection

The overall noise level in the electronics is determined by the thermal noise in the channel impedance and the current-to-voltage converter feedback resistor. Thermal noise increases as the square root of the system bandwidth. In order to detect high speeds, custom lock-in amplifiers were designed with optimized 5-pole band pass Bessel filters [21]. It is convenient to use lock-in amplifiers to remove from the signal a notable part of white and pink noises, due respectively to thermal and flicker noises. Furthermore, the Bessel characteristic preserves the pulse shape without undue distortion and the band pass was chosen to allow the fastest events to pass [21]. In figure 2.26 the detection circuit is schematized.

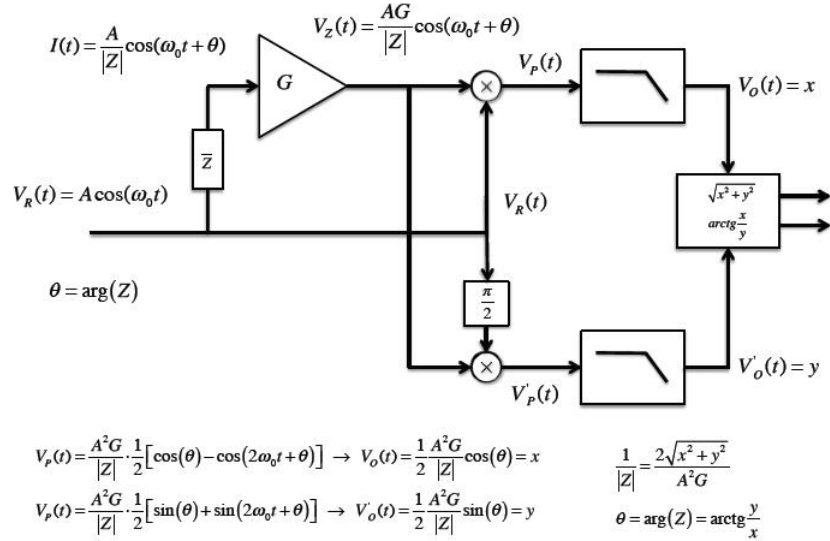


Figure 2.26: Complex Impedance detection by lock in amplifiers (From 'Transduction - Ionics' of Nanotechnology course).

$V_R(t)$ is the voltage signal supplied to the top electrodes, Z is the complex impedance of the cell (or particle) and $I(t)$ is the output signal measured at the bottom electrodes. The voltage signal $V_Z(t)$ is obtained by the current-to-voltage converter feedback resistor and is the impedance signal. In order to reduce the noise, from the impedance signal two signals are obtained through modulation: $V_P(t)$ and $V'_P(t)$. $V_P(t)$ is calculated multiplying $V_Z(t)$ with the reference signal $V_R(t)$; $V'_P(t)$ is calculated passing through a phase shifter $V'_R(t)$ and multiplying the obtained signal with $V_Z(t)$. The highest components in

frequency of the signals $V_P(t)$ and $V'_P(t)$ are removed by low pass filters. Lastly, the module and the phase of complex impedance are calculated through the signals $V_O(t)$ and $V'_O(t)$, which come out from the low pass filters.

2.3.2.6 Impedance spectrum of a single cell

If the geometrical parameters of the system are known, such as electrode size, channel dimensions, then the values of permittivity and conductivity of the system can be replaced by equivalent electrical components, as illustrated in figure 2.27. On the left, the electrode pair illustrates the equivalent circuit model without a cell between the electrodes, the right electrode pair has the cell present between the electrodes. Thus, the model includes the electrical characteristics of the microfluidic channel, the electrical double layer, the cell in the suspending medium and the amplifier circuit components.

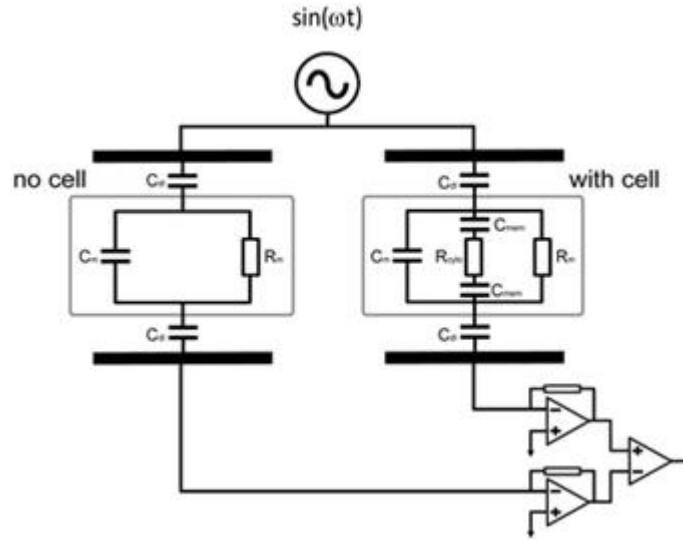


Figure 2.27: Simplified schematic of the impedance detection. C_{dl} represents the electrical double layer capacitance at the liquid electrode interface, C_m and R_m are the equivalent capacitance and resistance of the medium respectively. R_{cyto} is equivalent resistance of the cell cytoplasm, C_{mem} is the equivalent capacitance of the cell membrane [21].

Both electrical resistance $R_m = \frac{1}{\sigma} \frac{l}{S}$ and capacitance $C_m = \epsilon_0 \epsilon_r \frac{S}{l}$ of the medium depend on the height of the channel l and the area of the electrodes S . The resis-

tance depends on the conductivity of the medium σ and the capacitance depends on its permittivity ϵ_r . The double layer capacitance C_{dl} depends on both conductivity and permittivity of the medium: $C_{dl} = \frac{\epsilon}{\kappa^{-1}}$ and $\kappa^{-1} = \sqrt{\frac{D\epsilon}{\sigma}}$, where κ^{-1} is the Debye length (after that length from the electrode C_{dl} is negligible) and D is the diffusion coefficient of the medium. The equivalent complex permittivity of a heterogeneous system and the dielectric properties of the individual particles positioned between two measuring electrodes are described by Maxwell's mixture theory [15]. The electrical components of the cell are calculated on the base of Shell model. Including the double layer capacitance, the total impedance of the circuit is:

$$\tilde{Z}_{mixDL} = \frac{2}{j\omega C_{dl}} + \frac{R_m(2 + j\omega R_{cyto}C_{mem})}{j\omega R_m C_{mem} + (2 + j\omega R_{cyto}C_{mem})(1 + j\omega R_m C_m)} \quad (2.39)$$

The figure 2.28 shows how the impedance magnitude of each leukocyte population decreases with the frequency. At low frequencies the system is dominated by the electrical double layer.

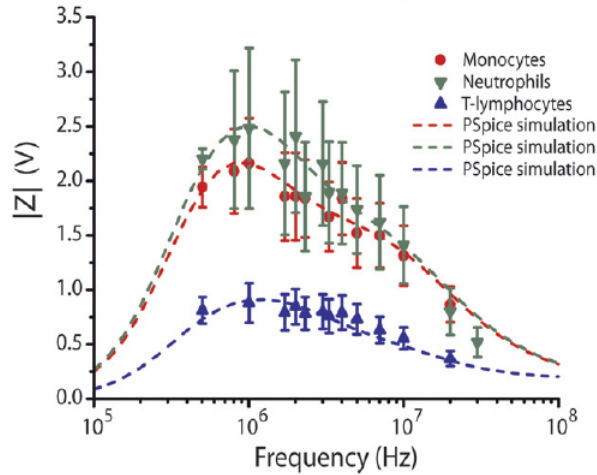


Figure 2.28: Typical frequency-dependent impedance magnitude signal for leukocytes [21].

In the frequency range 1MHz to 10 MHz the impedance of the cell decreases rapidly due to the interfacial relaxation of the cell membrane. The Maxwell-Wagner effect (or β -dispersion) is an interfacial relaxation process occurring in all systems where the electric current must pass an interface between two differ-

ent dielectrics [34]. Cell suspensions typically exhibit a significant β -dispersion in the radio frequency range and is due to the Maxwell-Wagner effect at the interface between the intra or extracellular solution and the phospholipid membrane [39]. At higher frequencies the properties of the system are dominated by the cytoplasmic resistance and, besides, by parasitic capacitances in the electrical circuit. Some differences between the simulations obtained by the equivalent model and the cell acquisitions have to be considered. The Maxwell's mixture theory is applicable only for low volume fractions ($<10\%$) and when the cell is located in an uniform electric field [5]. However the placement of the two parallel facing electrodes in the microfluidic cytometer creates a non-uniform field distribution due to the fringing field effect. The field distribution is relatively uniform only in the centre of the electrodes. Furthermore in the microfluidic cytometer the volume fraction is high ($>40\%$) and is modified by a cell constant which depends on the geometrical properties of the cytometer [21].

Chapter 3

Materials and methods

Introduction

In the first section of this chapter two lysis chemical protocols for WBC differentiation by impedance cytometry are described. The lysis procedure of both the methods is manual, simple and suitable for its implementation in automated fluidic platforms. Specifically, the standard chemical protocol used in the laboratory of hybrid biodevices, at the University of Southampton, for three-part leukocyte differentiation is reported and a specific chemical four-part differential protocol, that has been tested, is described. The results obtained by impedance cytometry after performing the experimented protocol do not provide the leukocyte four-part differentiation. Thus only the standard lysis protocol was performed in the sample preparation cartridge, developed previously in the laboratory. The cartridge consists of reservoirs, channels and active components, such as a rotating valve and a magnetic stirrer, that are capable to automate the RBC lysis. It is described in detail in the second section. The sample preparation device has been integrated into the microfluidic impedance cytometer so that leukocyte analysis is performed immediately after the erythrocyte lysis. The efficiency of the lysis, performed by the cartridge, according to the standard protocol, was tested. The leukocyte clusters obtained by the automated system were compared with those obtained by impedance cytometry after the manual lysis procedure. It has been observed that the lysis performed by the sample preparation cartridge is less effective than that performed manually. Then in the experimental work the WBC differentiation was improved by optimising the standard lysis protocol. The protocol was modified by changing some chemical concentrations and the variations are reported in the third section.

3.1 Chemical protocols used for RBC lysis and WBC differentiation

In order to differentiate leukocytes in subsets, several protocols which require the blood handling with a lytic reagent have been patented. They differ in chemicals which make up the reagent. Some of them involve the use of dyes for WBC differentiation, other ones the use of chemicals that effect changes in leukocyte shape to enhance the cell differentiation. Each protocol is suitable for specific analysis methods. The RBC lysis can be performed using hypotonic or hypoosmotic treatments. The hypotonic treatment makes use of the fact that leukocytes are more resistant than erythrocytes in hypotonic solutions. In this type of treatment an aqueous solution having a low osmolarity is used; some lytic chemicals can be added to accelerate the lysis process, that is extinguished by a subsequent hypertonic salt solution. Different lytic chemicals, such as saponin, surfactants, quaternary ammonium salts, are used in both hypotonic and hypoosmotic treatments. The saponin is the mildest cytolytic agent but it takes a prolonged time to complete leukocyte differentiation if it is used at low concentrations, such as 0.05-0.1% w/v, and it has a strong lytic effect at concentrations higher than 0.2% w/v [10]. The surfactants do not damage leukocytes as violently as quaternary ammonium salts but act more strongly on leukocytes than saponin [10]. In order to prevent leukocyte damage, in some methods fixatives, such as formaldehyde and glutaraldehyde [17], are used. In most cases the concentration of lytic reagent effects morphological changes on leukocytes, in addition to RBC lysis. In some cases the differentiation is improved by leukocyte staining with dyes, that have different affinity for leukocyte subtypes [42].

3.1.1 Standard lysis protocol for 3-part leukocyte differentiation

The standard lysis protocol for differential determination of three leukocyte populations, including neutrophils, lymphocytes and monocytes, derives from the chemistry patent *US 5155044 A*. It involves the use of two solutions, a lytic reagent and a quench solution. Besides erythrocyte lysis, the solutions dilute the sample so that coincidence of events, or rather the probability that two or more cells pass together through the micro-channel, is prevented in flow systems. The

two solutions are always maintained at a predetermined concentration, pH and osmolality [18].

The *lysis solution* is 0.12% v/v formic acid and 0.05% w/v saponin; it is used in the quantity 12 μ L per 1 μ L of whole blood. The lysis solution has a low pH, which is around 2.6-4.0, and a low osmolarity, less than 50 mOsm, and is selective toward red blood cells since leukocytes are more resistant than erythrocytes in hypotonic solutions; however a long exposition can damage leukocytes [18]. The formic acid is the main component that enables RBC lysis; the saponin reduces the debris volume and has a lytic effect only if it is present in high concentration. The concentration of lytic reagent has not to be effective only for lysing RBCs, but also should effect subtle changes in the leukocyte shape to facilitate the subsequent identification and analysis of the correspondent clusters. For example, exposure of saponin in an organic acid, formic acid, for a short period of time, modifies the properties of leukocytes changing the cell volume and cell membrane characteristics.

The *quench solution* is 0.6% w/v sodium carbonate, 3% w/v sodium chloride; it is used in the quantity 5.3 μ L per 1 μ L of whole blood. The quench solution has a high pH, around 10, so that the pH of the lysed blood sample is attained within the range 7-7.5, and a high osmolarity, around 1000 mOsm, in order to prevent WBC damage and to preserve the chemical balance of leukocytes. The concentration of the quench solution depends on the chemical concentration in the lysis solution. The protocol is suitable for leukocyte staining since it does not alter the immunochemical response of the leukocyte surface marker [18]. It is schematized in figure 3.1.

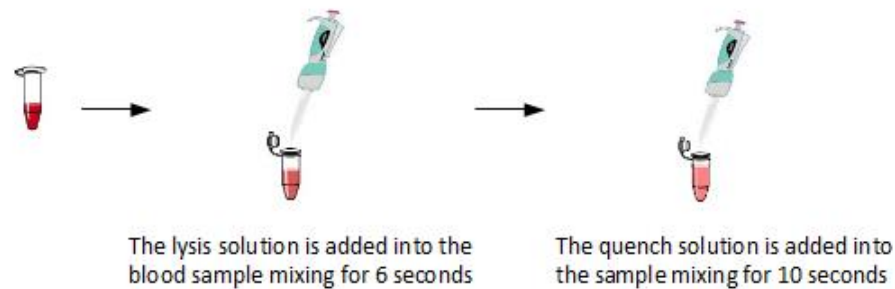


Figure 3.1: Scheme of the lysis protocol for 3-part leukocyte differentiation.

After the addition of the lysis solution, the sample is incubated for 6 sec-

onds at room temperature with continual agitation and the lytic reaction is interrupted by the quench reagent in order to preserve and distinguish white blood cells.

Following RBC lysis, blood samples can be analyzed by flow or impedance cytometry. In both analyses it is possible to distinguish three leukocyte clusters (lymphocytes, monocytes and neutrophils), as illustrated in figure 3.2.

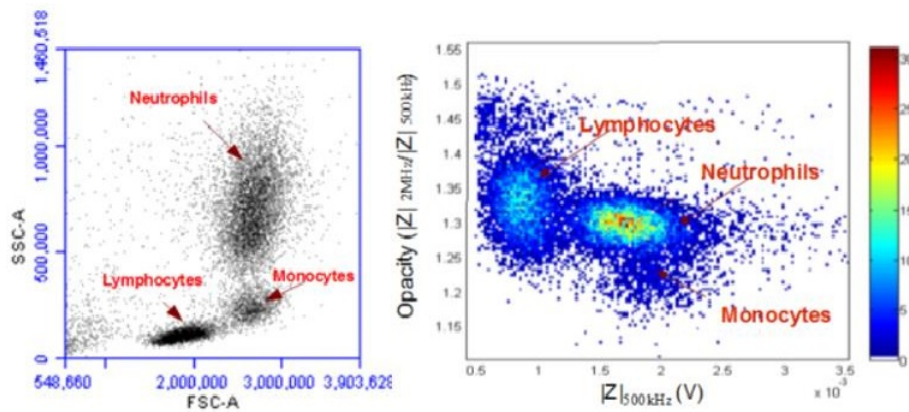


Figure 3.2: On the left three leukocyte subsets in the scatter plot SSC vs FSC. On the right the same populations in the scatter plot opacity vs electrical volume.

In the impedance acquisition the presence of saponin in formic acid allows to separate the cluster of monocytes from that of neutrophils, otherwise they would appear overlapped. The quench solution does not halt the reaction completely since the membrane capacitance of monocytes increases in the time. The membrane capacity increase of monocytes results in their opacity decrease [21] and occurs after 5 minutes from the addition of the quench solution, as shown in figure 3.3.

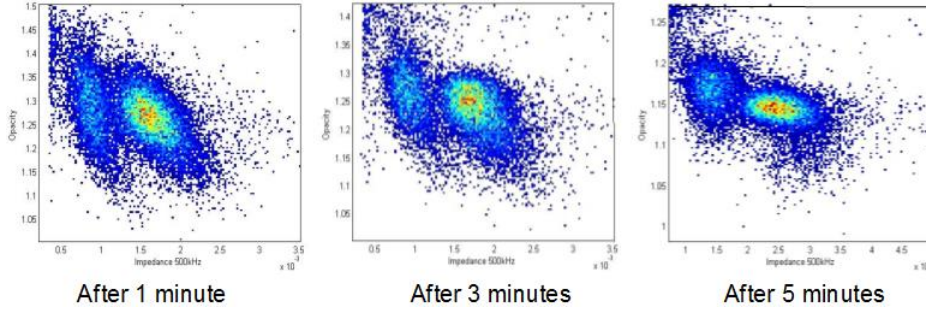


Figure 3.3: WBC differentiation obtained by MIC after implementing the 3 part leukocyte differential protocol in different quench times: 1 minute, 3 minutes and 5 minutes.

3.1.2 Lysis protocol for differential determination of four leukocyte populations

In order to distinguish eosinophils among leukocytes the chemistry patent *US 4,751,179* was tested. In normal conditions the eosinophil count is less than 350 cells per microliter but it increases in pathological conditions, such as acute hyper-eosinophilic syndrome, allergic reactions and parasitic infections [33]. In the patent for differential leukocyte determination of four populations (neutrophils, lymphocytes, monocytes and eosinophils) the reagent system comprises aqueous solutions of a lytic diluent containing saponin, and a fixing reagent containing a cross-linking compound, such as glutaraldehyde [17]. In this case blood cells are not subjected to an hypotonic treatment and a pH change, but erythrocytes are lysed by using a high concentration of saponin in the lysis solution and the reaction is interrupted by treatment with the cross-linking fixing reagent.

Saponin concentration in the *lytic diluent* is 0.40% w/v, about 8 times the saponin concentration of lytic reagent in the previous protocol. When the saponin is the only lytic chemical added in DI water in amounts barely sufficient to stromatolyse erythrocytes, it requires about 20 minutes for distinguish leukocytes from debris. When high saponin concentrations are used, the red blood cells are lysed in a few seconds and a long exposition can result in leukocyte damage [17]. The lysis solution contains also 0.2% sodium chloride to fix the pH, and additives to enhance the separation of the four white blood cell clusters and avoid the growth of microorganisms, such as 0.5% v/v 2-phenoxyethanol and 0.03% w/v methyl paraben preservative [17].

The *fixing reagent* comprises: 2.0% v/v glutaraldehyde, 0.4% sodium chlo-

ride, 0.1% w/v buffer salt, such as sodium bicarbonate. Salts adjust the pH that is maintained within the range of 7.0 to 8.0 throughout the procedure. The glutaraldehyde in the quench solution protects the leukocytes against damage and effects changes in leukocyte shape [17]. It is a rapidly active cross linking fixing reagent and slow acting monoaldehydes, such as formaldehyde, are inefficient for preserving the leukocytes from the lytic effect of saponin. The protocol involves the use of the lysis solution in the quantity $6\mu\text{L}$ per $1\mu\text{L}$ whole blood, and the quench solution in the quantity $10\mu\text{L}$ per $1\mu\text{L}$ whole blood [17]. The quantity of lysis solution is half that in the standard protocol because of the high saponin concentration that has a strong lytic effect. The volume of fixing reagent added to the lysed blood is about the double that of the lysing reagent, so that the concentration of glutaraldehyde in the lysed and fixed blood solution is about 1% v/v. The protocol is schematized in figure 3.4.

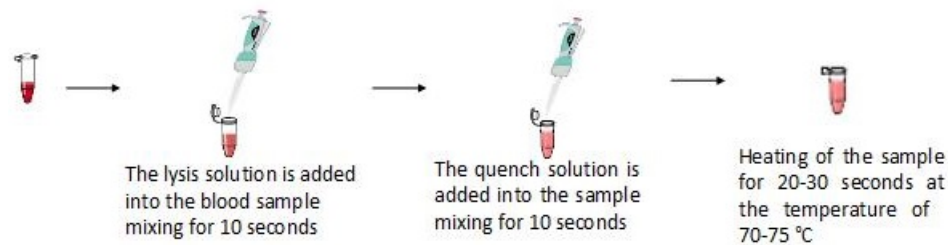


Figure 3.4: Scheme of the lysis protocol for 4-part leukocyte differentiation.

Heating of the lysed and fixed blood solution often is useful to accelerate leukocyte modification and rapidly give stable clusters for flow analysis. In manual preparations, it is convenient to immerse the blood solution, contained in a test tube, into a 70° to 75° C water bath with swirling to achieve heating [17].

Blood sample taken by finger prick from a healthy volunteer and stored in Vacutainer tubes (EDTA K3E15%) was used for testing the protocol by flow and impedance cytometry. Data acquired after implementing the four part differential protocol was compared with that obtained from the standard protocol by analyzing the cluster shape and counting leukocyte subpopulations. According to the standard lysis, $30\mu\text{L}$ whole blood was mixed with $360\mu\text{L}$ lysis solution for 6 seconds and subsequently with $159\mu\text{L}$ quench solution for 10 seconds. The figure 3.5 shows the three main leukocyte populations acquired by flow cytometry

after performing the standard lysis protocol.

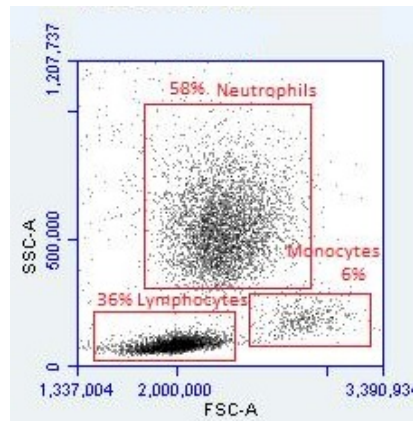


Figure 3.5: Leukocyte clusters obtained by flow cytometry after performing the standard lysis protocol.

The figure 3.6 illustrates leukocyte subsets in the scatter plot SSC vs FSC, obtained by flow cytometry after performing the four part differential protocol for different times of heating. For each experiment, according to the protocol, $30\mu\text{L}$ whole blood was mixed with $180\mu\text{L}$ lysis solution for 10 seconds and subsequently with $300\mu\text{L}$ quench solution for 10 seconds more. Furthermore three of the lysed and fixed blood solutions were heated for different times: 15, 20, 30 seconds. Erythrocyte fragments do not interfere with leukocyte analysis and the cluster shape does not vary changing the heating time of the blood solution. The eosinophil cluster is well distinguishable, even if the eosinophil percentage in healthy donors' blood is low, between 2-6% of all leukocytes. The position of the cluster is consistent with eosinophil morphological characteristics since the eosinophils are slightly larger and have more granules than neutrophils (FSC is proportional to the cell size and SSC is proportional to the cell complexity). Lymphocytes are distinguished from the other subpopulations and their percentages are comparable with the one calculated using the standard protocol lysis. Lastly the monocyte and neutrophil clusters are merged each other, as shown in the enlargement provided for each experiment (right diagrams in figure 3.6). The distinction of monocytes from neutrophils may be inhibited by the presence of glutaraldehyde in the quench solution since it changes the cell structure.

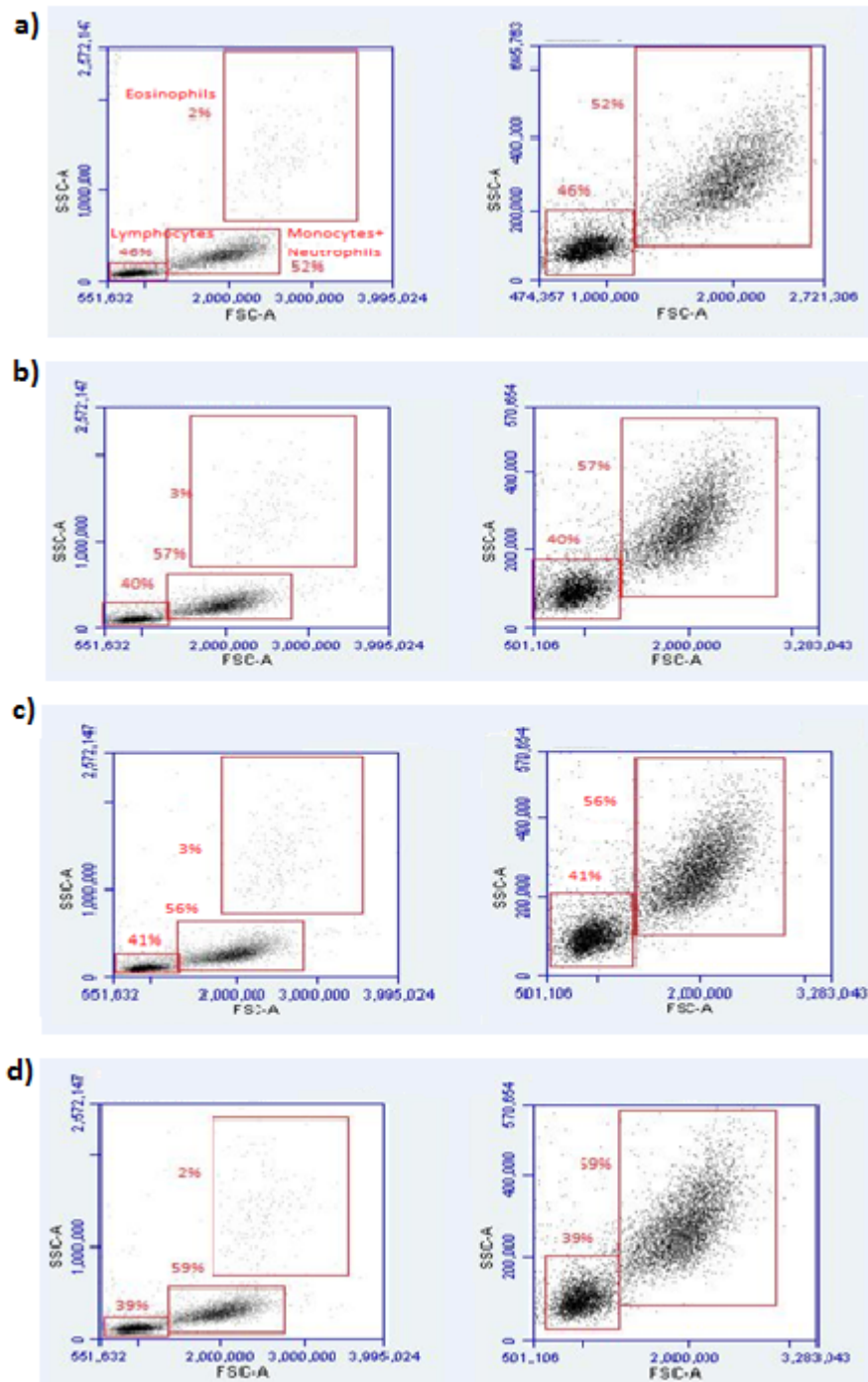


Figure 3.6: Leukocyte analysis by flow cytometry from the four part differential protocol. The four experiments were performed by immersing the lysed and fixed blood solution into a 70° C water bath with swirling for different times: a) no heating b) 15 seconds c) 20 seconds d) 30 seconds.

Leukocyte subsets are not clearly distinguishable by impedance cytometry, as shown in figure 3.7, in the scatter plot opacity vs impedance magnitude at low frequency. Data was acquired after implementing the four part differential protocol and immersing the fixed blood solution into a 70° C water bath for 20 seconds. The left cluster corresponds to lymphocytes, which are smaller than granulocytes and monocytes. Neutrophils, monocytes and eosinophils have similar size and, as they do not present different electrical properties, it is not possible to distinguish them. In summary, the protocol does not enable the differential classification of four leukocyte populations, but only eosinophil distinction from other leukocyte subsets by flow cytometry.

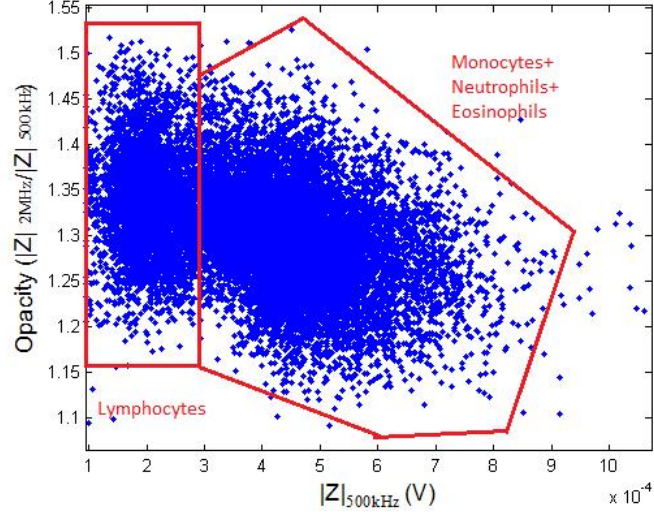


Figure 3.7: Leukocyte analysis by impedance cytometry after performing the 4 part differential protocol.

3.2 Sample preparation cartridge for automated RBC lysis

The simplicity and portability of the microfluidic impedance chip offer a range of potential applications in cell analysis including point-of-care diagnostic systems using label-free techniques. It has been integrated into a sample preparation cartridge to automate erythrocyte lysis before leukocyte differentiation.

3.2.1 Integrated cartridge components

The cartridge performs semi-automatically RBC lysis of 30 μ L of blood. It consists of a rotating valve and a magnetic stirrer, so that the lysis and quench solutions are mixed alternately with the blood sample. The figure 3.8 shows a schematic diagram of the integrated sample preparation cartridge.

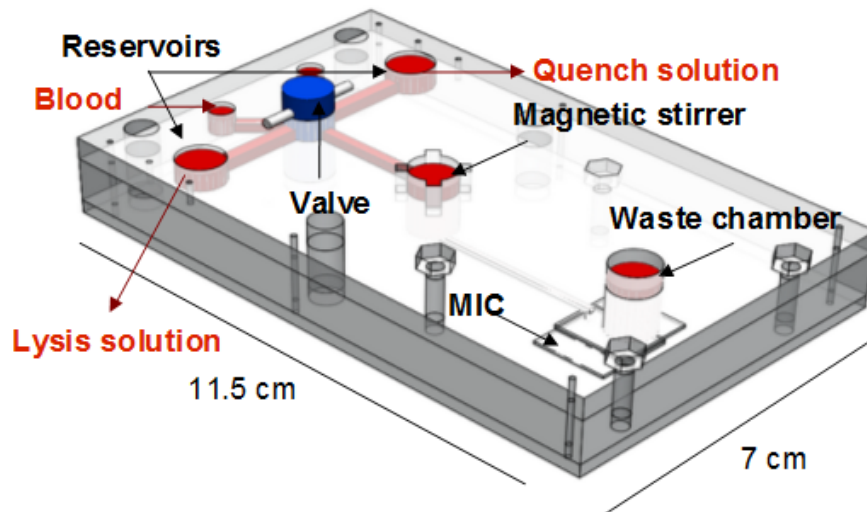


Figure 3.8: Schematic diagram of the integrated sample preparation cartridge.

The size of the cartridge is 11.5 cm x 7 cm. The channel contained in the rotating valve is filled with 30 μ L whole blood by pipette. The two reservoirs are filled with the lysis and quench solutions respectively. After rotating the valve, 360 μ L lysis solution ($\times 12$ whole blood volume) is pushed with 30 μ L blood into the mixing chamber, whose diameter is 0.9 cm. RBC lysis is performed by the magnetic stirrer. It has been tested that the optimal lysis is achieved mixing the sample with the lysis solution for 10-15 seconds at the 2000 rpm frequency of rotation. Once turned the valve again, 159 μ L quench solution ($\times 5.3$ whole blood volume) is mixed with the lysed blood solution for about 20 seconds. Then the lysed blood is pumped into the MIC at the flow rate of 40 μ L/min.

Without applying any pressure, the lysed blood remains in the chamber because of the capillary action related to the narrow size of the channel underlying the mixing chamber. The channel is 300 μ m in diameter and 1 mm in length. The liquid does not pass through the micro-channel because the surface of the

liquid in contact with it is elevated depending on the relative attraction of the molecules of the liquid for each other and for those of the channel. The remaining part of the channel that connects the mixing chamber to the micro-impedance channel is 1 mm wide.

The size of the MIC is 15 mm x 20 mm. The length of the channel is 8 mm; in the correspondence of the inlet and the outlet the channel is 200 μm deep, the narrow part of the channel is 40 μm deep and represents the detecting area made of two pairs of microelectrodes. The distance of the two pairs of microelectrodes is 50 μm and their width is 30 μm ; then the detection area is 110 μm length. When the lysed blood passes through the detection channel impedance signals from leukocytes are acquired and data is saved for a further analysis. The electrodes of the chip are in contact with spring connectors of two PCBs, one used for supplying the top electrodes and the other one used to acquire the current signal from the two bottom electrodes. The resulting current signal is converted into voltage signal and processed by lock in amplifiers.

In the figure 3.9 the top view of the integrated cartridge is shown.

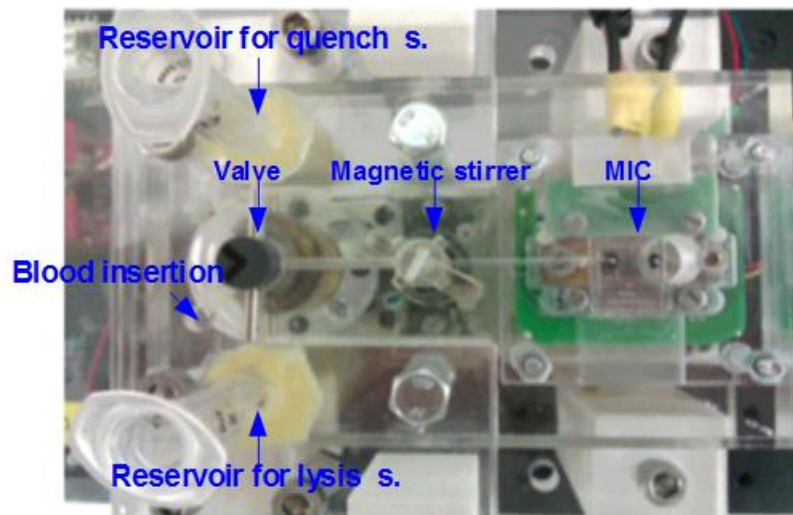


Figure 3.9: Top view of the integrated cartridge.

The valve and the magnetic stirrer are activated by commands. In each reservoir a piston is inserted so that the solutions are pushed into the mixing chamber by applying a pressure. In the mixing chamber there is a magnetic bar (flea) that interacts with the stirrer. The lysed blood is pushed into the

MIC by a pump that is mounted over the mixing chamber and is activated by a specific command. The commands for the valve, the stirrer and the pump are controlled by Arduino boards.

3.2.2 Comparison of data acquired by the integrated system and that acquired by MIC after manual sample preparation

RBC lysis performed by the sample preparation cartridge (*stirring lysis*) according to the standard protocol is less effective than lysis performed by pipettes (*bulk lysis*) because of the reduced shear stress in the mixing by the magnetic stirrer. The figure 3.10 shows the three leukocyte populations acquired by the microfluidic impedance cytometer after both bulk lysis and stirring lysis. About 15000 leukocytes, acquired in 80 seconds, are shown in the scatter plots. The color bar is used for quantifying the number of cells making up the three clusters; the blue color corresponds to low number of leukocytes and the red one to high number.

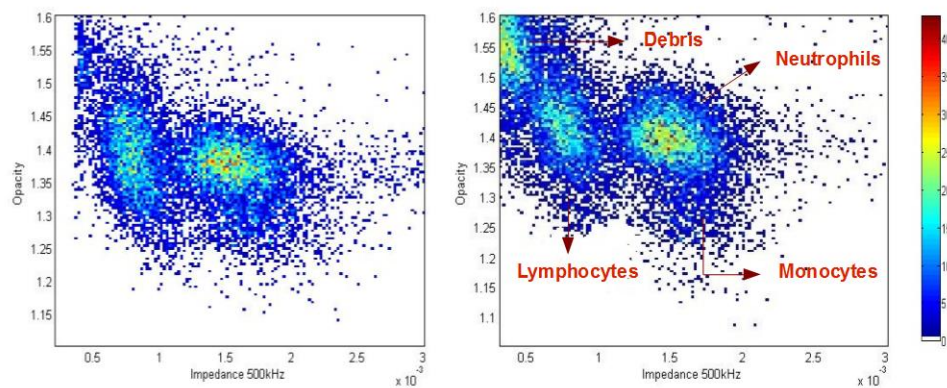


Figure 3.10: Three leukocyte populations in the scatter plot opacity vs Z_{500kHz} : on the left, clusters from the bulk lysis; on the right, clusters from the stirring lysis.

In the bulk lysis 30 μ L whole blood was mixed with the lytic reagent for 6 seconds and the reaction was extinguished by adding the quench solution. In

the stirring lysis 30 μ L whole blood was mixed with the lytic reagent for 15 seconds at 2000 rpm frequency of rotation and subsequently with the quench solution at 200 rpm. In both lyses leukocytes were acquired after 4 minutes from the quench addition. In order to prevent cell sedimentation, before leukocyte acquisition, the lysed blood was stirred at the 200 rpm frequency of rotation. Leukocyte populations detected by MIC after performing the stirring lysis are well distinguishable and comparable with the ones from the bulk lysis. The number of points that make up the different clusters is consistent with the percentages of leukocyte subpopulations which characterize healthy adults' blood. The difference between data obtained after the two lyses concerns the number and the volume of debris, or RBC fragments. The opacity diagram from the stirring lysis shows a high number of debris, whose volume is slightly larger than that from the bulk lysis. The large debris volume affects the differentiation of lymphocytes, which are smaller than monocytes and neutrophils. The difference in debris volume between the two lyses is confirmed by observing the measured time traces of impedance signals from leukocytes; they are shown in figure 3.11. The noise amplitude is proportional to the debris volume. The noise amplitude for the stirring lysis is double that for the bulk lysis.

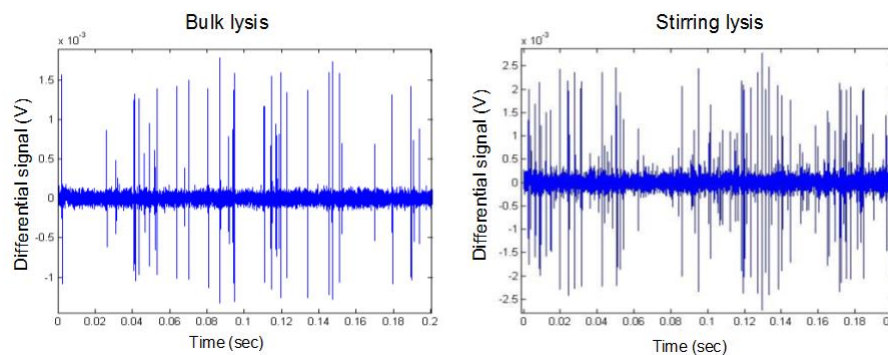


Figure 3.11: Time traces (0.2 seconds) of impedance signals from leukocytes obtained after performing bulk lysis (on left) and stirring lysis (on right).

Furthermore in both lyses, the differentiation between monocytes and neutrophils occurs after 5 minutes, as shown in figure 3.12. This is related to the presence of saponin in formic acid, that induces morphological changes in monocyte membrane after a few minutes. Membrane capacitance of monocytes increases in the time resulting in opacity decrease.

For the two lysers, two blood samples taken by finger prick from different healthy volunteers have been used. There is a high variability in leukocyte shape and count between blood samples.

The difference in electrical volume between the smaller lymphocytes and the two larger populations does not change for different quench times; only the level of separation between neutrophils and monocytes is dependent on quench time. It is easier to distinguish monocytes from neutrophils after 5 minutes of quench compared to 1 minute of quench.

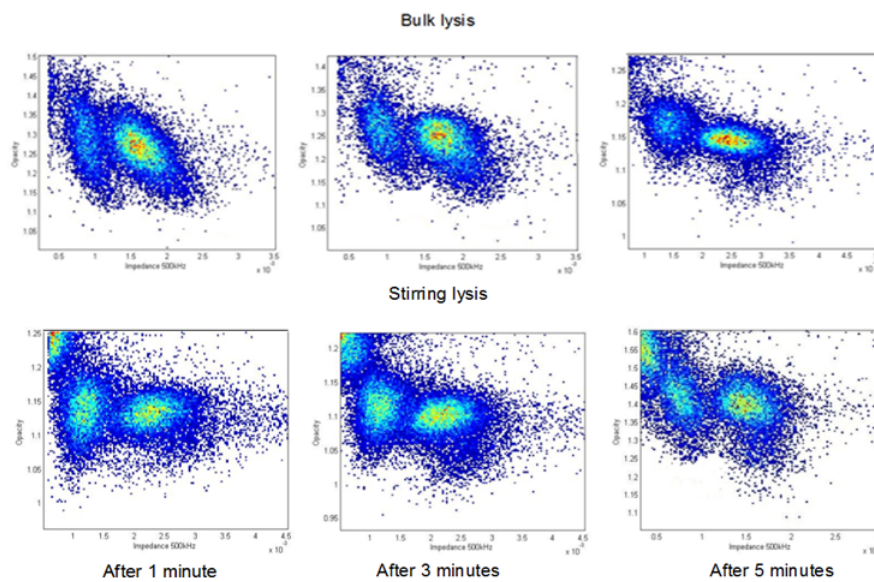


Figure 3.12: Scatter plots obtained after 1 minute, 3 minutes and 5 minutes of quench by implementing the bulk lysis and the stirring lysis according to the 3 part leukocyte differential protocol.

3.3 Variations in the 3-part leukocyte differential protocol

The sample preparation cartridge automates the blood sample preparation before WBC acquisition by MIC, making the integrated system a potential point-of-care device for WBC differentiation and count. Several point-of-care systems are being developed in recent years for enabling fast on-site diagnoses using a small amount of capillary blood. They have the advantage to be portable, cheaper and simpler than traditional hematology analyzers. Applications of

point-of-care leukocyte count in the field of telemedicine, out-patient monitoring and medical care in resource limited settings have been previously evaluated.

In order to improve WBC differentiation by the integrated cartridge, in this research work the standard lysis protocol has been optimised. The aim of the work was increasing the distinction of lymphocytes from debris and accelerating the differentiation between monocytes and neutrophils that normally occurs after 5 minutes by optimizing the lytic reaction. The effect of two chemicals was analyzed by changing their concentration in lysis and quench solutions. In particular, it was tested the effect of different saponin concentrations in the lysis solution and the presence of glutaraldehyde in the quench solution. Saponin concentration was increased for reducing the debris volume and glutaraldehyde was added in the quench solution because it is a rapidly active cross linking fixing reagent capable to protect leukocytes from the lytic effect of saponin. In the next chapter results relative to these variations will be shown and discussed.

3.3.1 Saponin concentration variations in the lysis solution

Different lysis solutions were prepared with the following saponin concentrations: 0.065%, 0.075% and 0.01% w/v, respectively 1.3, 1.5 and 2 times that in the standard lysis protocol (0.05%). The concentration of formic acid, that is 0.15% v/v, has not been modified.

The effectiveness of saponin, as a lytic reagent is highly concentration dependent, as specified in the four part leukocyte differential protocol, where the hypotonic treatment with formic acid is replaced by 0.40% w/v saponin. Since the saponin, where present at a lytic effective concentration, can also cause the lysis of leukocytes, the glutaraldehyde in the quench solution has the capacity to protect the leukocytes.

In the three part leukocyte differential patent the concentration of saponin that has been determined as effective for reducing red cell fragments is from about 0.006 to about 0.012 grams per milliliter of whole blood [18]. In the standard lysis protocol the saponin concentration is 0.006 grams per milliliter of whole blood and it was increased until 0.012 grams per milliliter of whole blood, that corresponds to 0.01% w/v saponin in the lysis solution. Furthermore it has been demonstrated that the presence of saponin in an organic acid, such as formic acid, modifies the membrane shape of the monocytes and enhances their

separation from the neutrophils in the opacity/electrical volume diagram [21]. In the impedance measurements the differentiation between monocytes and neutrophils occurs after a few minutes from the addition of the quench solution; this confirms that the quench does not totally eliminate the lytic effect upon the leukocytes but it only retards the lytic activity. The velocity of monocyte morphological variation depends on the concentration of lytic reagent. Thus it has been analyzed how different saponin concentrations influence the differentiation process of monocytes from neutrophils.

3.3.2 Glutaraldehyde addition in the quench solution

The quench solution with 1% v/v glutaraldehyde was prepared without changing the salt concentration. The choice of glutaraldehyde derives from the four part leukocyte differential protocol. The glutaraldehyde has been added into the quench solution to protect leukocytes from the lytic effect of higher saponin concentrations. In the three part leukocyte differential patent it was specified that the quench solution does not halt completely the lysis process and the use of a fixative is recommended to preserve the characteristic size and shape of the white blood cells over the time. The glutaraldehyde is a fixative capable to form cross-linkage with the target proteins. Glutaraldehyde is a large molecule that has two aldehyde groups, that allow the link between distant pairs of protein molecules, and a flexible hydrocarbon chain. The cross-linkage is schematised in figure 3.13. If two proteins physically interact with each other, they are covalently cross-linked. This technique involves the formation of covalent bonds between the amino group of each protein and the aldehyde, that is the reactive end group of each side of the glutaraldehyde.

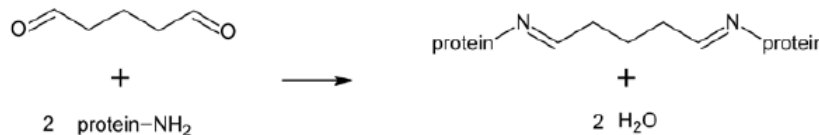


Figure 3.13: Protein cross-linkage by glutaraldehyde.

Glutaraldehyde can also react with phospholipids containing free amino groups. Ideally, a good fixation method should preserve the cell structure with minimum change from the living state (volume, morphology, localization of

macromolecules and organelles). In practice, glutaraldehyde alters the cells on a molecular level to increase their mechanical strength or stability. This increased strength and rigidity can help preserve the shape and the structure of the sample.

Chapter 4

Results and discussion

4.1 Leukocyte subpopulation gating and count

The solutions described in the previous chapter were tested for improving RBC lysis and WBC differentiation by the integrated cartridge. For each modified protocol the manual lysis and the stirring lysis were performed. Each data was acquired in different times (1 minute, 3 minutes and 5 minutes) from the addition of the lysis solution and compared with WBC differentiation obtained after 5 minutes of quench by performing the standard lysis protocol manually (standard bulk lysis). The cluster shape and the leukocyte count between acquisitions were compared. The numbers of leukocytes in each cluster were enumerated to calculate the total leukocyte count and the differential count of each leukocyte subtype. The clusters were gated by polygons, as shown in figure 4.1. The total leukocyte count was calculated by dividing the total number of leukocytes by the volume of the blood sample. The differential count was calculated as the percentages of each cluster among the total leukocytes. Leukocyte count was compared also with that obtained by HemoCue, a point-of-care testing device shown in figure 4.2. It analyzes and counts five leukocyte sub-populations (neutrophils, lymphocytes, monocytes, eosinophils and basophils) using 10 μ L of blood. The blood drop is drawn by capillary forces into a disposable micro-cuvette containing the dried reagents for leukocyte staining. Leukocyte differentiation is performed using a photo microscope and image processing techniques. The HemoCue has been validated comparing the total WBC count with that obtained with a hematology analyser. It has been found to be accurate within 12% for all 200 clinical samples [26].

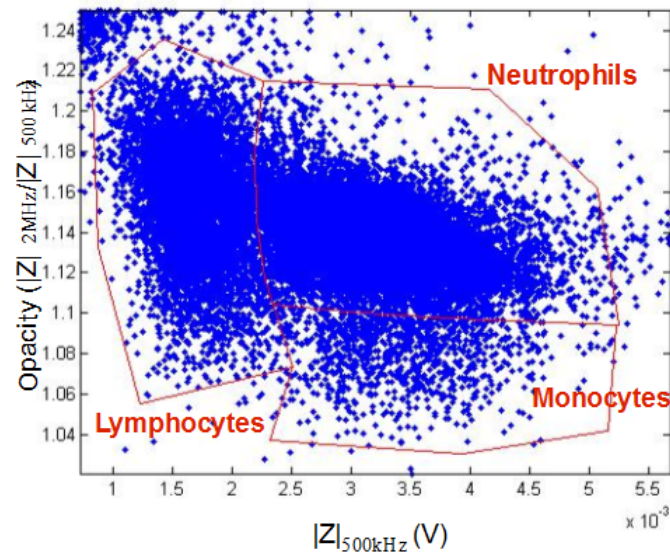


Figure 4.1: Cluster gating by polygons for sub-population count.



Figure 4.2: HemoCue for WBC count and monitor with the corresponding leukocyte percentages from a blood sample (Left image from [26]).

4.2 Saponin variation effects

The effects of increasing saponin concentration in the lysis solution were evaluated in both the lysers. First the results from bulk lysis are reported and discussed. Secondly the results from the stirring lysis are shown and compared.

Every result from each modified protocol is compared with the scatter plot designated 'standard bulk lysis', since it is obtained after 5 minutes from the addition of the quench solution according to the standard lysis protocol performed manually.

4.2.1 Evaluation of results in bulk lysis

First, it was used the lysis solution with 0.1% *w/v* *saponin*; the concentration is double that in the standard protocol. The clusters obtained for different quench times in the bulk lysis are illustrated in figure 4.3.

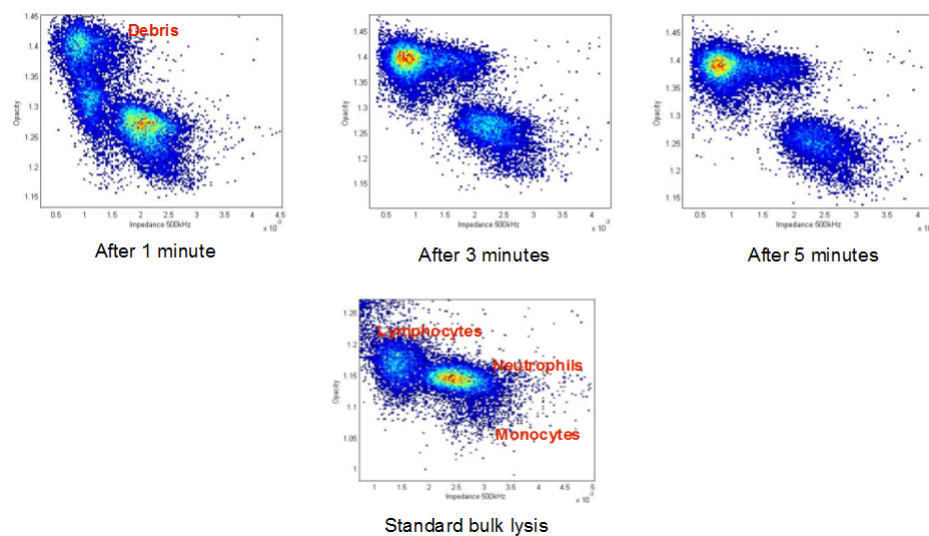


Figure 4.3: WBCs acquired in different quench times (1 minute, 3 minutes and 5 minutes) from bulk lysis using the 0.1% *w/v* *saponin* lysis solution. Clusters are compared with those from the standard bulk lysis.

The lymphocyte cluster obtained after 1 minute of quench is shifted toward up compared with that from the standard lysis since lymphocytes were damaged. After 3 minutes all the lymphocytes were lysed, but neutrophils and monocytes were not modified as they are more resistant to higher *saponin* concentrations. There are not differences between the acquisitions after 3 minutes and 5 minutes of quench since the lymphocyte cluster appears completely merged with debris and the monocyte cluster does not change position. Furthermore it is noticeable that the differentiation between monocytes and neutrophils occurs

after one minute of quench. Thus the saponin concentration increase results in a fast change of monocyte membrane that allows monocyte differentiation from neutrophils.

Secondly, it was used the lysis solution having 0.075% *w/v* saponin, that is an intermediate concentration between the previous one and that in the standard protocol. In figure 4.4 WBC clusters obtained after performing the bulk lysis are illustrated for different quench times.

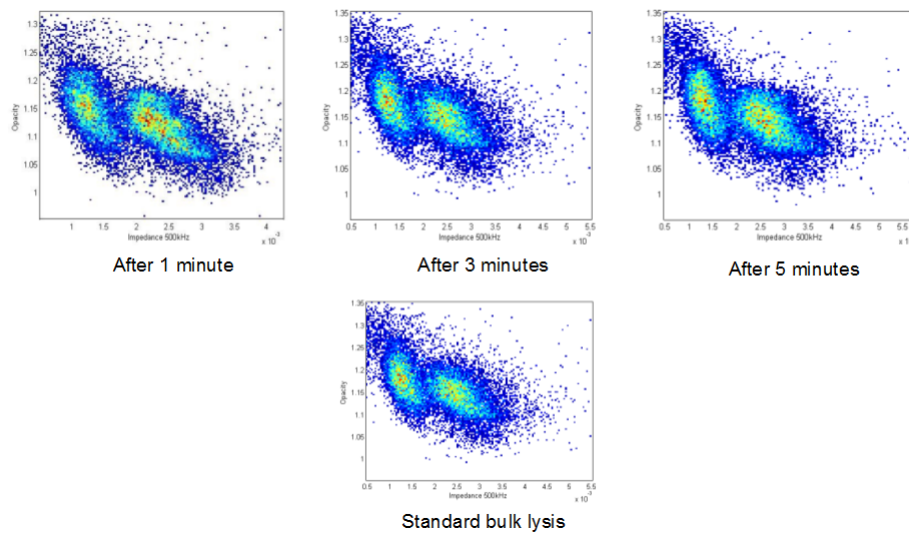


Figure 4.4: WBCs acquired in different quench times (1 minute, 3 minutes and 5 minutes) from bulk lysis using the 0.075% *w/v* saponin lysis solution. Clusters are compared with those from the standard bulk lysis.

The three clusters are totally comparable with those obtained according with the standard lysis protocol. It was confirmed by leukocyte count that was performed gating the clusters. The advantage of using the lysis solution with 0.075% *w/v* saponin is that monocytes are differentiated from neutrophils after 1 minute of quench. The percentages of each sub-population among the total leukocytes calculated in every experiment are reported in the table 4.1. The percentages are compared with those obtained by HemoCue.

	HemoCue	Standard bulk lysis	1 min	3 min	5 min
Neutrophils	52%	53%	55%	53%	53%
Lymphocytes	41%	43%	41%	42%	42%
Monocytes	4%	4%	4%	5%	5%

Table 4.1: WBC sub-population count corresponding to data shown in figure 4.4.

The same results are obtained using the 0.065% *w/v* saponin lysis solution, as shown in figure 4.5.

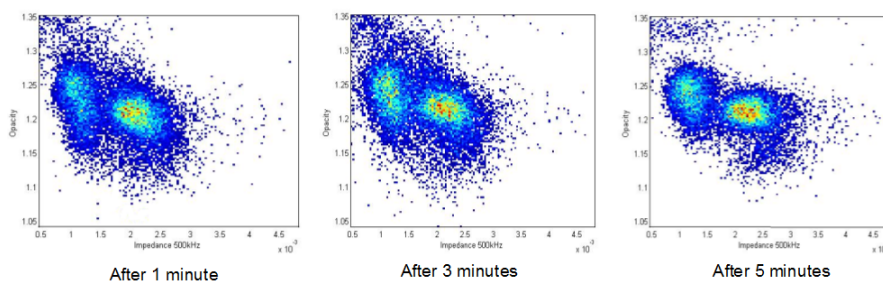


Figure 4.5: WBCs acquired in different quench times (1 minute, 3 minutes and 5 minutes) from bulk lysis using the 0.065% *w/v* saponin lysis solution.

The three clusters are well distinguishable from the first minute of quench even if they appear more clearly defined after 5 minutes. Thus even a slightly higher saponin concentration in the lysis solution effects a faster change in monocyte membrane resulting in the distinction of monocytes from neutrophils after 1 minute of quench. The correspondent WBC sub-population count is shown in the table 4.2.

	HemoCue	after 1 minute	3 minutes	5 minutes
Neutrophils	49%	53%	55%	52%
Lymphocytes	45%	41%	39%	43%
Monocytes	4%	6%	6%	5%

Table 4.2: WBC sub-population count corresponding to data shown in figure 4.5.

4.2.2 Evaluation of results in stirring lysis

The lytic effect of 0.1% *w/v* saponin lysis solution was verified also performing the stirring lysis, as shown in figure 4.6. WBC differentiation obtained after 1

minute is compared with data obtained by bulk lysis according to the standard protocol after 5 minutes of quench.

WBC differentiation is not improved because the high saponin concentration results in lymphocyte damage and it was verified by counting that a small part of lymphocytes were lysed even after 1 minute of quench.

The two lysis solutions, having respectively 0.065% and 0.075% w/v saponin, were used in the stirring lysis to test the saponin effect on debris volume. The figure 4.7 shows the clusters acquired by the integrated cartridge using 0.075% w/v saponin lysis solution for different quench times. They are compared with WBC differentiation obtained according with the standard lysis protocol performed by pipettes.

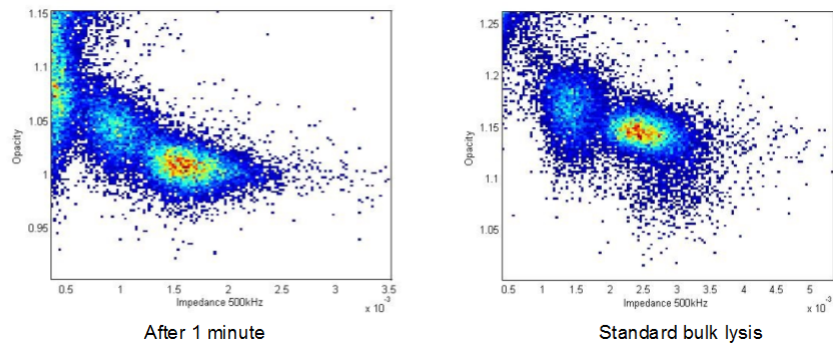


Figure 4.6: On left, WBCs from stirring lysis using 0.1% w/v saponin lysis solution after a quench time of 1 minute; on right, WBCs from the standard bulk lysis.

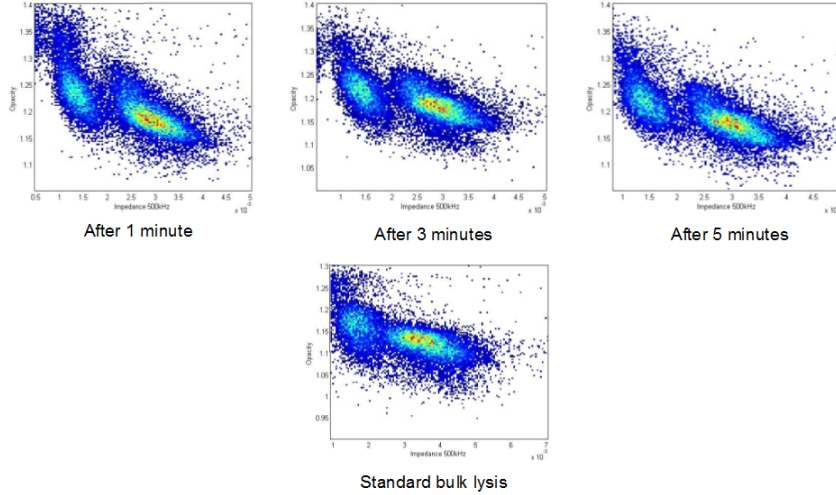


Figure 4.7: WBCs acquired in different quench times (1 minute, 3 minutes and 5 minutes) from stirring lysis using the 0.075% w/v saponin lysis solution. Clusters are compared with those from the standard bulk lysis.

The cluster shapes obtained by the stirring lysis are slightly different from those in the reference scatter plot. It is difficult to define if it depends on the different saponin concentration or it is the result of acquisition artifacts. However the three leukocyte populations from stirring lysis are well-defined and they do not change significantly for different times of quench. The debris volume is reduced and RBC fragments do not interfere with lymphocyte acquisition. The leukocyte count was performed for each experiment and it has been found that the lymphocyte count is slightly lower in the experiments where 0.075% saponin lysis solution is used. The difference in lymphocyte count between the modified protocol and the standard one is within 5%. The percentages of each leukocyte population are reported in the table 4.3.

	HemoCue	Standard bulk lysis	1 min	3 min	5 min
Neutrophils	59%	61%	64%	65%	62%
Lymphocytes	37%	35%	33%	32%	34%
Monocytes	2%	4%	4%	5%	5%

Table 4.3: WBC sub-population count corresponding to data shown in figure 4.7.

The results obtained using the 0.065% w/v saponin lysis solution are shown

in figure 4.8.

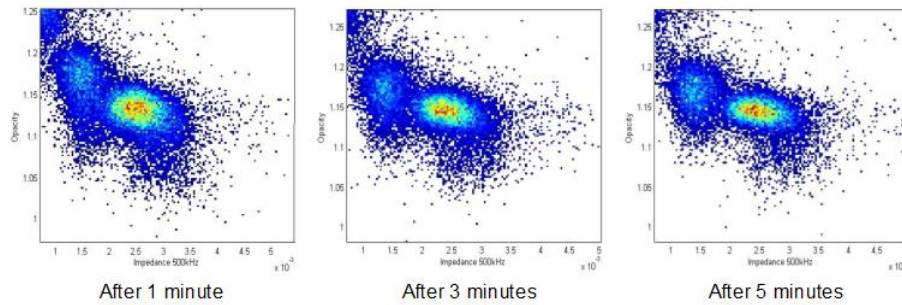


Figure 4.8: WBCs acquired in different quench times (1 minute, 3 minutes and 5 minutes) from stirring lysis using the 0.065% w/v saponin lysis solution.

The three clusters are well distinguishable after 1 minute of quench, even if the separation between debris and lymphocytes increases after 3 minutes. The leukocyte count is comparable with that obtained by HemoCue, as shown in the table 4.4.

	HemoCue	after 1 minute	3 minutes	5 minutes
Neutrophils	59%	62%	63%	59%
Lymphocytes	35%	33%	32%	36%
Monocytes	4%	5%	5%	5%

Table 4.4: WBC sub-population count corresponding to data shown in figure 4.8.

Therefore using the 0.065% saponin lysis solution lymphocytes are not damaged, the debris volume is reduced and the differentiation between monocytes and neutrophils is accelerated. The results obtained using the 0.065% saponin lysis solution are confirmed by performing the same experiments with blood samples taken from different donors. The figure 4.9 illustrates the results obtained using the blood from another donor. The clusters obtained after 1 minute and 3 minutes of quench are compared with those from the standard bulk lysis.

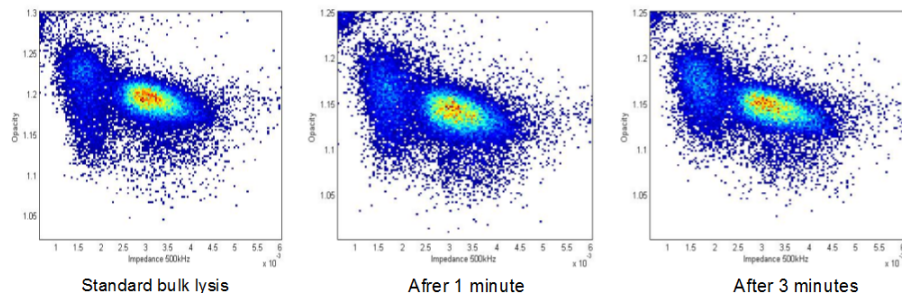


Figure 4.9: WBCs from stirring lysis using the 0.065% w/v saponin lysis solution acquired after 1 minute and 3 minutes of quench and compared with the standard bulk lysis.

4.3 Glutaraldehyde addition effects

Each experiment was repeated substituting the quench solution for that containing 1% w/v glutaraldehyde. The effect of the cross-linking fixative was evaluated for different saponin concentrations.

4.3.1 Evaluation of results obtained using 0.05% saponin solution

First, the lysis protocol was modified substituting only the quench solution for that containing 1% v/v glutaraldehyde. The results from the *bulk lysis* after 1 minute and 5 minutes of quench are illustrated in figure 4.10 and compared with the standard bulk lysis.

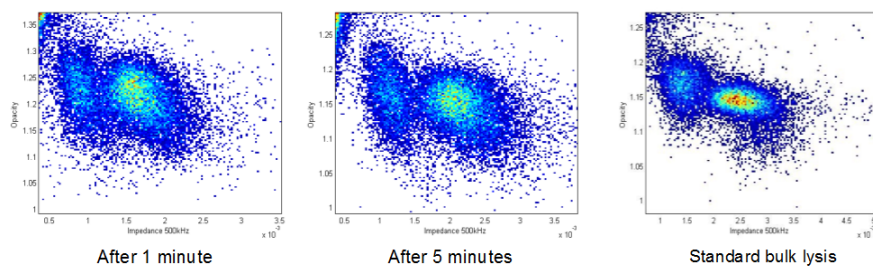


Figure 4.10: WBCs from bulk lysis using the 1% v/v glutaraldehyde quench solution acquired after 1 minute and 5 minutes of quench and compared with the standard bulk lysis.

The cluster shape is different from that in the scatter plot from the standard lysis but it was tested that the total leukocyte count is analogous. After one minute of quench the cluster position is shifted toward up and left compared with that from the standard lysis. This suggests that the immediate effect of glutaraldehyde on cells is the reduction of the volume and the membrane capacitance. After five minutes of quench the cluster shape does not change, presumably it is due to the strong glutaraldehyde effect in halting the reaction and in preventing morphological cell modification. The lymphocyte cluster is well distinguishable from the neutrophil cluster but monocytes are not differentiated from neutrophils. Furthermore, after five minutes, it is observable that the cell volume and the cell membrane capacitance increase since the clusters move toward right and down. The same results are obtained from the *stirring lysis*, as shown in figure 4.11.

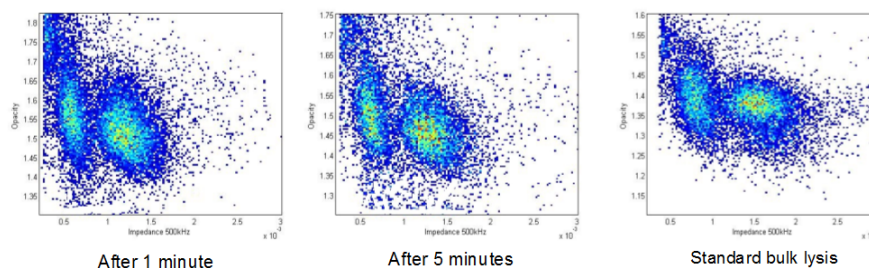


Figure 4.11: WBCs from stirring lysis using 1% v/v glutaraldehyde quench solution acquired after 1 minute and 5 minutes of quench and compared with the standard bulk lysis.

The only improvement in WBC differentiation due to the use of 1% glutaraldehyde quench solution is the reduction of debris volume, that enhances the differentiation between lymphocytes and debris in the stirring lysis.

4.3.2 Evaluation of results obtained using 0.1% saponin solution

In order to test the fixing effect of glutaraldehyde, the 1% glutaraldehyde quench solution was used for extinguishing the lytic effect of the saponin double concentrated lysis solution. The results from the *bulk lysis* are illustrated in figure 4.12.

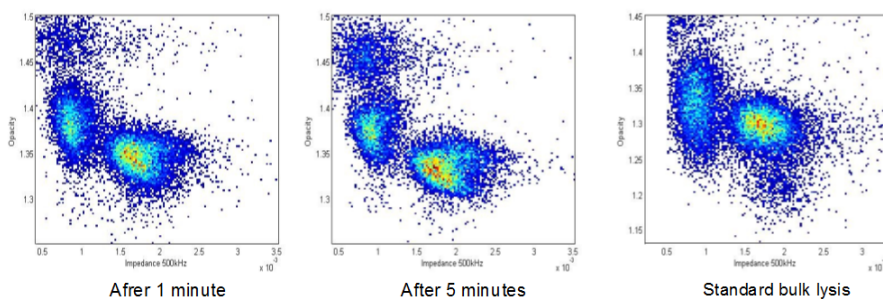


Figure 4.12: WBCs from bulk lysis using 0.1% w/v saponin lysis solution and 1% v/v glutaraldehyde quench solution acquired after 1 minute and 5 minutes of quench and compared with the standard bulk lysis.

The 1% glutaraldehyde quench solution halts almost totally the lytic reaction since it prevents the lymphocyte lysis. In contrast, lymphocyte lysis normally occurs after one minute from the addition of the quench solution without glutaraldehyde. The clusters are well defined even if the monocytes are not easily distinguishable from the neutrophils. Leukocyte count from the modified protocol is comparable with that from HemoCue but the lymphocyte count from the modified protocol decreases in the time by approximately 3%. The percentages of each WBC population are reported in the table 4.5. The lymphocyte count suggests that a small number of lymphocytes were lysed after five minutes of quench. It is supported by the comparison of the opacity vs electrical volume diagrams obtained from the modified protocol after one minute and five minutes of quench: after five minutes the size of the lymphocyte cluster decreases and the number of debris increases. The lymphocyte damage presumptively may be prevented increasing the concentration of glutaraldehyde in the quench solution.

	HemoCue	Standard bulk lysis	1 minute	5 minutes
Neutrophils	52%	56%	64%	67%
Lymphocytes	42%	38%	36%	33%
Monocytes	3%	6%	-	-

Table 4.5: WBC sub-population count corresponding to data shown in figure 4.12.

The results from the *stirring lysis* are not shown. They are completely different from those from the bulk lysis because of the leukocyte damage. This may be due to the reduced sheared stress that occurs in the mixing by the magnetic stirrer.

4.3.3 Evaluation of results obtained using 0.075% saponin solution

Then some experiments were performed by the integrated cartridge, using the 1% glutaraldehyde quench solution to halt the lytic effect of the solution having lower saponin concentration. The figure 4.13 shows the WBC clusters obtained after performing the *stirring lysis* using 0.075% saponin lysis solution and 1% glutaraldehyde quench solution.

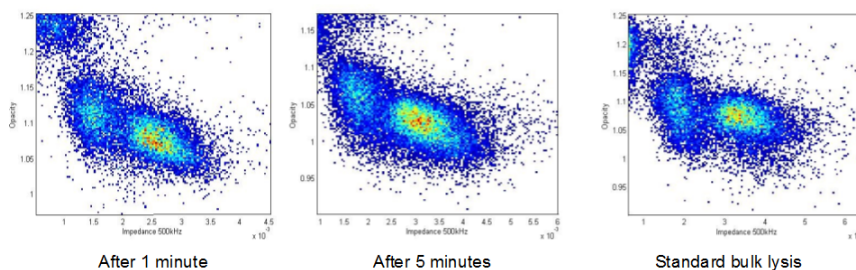


Figure 4.13: WBCs from bulk lysis using 0.075% w/v saponin lysis solution and 1% v/v glutaraldehyde quench solution acquired after 1 minute and 5 minutes of quench and compared with the standard bulk lysis.

The only difference between the results from the modified protocol and that from the standard lysis protocol concerns the separation of monocytes from neutrophils. While they are separated in the scatter plot from the standard protocol, monocytes and neutrophils are merged each other in that from the modified protocol even after five minutes of quench. On the other hand the leukocyte count is analogous in the two acquisitions.

Although the presence of glutaraldehyde inhibits the distinction between monocytes and neutrophils, it halts the lytic reaction preventing the leukocyte damage and reduces the debris volume improving the differentiation of lymphocytes from RBC fragments.

4.4 Variability in the data acquisition

For all the experiments performed using the sample preparation cartridge the blood was mixed with the lysis solution for 15 seconds at 2000 rpm. It was tested that the same result is obtained reducing the mixing time to 10 seconds. The figure 4.14 shows the three clusters acquired after performing the stirring

lysis by mixing the blood with the lysis solution for 10 and 20 seconds. In the experiments the 0.065% saponin lysis solution has been used and data has been saved after 3 minutes of quench.

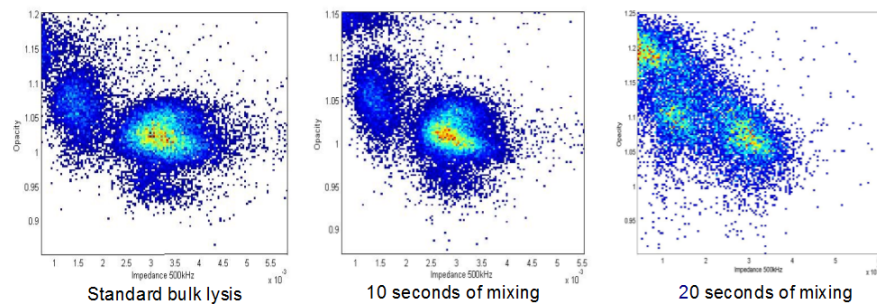


Figure 4.14: WBC clusters acquired after 3 minutes from the bulk lysis mixing the 0.065% saponin lysis solution with the whole blood for 10 seconds and 20 seconds. Clusters are compared with the standard lysis protocol.

The results have been compared with that from the bulk lysis performed according to the standard lysis protocol. The three clusters obtained by mixing the lysis solution with the blood for 10 seconds are totally comparable with those from the standard lysis protocol. The leukocyte count has been compared also with that from HemoCue and it is analogous. In contrast, the mixing of the blood with the lysis solution for 20 seconds resulted in leukocyte damage.

Experiments were performed within 5 hours from the blood collection since the morphology of blood cells in EDTA, anticoagulant used for blood storage, is well known to deteriorate after a few hours [19]. The figure 4.15 shows how leukocyte clusters change after 5 hours from the blood collection.

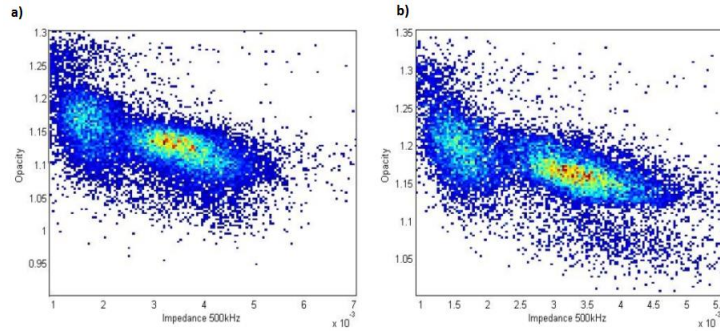


Figure 4.15: WBC acquisitions from the the standard bulk lysis obtained using the same blood sample a) after 30 minutes and b) after 5 hours from the collection.

The cluster position is modified and the three populations are shifted toward up and left. This means that the size of the cell is slightly reduced and the electrical properties of the cells are changed. Specifically, the opacity increase corresponds to the membrane capacitance decrease.

All the types of experiments were repeated three times to make sure that the results were not influenced by specific parameters, such as temperature, presence of air bubbles in the blood sample, asymmetries in the electrodes of the impedance chips, and cell sedimentation in the mixing chamber.

The temperature affects the rate of reaction. The experiments were performed at room temperature but higher room temperature can increase the rate of reaction.

When there are air bubbles in the blood samples, the total volume taken by pipette does not correspond to the blood volume but it is the sum of the blood volume and the volume of air bubbles. If the blood volume is reduced the blood-solution ratio changes resulting in leukocyte damage.

Since dirty electrodes affect the electrical signal, the electrodes of the impedance chips were regularly cleaned flushing 1 M NaOH solution for 10 min through the micro-channel and then rinsing it with 1mL of DI water. Furthermore, after each experiment, all the system was flushed with DI water and dried. The time taken for cleaning is necessary for avoiding clogs in the channels, and the drying process prevents leukocyte damage since the water has a lytic effect.

If leukocytes are acquired continuously from the same lysed blood sample, the leukocyte count decreases in the time because of cell sedimentation in the mixing chamber. The figure 4.16 illustrates the three clusters, in the scatter

plot opacity vs electrical volume, acquired in a continuous flow after 1 minute and 5 minutes from the quench solution addition.

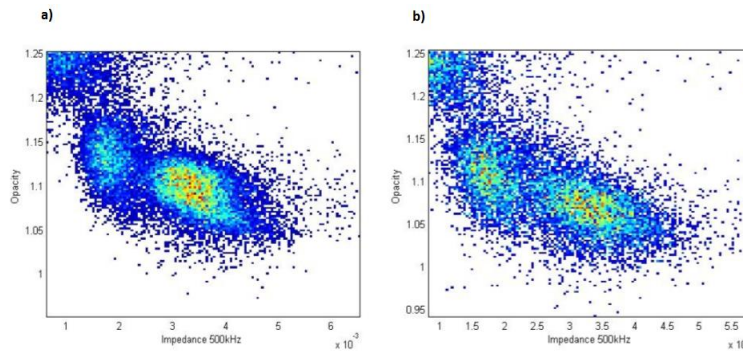


Figure 4.16: Clusters from the stirring lysis with 0.065% saponin solution obtained by pumping the lysed blood continuously at the flow rate of 40 $\mu\text{L}/\text{min}$, and acquired a) after 1 minute, and b) after 5 minutes of quench.

Data was obtained after performing the stirring lysis with 0.065% saponin lysis solution. In both acquisitions data was collected for 80 seconds but the total leukocyte count is different. The total leukocyte count from the first acquisition is 300 leukocytes per $1\mu\text{L}$ of diluted blood, and it corresponds to 6000 leukocytes per $1\mu\text{L}$ of whole blood since the blood sample has been diluted 20 times. The total leukocyte count from the second acquisition is 200 leukocytes per $1\mu\text{L}$ of diluted blood, which corresponds to 4000 leukocytes per $1\mu\text{L}$ of whole blood. Then, in order to avoid cell sedimentation, two data from the same lysed blood were acquired mixing the lysed blood in the time between the acquisitions.

Moreover, as the cartridge is semiautomatic, some actions are made manually and they are dependent on operator's promptness. The manual actions concern the command of the valve and the magnetic stirrer, and the pressure applied to pistons to push the two solutions into the mixing chamber. Thus variations can occur in the mixing time and may affect the erythrocyte lysis. The dependence of results on the operator's action has been reduced in the time by practice.

Furthermore it has been useful to analyze samples from different adult donors since they differ from each other resulting in different cluster position and shape. For example, the variability may concern the number of erythrocytes and leukocytes, and the leukocyte shape. A large number of erythrocytes affects the number of debris which can interfere with lymphocyte acquisition, and the leukocyte shape and count influence the cluster contours.

Chapter 5

Conclusion and future direction

5.1 Conclusion

The RBC lysis is a relevant step before WBC analysis by flow or impedance cytometry. It eliminates cell interferences and improves WBC differentiation. The RBC lysis, normally performed manually, has been automated by the sample preparation cartridge. The integrated system, consisting of the cartridge and the microfluidic impedance cytometer, represents a point-of-care device for WBC differentiation and count. As the lysis performed by the cartridge was less effective than that performed by pipette, in this research work the point-of-care leukocyte differentiation was improved by optimizing the standard lysis protocol for 3-part WBC differentiation (neutrophils, lymphocytes and monocytes). The protocol consists of two solutions: the lysis solution that is selective toward erythrocytes, and the quench solution that extinguishes the lytic reaction and restores the ionic balance of the leukocytes. The standard protocol was modified after analyzing the effect of specific chemicals on RBC lysis and WBC differentiation. Specifically, the saponin concentration was increased in the lysis solution for reducing the volume of RBC fragments and for accelerating the differentiation between neutrophils and monocytes, and the glutaraldehyde was added in the quench solution to preserve leukocyte morphology from the lytic effect. It was demonstrated that glutaraldehyde halts the lytic reaction preserving the leukocyte structure, but it does not improve WBC differentiation since it inhibits the separation of monocytes from neutrophils. Lastly, it was found the optimal saponin concentration in the lysis solution for obtaining a good point-

of-care leukocyte differentiation. It was proved that the 0.065% w/v saponin lysis solution contributes to reduce the debris volume and accelerate the differentiation between monocytes and neutrophils without damaging leukocytes. Thus a good three-part WBC differentiation is achieved within one minute from the addition of the quench solution. In the future, other protocols will be tested and modified for the detection of the eosinophils, besides the three main leukocyte subpopulations, by the integrated cartridge. The eosinophil count would complete the leukocyte count obtained by the point-of-care system.

5.2 Future direction

The microfluidic impedance chip is capable to detect different cell subtypes, not only the three main leukocyte populations, by the use of specific coated particles that modify the cell dielectric properties. Specifically, it has been tested that CD4 antibody coated beads can modify dielectric CD4 T cell properties and enable their differentiation by impedance cytometry. CD4 T-cells are recognized by CD4 antigens present on their surface and CD4+ T-lymphocyte count represents one of the most widely used method for HIV diagnosis and for monitoring its progression. In addition, low CD4 T-cell count is associated with a variety of conditions, including many viral, bacterial and parasitic infections. It would be advantageous to integrate the micro impedance chip into a microfluidic system, that performs continuous CD4 T cell labeling. The integrated system for CD4+ T-lymphocyte detection and counting would represent a great resource for developing countries, where cases of HIV infected people are more frequent, thanks to its portability and limited cost.

The last section of the thesis consists in the analysis of the interaction between CD4 antibodies and T helper cell antigens. Different quantities of fluorochrome conjugated CD4 antibody solution were mixed with small aliquots of blood in order to find the quantity that enables the saturation of the antigenic markers on T lymphocytes. In addition, the antigen-antibody interaction was analyzed in the time.

In the first paragraph the T lymphocytes labeling with CD4 antibodies is discussed. In the second paragraph different micro-mixers are evaluated for the design of the new point-of-care system. The last part of the work represents the starting point for the development of a microfluidic system for real time cell labelling.

5.2.1 CD4 T-cell labeling

As mentioned previously, lymphocytes can be distinguished in 3 main subsets: T helper, cytotoxic T cells and Natural Killer T cells. T helper cells show CD4 antigens on their surface and regulate the presence of cytokines modifying the adaptive immune response.

CD4+ T-lymphocyte count is the most widely used method for monitoring disease progression, staging, and response to drug therapy in HIV infected individuals [14]. It has been proposed that during the non-symptomatic phase of HIV infection, the virus has a relatively low affinity towards T cells and has a higher affinity for macrophages, resulting in a slow kill rate of CD4+ T cells by the immune system. This is initially compensated for via the production of new helper T cells. Once the virus becomes lymphotropic, it begins to infect CD4+ T cells far more efficiently and the immune system is overwhelmed [6].

The CD4+ T-cells express a large number of CD4 antigens on their surface; they are about 50 thousands on the surface of one cell. In 20 μL of blood there are from 10 thousands to 24 thousands of CD4 cells [20]; therefore in 20 μL of blood there are from $0.5 \cdot 10^9$ to $1.2 \cdot 10^9$ CD4 sites.

T helper cells can be detected from a blood sample by flow cytometry. Generally the blood is stained with fluorochrome conjugated CD4 antibodies before performing the RBC lysis. The antigenic sites saturate after about 20 minutes, because the motion of antibodies suspended in the blood is Brownian; however the phenomenon can be accelerated using an active mixer. The interaction between antibodies and a lymphocyte is illustrated in figure 5.1.

In order to analyze T helper cells by impedance cytometry, the blood has to be mixed with CD4 antibody coated beads, which lead T cells to a change in electrical properties and in size. The interaction between beads and CD4 cells is schematized in figure 5.2.

Before choosing a mixer capable to perform a continuous real time cell labeling with antibodies, it has been found the concentration of antibodies that saturate all the antigenic markers and it has been analyzed the molecular dynamics of CD4 antibodies. Changing the volume concentration of the reagent in the blood aliquot is a typical approach to find optimal sample preparation condition in cytometric analyses. Different amounts of APC labeled antibodies were titrated with a volume of 20 μL of whole blood before analysis by flow cytometry. As the mean fluorescent value from lymphocytes is proportional to the quantity of antibodies bound to antigenic markers, it gives information about the amount

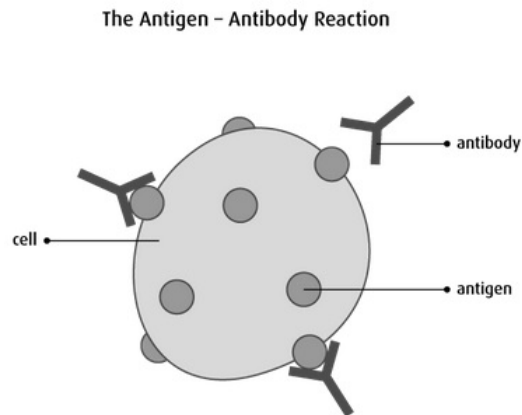


Figure 5.1: Scheme of the interaction between a lymphocyte and antigen specific antibodies (<http://www.cancer.ca/the-immune-system/>).

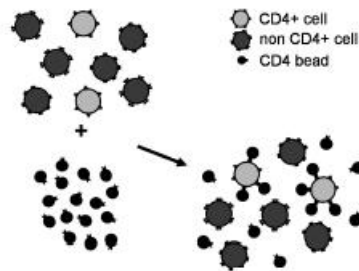


Figure 5.2: Scheme of the interaction of CD4 coated beads with T helper cells [14].

of antibodies that saturates the binding sites on cells. It was used a solution of antibodies having a concentration equal to 0.1 mg/ml. The following volumes of APC labeled antibody solution were used for each sample: 0.2, 0.3, 0.4, 1, 1.5, 2, 2.5, 3, 3.5, 4, 4.5, 5 [μL]. Three blood samples were taken by finger prick from different patients and divided into 20 μL aliquots mixed respectively with the mentioned antibody volumes. After cell labeling the blood was incubated for 20 minutes on a blood roller mixer and before data acquisition RBCs were lysed according to the standard lysis protocol in order to avoid cell interferences. In figure 5.3 the mean APC fluorescence from lymphocytes is plotted against the quantity of APC labeled antibody solution in the logarithmic diagram.

For each antibody concentration the arithmetic mean of fluorescence inten-

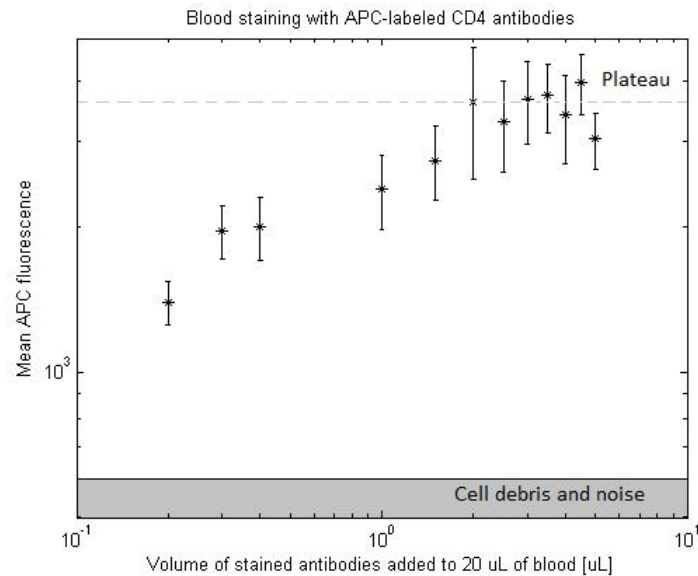


Figure 5.3: Dependence of the mean APC fluorescence from lymphocytes on the volume of the APC-CD4 staining antibody solution added to 20 μ L blood sample.

sities relative to different samples is marked out as star. The error bars indicate the dispersion of the distribution. The grey area corresponds to background fluorescence of cell debris and noise. The fluorescence intensity increases until it reaches a plateau for a quantity of CD4 antibody solution of about 2 μ L. This threshold value has been assumed as the quantity of antibodies which saturate all the binding sites.

That quantity of antibody solution has been used to analyze how the interaction antibody-cell develops in the time, or rather how the mean APC fluorescence from lymphocytes varies changing the incubation time. The curve corresponding to molecular dynamics is shown in figure 5.4. Data is relative to one sample and has been acquired after dividing the sample into 20 μ L aliquots and mixing them with 2 μ L of APC labeled CD4 antibody solution. The different aliquots were stored on a roll mixer and analyzed by flow cytometry in the following times after RBC lysis: 3, 3.5, 5.5, 8, 10, 12, 15, 20. After 6 minutes the most of CD4 antibodies are bound to T cells and after 15 minutes antibodies saturate the antigenic markers. An active mixer could accelerate the binding process contributing to a fast diagnosis.

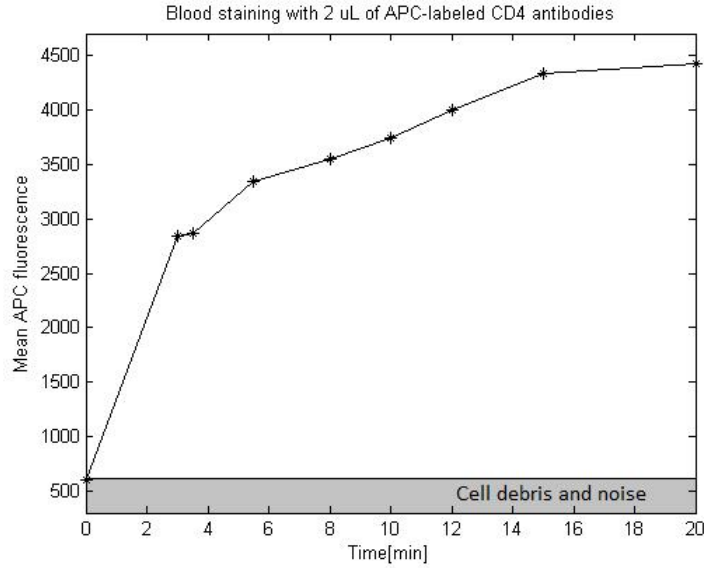


Figure 5.4: Evolution of the APC fluorescence from lymphocytes in the time. 20 μ L blood sample was stained with 2 μ L APC-CD4 antibody solution.

5.2.2 Choice of the mixer

In microfluidic platforms networks of micro-channels can be designed and tuned to achieve desired mixing and dilution ratios while minimizing the need for externally driven valves or pumps [41]. Microfluidic mixing schemes can be categorized as either “active”, where an external energy force is applied to perturb the sample species, or “passive”, where the contact area and contact time of the samples are increased through specially-designed micro-channel configurations. In *passive mixing* the flows are controlled by varying the length of the different sections. In order to have the desired flow profile at a predetermined Reynolds number, the behavior of different types of junction has to be modeled. Increasing the contact area between the species to be mixed is one of the most efficient means of enhancing the diffusive mixing effect [41]. Passive mixers consist of complex paths and are time consuming, therefore not suitable for real time cell labeling.

Active microfluidic mixers enhance the mixing performance by stirring or agitating the fluid flow using some forms of external energy supply. Active mixers typically use acoustic/ultrasonic, dielectrophoretic, pressure perturbation, electro-hydrodynamic or magnetic techniques to enhance the mixing perfor-

mance [24, 38].

In the design of *acoustic* mixer, a piezoelectric disk is used to excite air bubbles trapped in the top layer of the chamber. The disk is supplied using a AC voltage signal; the process mixing is accelerated by increasing the amplitude and the frequency [38].

The *dielectrophoretic* (DEP) force is executed by the particles present in a non-homogeneous electric field. Non-uniform alternating electrical fields are originated from electrodes supplied with different AC voltage signal. The electrical field generates a dipole moment on the particles and the interaction between the induced dipole charges and the electrical field generates a net force which drives the particles either towards or away from the electrode. The velocity of the particles increases with the magnitude of DEP force and with the size of the particle. In order to enhance the efficiency of the mixing it is used a flow rate that maximizes the speed of the particles and minimizes the diffusion of the reagents [24]. The disadvantage of dielectrophoretic mixers is due to their inappropriateness for particles of large sizes.

In *pressure perturbation* mixers, perturbations within the fluid streams are generated by velocity pulsing. In a typical device, the mixer comprises a single main channel and multiple side channels, and the fluids within the main channel are stirred by velocity pulsing of the fluids flowing through the side channels. The resulting stretching and folding of the fluids in the main and side channels induce a chaotic advection effect, which enhances the mixing [38].

A micro-mixers based on the *electro-hydrodynamic* (EHD) use force present when the fluids to be mixed have different electrical properties and are subjected to an electric field. The electrodes are arranged so that the electric field is perpendicular to the interface between the two fluids, creating a transversal secondary flow [38].

The *magneto-hydrodynamic* (MHD) flow effect has been used by various researchers to realize micro-mixers. Normally these micro-mixers use either DC or AC electrical and magnetic fields to generate Lorentz forces. These forces induce MHD flows in an electrolyte solution and result in a stretching and folding of the fluid in the mixing chamber [24].

The choice of the mixer depends on several factors, such as simplicity, efficiency, severity and cost. It has been thought to design a pressure perturbation mixer using a *braille cell* which consists of pins moved by a piezoelectric system. There are braille cells having different number of pins and different size in order to adapt to the pattern of the microfluidic system. They may have

different applications: braille pins are used for elastomeric valves, and pins in specific configurations are used for peristaltic pumps or for mixing solutions [9, 40, 23, 12]. Generally pins are in contact with elastomeric PDMS membranes and their displacement is enabled by a piezoelectric system activated via software. The effect of the braille pin depends on the force acting on it, the maximum displacement of the actuation, the stiffness and the thickness of the elastomeric membrane, and the geometry of the channel. It has been thought to use the 8-dot Braille cell for applying pressures which result in a stretching and folding of the blood sample in the main chamber to enhance the mixing with antibodies. Different mixer designs are suitable for specific configurations of pin actuation and several parameters which involve the efficiency of the actuation have to be tested in order to optimize the mixing and avoid cell damage. The use of the Braille cell could enable the fabrication of a simple, non-invasive and cheap active mixer.

Bibliography

- [1] C.M.A. Brett and A.M.O. Brett. *Electrochemistry: principles, methods, and applications*. Oxford University Press, 1993.
- [2] K. C. Cheung, M. Di Berardino, G. Schade-Kampmann, M. Hebeisen, A. Pierzchalski, J. Bocsi, A. Mittag, and A. Tarnok. Microfluidic impedance-based flow cytometry. *Cytometry A*, 77, 648-666, 2010.
- [3] D. Das, F.A. Kamil, K. Biswasa, and S. Dasa. Evaluation of single cell electrical parameters from bioimpedance of a cell suspension. *RSC Advances* 4, 18178-18185, 2014.
- [4] M. Frankowski, J. Theisen, A. Kummrow, P. Simon, H. Ragusch, N. Bock, M. Schmidt, and J. Neukammer. Microflow cytometers with integrated hydrodynamic focusing. *Sensors* 13, 4674-4693, 2013.
- [5] S. Gawad, D. Holmes, G. Benazzi, P. Renaud, and H. Morgan. *Micro-engineering in Biotechnology, Methods in Molecular Biology* 583, 149-179. Humana Press, 2010.
- [6] M. T. Glynn, D. J. Kinahan, and J. Ducree. Cd4 counting technologies for hiv therapy monitoring in resource-poor settings—state-of-the-art and emerging microtechnologies. *Lab on a Chip* 13, 2731-48, 2013.
- [7] D. R. Gossett, Weaver, W. M., A. J. Mach, S. C. Hur, H. T. Tse, W. Lee, H. Amini, and D. Di Carlo. Label-free cell separation and sorting in microfluidic systems. *Analytical and Bioanalytical Chemistry* 397, 3249-67, 2010.
- [8] E.H. Grant, R. J. Sheppard, and G. P. South. *Dielectric behaviour of biological molecules in solution*. Oxford University Press, 1978.
- [9] W. Gu, X. Zhu, N. Futai, B. S. Cho, and S. Takayama. Computerized microfluidic cell culture using elastomeric channels and braille displays. *Proceedings of the National Academy of Sciences* 101, 15861-6, 2004.
- [10] Hamaguchi and et al. Us patent 5,389,549. (5389549), 1995.

- [11] X. Han, C. van Berkel, J. Gwyer, L. Capretto, and H. Morgan. Microfluidic lysis of human blood for leukocyte analysis using single cell impedance cytometry. *Analytical Chemistry* 84, 1070-5, 2012.
- [12] Y. S. Heo, L. M. Cabrera, C. L. Bormann, G. D. Smith, and S. Takayama. Real time culture and analysis of embryo metabolism using a microfluidic device with deformation based actuation. *Lab on a Chip* 12, 2240-6, 2012.
- [13] V. S. Hollis, J. A. Holloway, S. Harris, D. Spencer, C. van Berkel, and H. Morgan. Comparison of venous and capillary differential leukocyte counts using a standard hematology analyzer and a novel microfluidic impedance cytometer. *PLoS One*, 7, e43702, 2012.
- [14] D. Holmes and H. Morgan. Single cell impedance cytometry for identification and counting of cd4 t-cells in human blood using impedance labels. *Analytical Chemistry* 82, 1455-1461, 2010.
- [15] D. Holmes, D. Pettigrew, C. H. Reccius, J. D. Gwyer, C. van Berkel, J. Holloway, D. E. Davies, and H. Morgan. Leukocyte analysis and differentiation using high speed microfluidic single cell impedance cytometry. *Lab on a Chip* 9, 2881-9, 2009.
- [16] G. Jerkiewicz. *Solid-Liquid Electrochemical Interfaces*, 1-12. American Chemical Society, 1997.
- [17] Ledis and et al. Us patent 4,751,179. (4,751,179), 1988.
- [18] Ledis and et al. Us patent 5,155,044 a. (5,155,044 A), 1992.
- [19] H. P. Mansberg, A. M. Saunders, and W. Groner. The hemalog d white cell differential system. *Journal of Histochemistry & Cytochemistry* 22, 711-724, 1974.
- [20] M. McKinley and V. O'Loughlin. *Human Anatomy*. McGraw-Hill Higher Education, 2011.
- [21] H. Morgan, D. Holmes, and N. G. Green. High speed simultaneous single particle impedance and fluorescence analysis on a chip. *Current Applied Physics* 6, 367-370, 2006.
- [22] H. Morgan, T. Sun, D. Holmes, S. Gawad, and N. G. Green. Single cell dielectric spectroscopy. *Journal of Physics D: Applied Physics* 40, 61-70, 2007.
- [23] B. Mosadegh, A. D. Mazzeo, S. A. Shepherd, R. F. and Morin, U. Gupta, I. Z. Sani, D. Lai, S. Takayama, and G. M. Whitesides. Control of soft machines using actuators operated by a braille display. *Lab on a Chip* 14, 189-99, 2014.
- [24] N.T. Nguyen and Z. Wu. Micromixers - a review. *Journal of Micromechanics and Microengineering* 15, R1-R16, 2005.

- [25] M.G. Ormerod, editor. *Flow cytometry - A practical approach. 3rd edition.* Oxford University Press, 2000.
- [26] A. Osei-Bimpong, C. Jury, R. McLean, and S. M. Lewis. Point-of-care method for total white cell count: an evaluation of the hemocue wbc device. *International Journal of Laboratory Hematology* 31, 657-64, 2009.
- [27] A. Osei-Bimpong, R. McLean, E. Bhonda, and S. M. Lewis. The use of the white cell count and haemoglobin in combination as an effective screen to predict the normality of the full blood count. *International Journal of Laboratory Hematology* 34, 91-7, 2012.
- [28] R. Parsons. The electrical double layer: recent experimental and theoretical developments. *Chemical Review* 90, 813-826, 1990.
- [29] R.R. Pethig and S. Smith. *Introductory Bioelectronics: For Engineers and Physical Scientists.* Wiley, 2012.
- [30] R. Pethig. *Dielectric and electronic properties of biological materials.* Wiley, 1979.
- [31] M. E. Piyasena and S. W. Graves. The intersection of flow cytometry with microfluidics and microfabrication. *Lab on a Chip* 14, 1044-59, 2014.
- [32] J.P. Robinson. *Handbook of flow cytometry methods.* Wiley, 1993.
- [33] Sakata and et al. *US Patent 5,175,109, (5,175,109), 1992.*
- [34] H.P. Schwan. Electrical properties of tissues and cell suspensions: mechanisms and models. In *Engineering in Medicine and Biology Society. Engineering Advances: New Opportunities for Biomedical Engineers. Proceedings of the 16th Annual International Conference of the IEEE., 1994.*
- [35] H.M. Shapiro. *Practical flow cytometry. Fourth edition.* Wiley, 2003.
- [36] D. Spencer. *Advanced microfluidic impedance cytometry for point of care analysis.* PhD thesis, University of Southampton, 2013.
- [37] D. Spencer and H. Morgan. Positional dependence of particles in microfluidic impedance cytometry. *Lab on a Chip* 11, 1234-9, 2011.
- [38] Y. K. Suh and S. Kang. A review on mixing in microfluidics. *Micromachines* 1, 82-111, 2010.
- [39] T. Sun and H. Morgan. Single-cell microfluidic impedance cytometry: a review. *Microfluidics and Nanofluidics* 8, 423-443, 2010.
- [40] Y. C. Tung, N. Torisawa, Y. S. and Futai, and S. Takayama. Small volume low mechanical stress cytometry using computer-controlled braille display microfluidics. *Lab on a Chip* 7, 1497-503, 2007.

- [41] C. van Berkel, J. D. Gwyer, S. Deane, N. G. Green, J. Holloway, V. Hollis, and H. Morgan. Integrated systems for rapid point of care (poc) blood cell analysis. *Lan on a Chip* 11, 1249-55, 2011.
- [42] S. Zheng, J. Lin, H. Kasdan, and Y. Tai. Fluorescent labeling, sensing, and differentiation of leukocytes from undiluted whole blood samples. *Sensors and Actuators B* 132, 558-567, 2008.

Acknowledgments

Ringrazio il prof. Marco Tartagni per avermi dato l'opportunità di trascorrere alcuni mesi nel laboratorio di Southampton e per i suoi feedback durante la permanenza all'estero. I would like to thank Hywel Morgan for having received me in his research group and for the helpful meetings along the work period. I thank Dan for his help in the lab, for having explained me the operating principles of several devices and I'm sorry if I asked senseless questions at the beginning. I thank all my colleagues who worked/work in the laboratory of hybrid biodevices for their availability to clear up my doubts, for having been 'spontaneous' bleeding volunteers and for the pleasant company. Ringrazio tutti i miei amici di Cesena; ognuno sa l'importanza che ha avuto durante il mio percorso universitario. Grazie anche agli amici incontrati a Taranto e Coimbra per il loro costante sostegno. Un grazie speciale ai miei genitori per avermi 'finanziato' durante tutti questi anni accademici, soprattutto, durante il periodo di ricerca a Southampton. Senza di loro non avrei raggiunto questo traguardo, che rappresenta il punto di partenza del mio futuro percorso lavorativo. Grazie anche a mio fratello per il suo aiuto in campo linguistico durante i periodi di permanenza all'estero.

Appendix - Results obtained by the stirring lysis using 0.065% w/v saponin solution

Patient 1

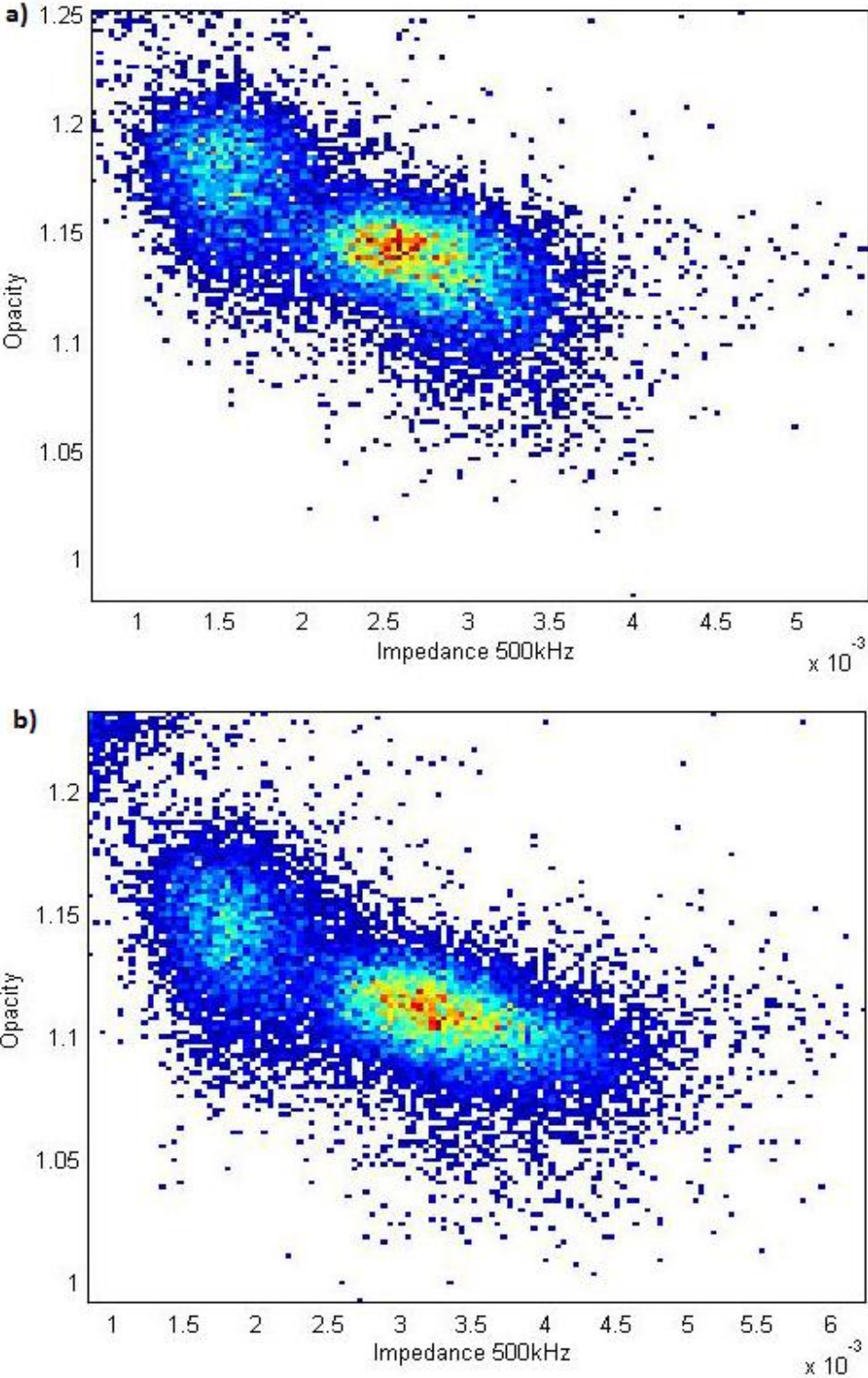


Figure 1: a) Standard bulk lysis b) Stirring lysis (1 minute of quench)

Patient 2

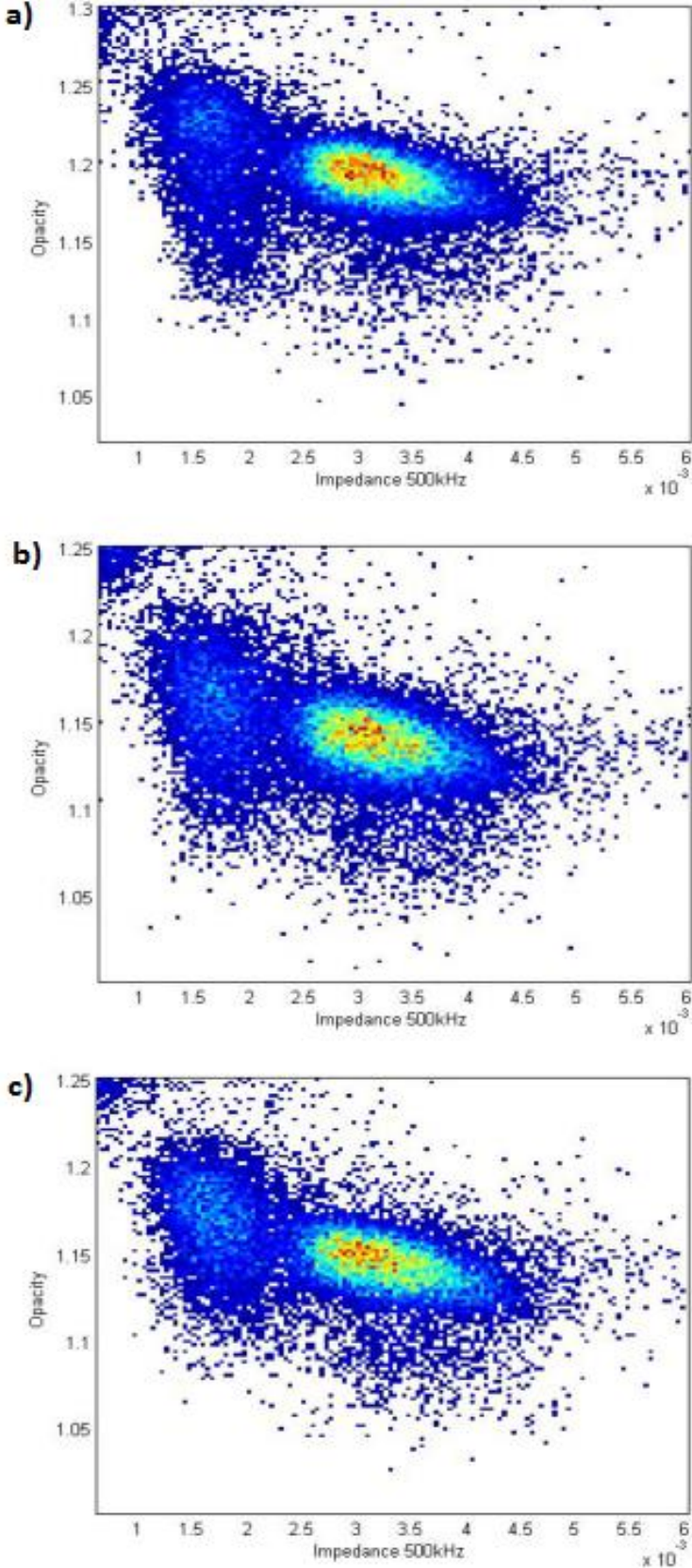


Figure 2: a) Standard bulk lysis b) Stirring lysis (1 minute of quench)
c) Stirring lysis (3 minutes of quench)

Patient 3

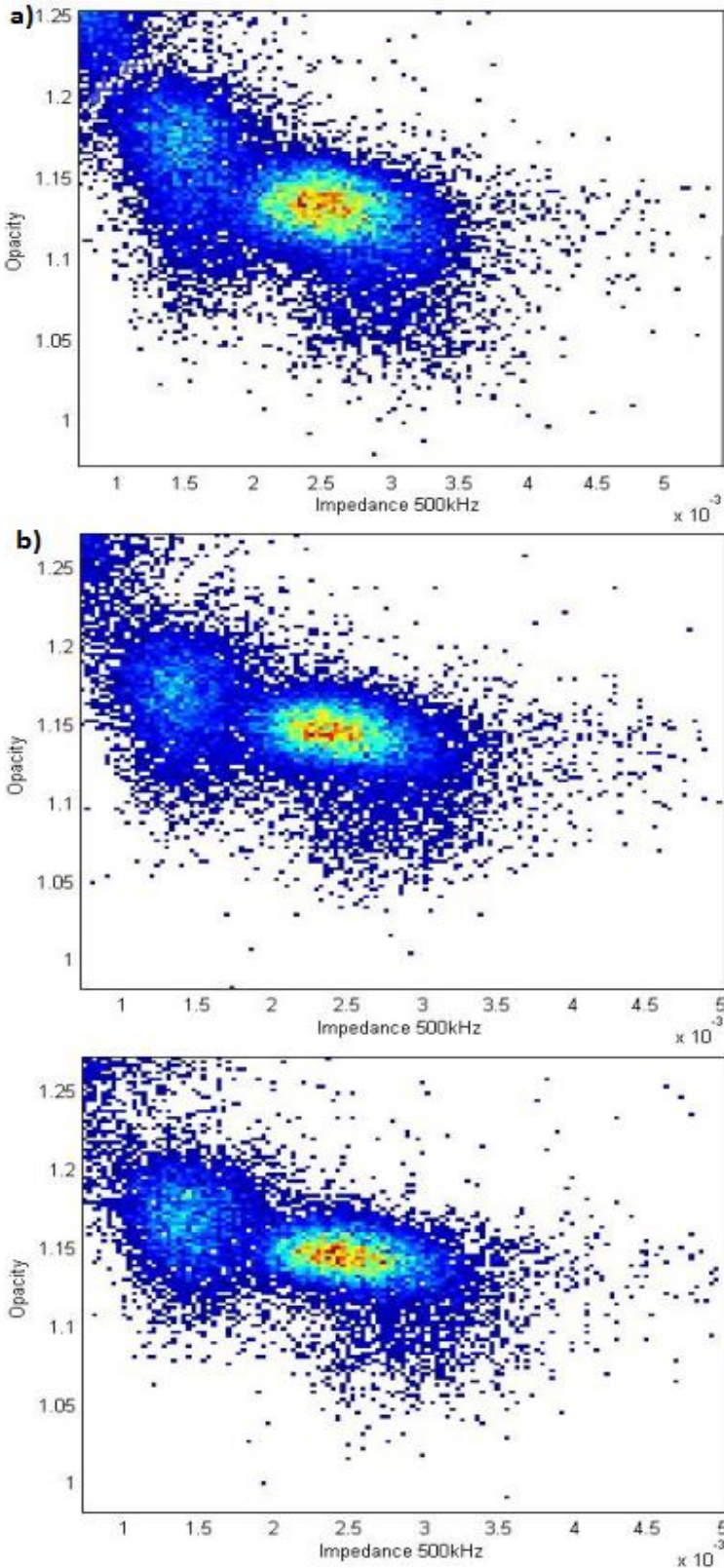


Figure 3: a) Stirring lysis (1 minute of quench) b) Stirring lysis (3 minutes of quench)
c) Stirring lysis (5 minutes of quench)

Patient 4

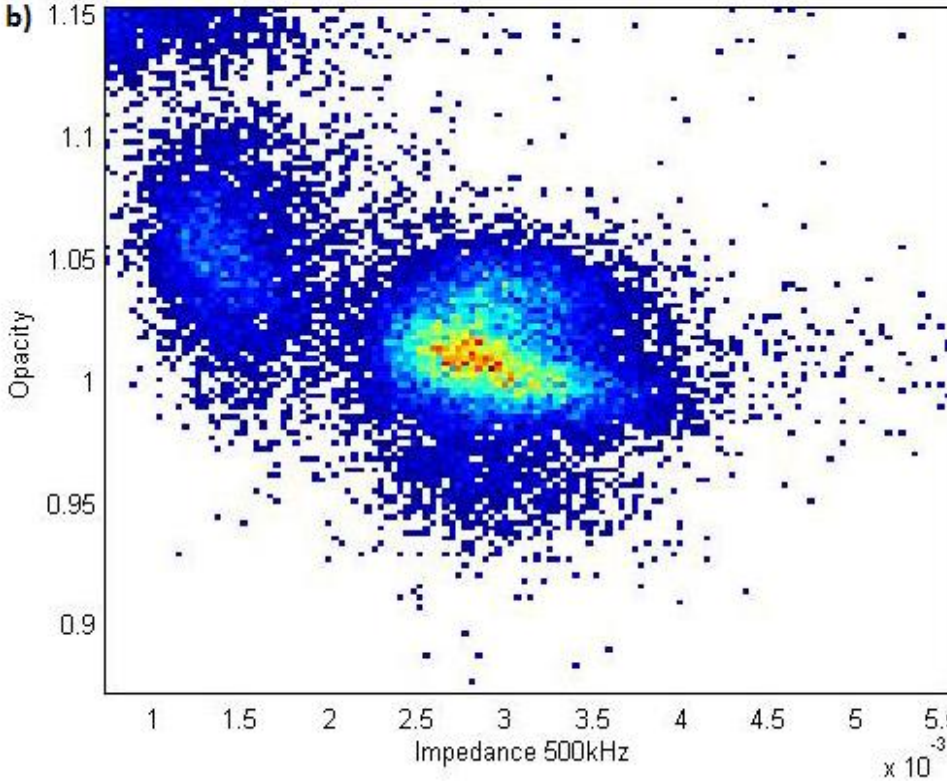
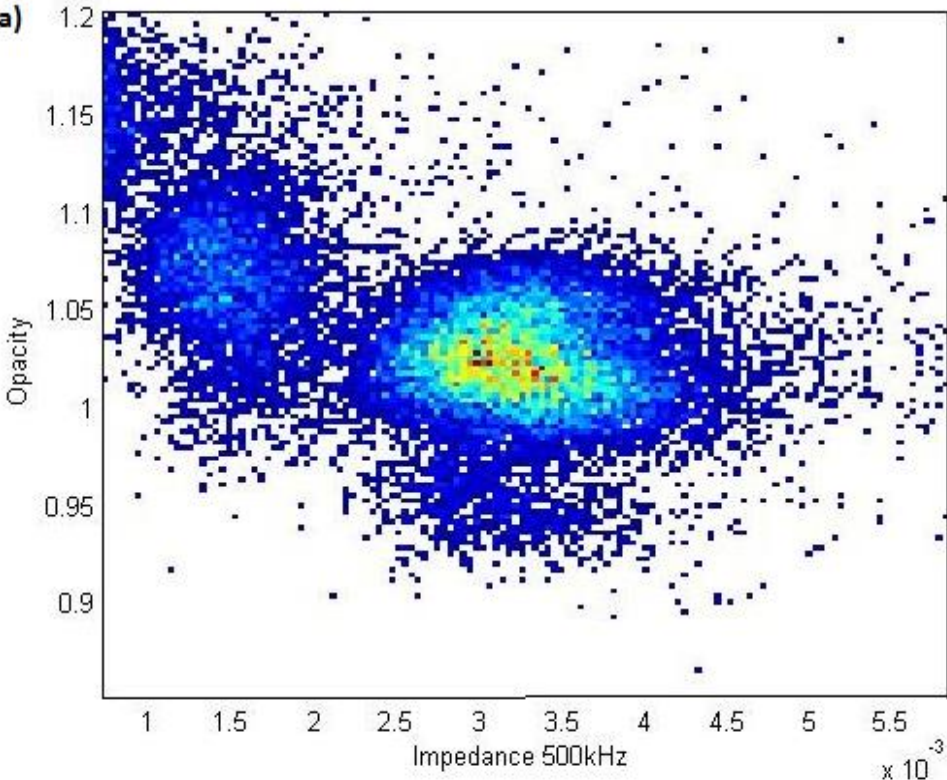


Figure 4: a) Standard bulk lysis b) Stirring lysis (3 minutes of quench)

Patient 5

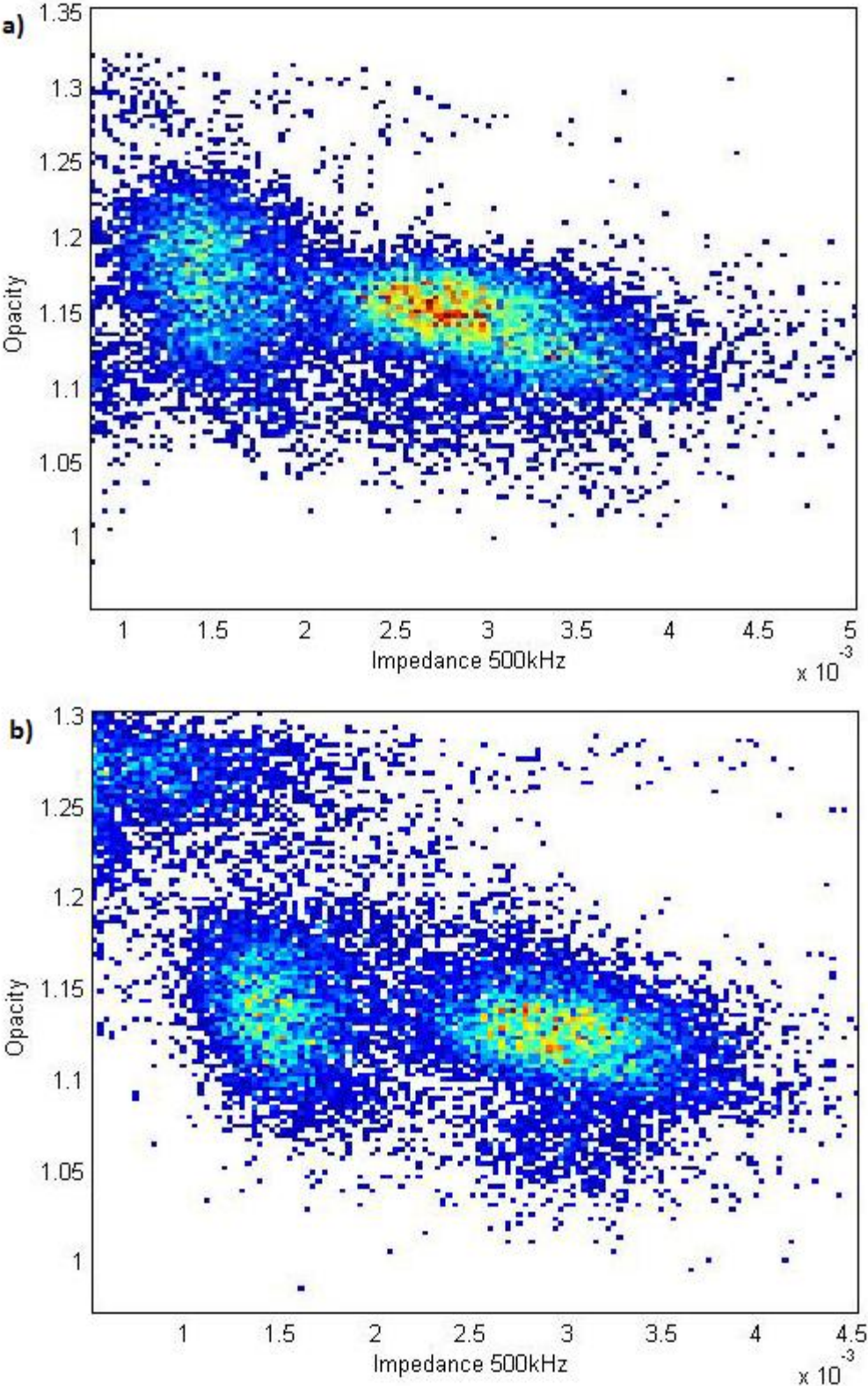


Figure 5: a) Standard bulk lysis b) Stirring lysis (5 minutes of quench)